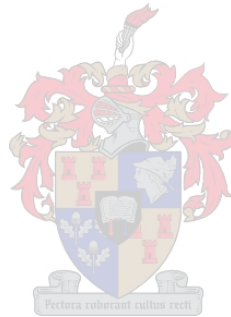


Exploratory Investigation of Extending Rainfall Records in the Western Cape by Means of Dendroclimatology

Lauren A. Lester



Masters project presented in partial fulfilment of the requirements for the degree of
Masters of (Civil) Engineering
in the Faculty of Engineering at Stellenbosch University

Supervisor: Prof JA du Plessis

Department of Civil Engineering

December 2019

Declaration

By submitting this project electronically, I declare that the entirety of the work contained therein is my own, original work, that I am the sole author thereof (save to the extent explicitly otherwise stated), that reproduction and publication thereof by Stellenbosch University will not infringe any third party rights and that I have not previously in its entirety or in part submitted it for obtaining any qualification.

Signature:

Date: December 2019

Copyright © 2019 Stellenbosch University

All rights reserved

Abstract

Water security is a pressing global issue, although given the recent “Day Zero” crisis experienced in the Western Cape the concern for securing water supplies and sustainable water management is of utmost importance in South Africa. This threat of limited water supplies is only compounded by the growing population and indication of climate change resulting in the country becoming hotter and drier, therefore necessitating more research being done with respect to the effects of climate on South African water surety, and in so doing supporting better, more sustainable, water use and management schemes.

Centuries old rainfall records are particularly useful in developing robust climate models, as they may provide insight into any seasonality and cyclicity found within a region’s climate. South Africa, however, has limited reliable rainfall records, with few being in excess of a hundred years therefore leaving much room for improvement in both ascertaining reliable models and in the development of robust, predictive climate models.

Successfully used to augment climatic records in parts of Asia, Europe and North America, dendroclimatology offers an opportunity to derive longer rainfall records. Dendroclimatology, a sub-branch of the greater discipline of dendrochronology, is the study and use of trees’ annual growth rings to date and subsequently approximate climatic information, such as rainfall. The ability to extract climatic information from the annual growth ring series is possible since the growth of a tree is not only driven by age or competition but also by climatic factors. To isolate the effect of the climatic factors on the growth, however, the annual growth ring series does need to be detrended through a statistical process known as standardisation and cross-dating. Once the ring series is standardised and cross-dated, a nearby climatic record can be used to establish the correlation between the relevant climatic variable and the tree’s growth thereby allowing the effect of the climate on the growth to be quantified and, if there is a good correlation, projected back or forward to extend the climatic record.

Previously, there has not been much success in applying dendroclimatological principles in South Africa – mostly due to the sparse number of indigenous species limiting the sample size and, thus, the accuracy and reliability of the results. The most significant study undertaken in South Africa, at least in terms of prompting greater interest in dendroclimatology, was the “Die Bos” study undertaken by LaMarche and Dunwiddie in the late 1970s. The “Die Bos” study focused on using indigenous *Widdringtonia cedarbergensis (wallichii)* with the hopes of quantifying a significant correlation between rainfall and the tree growth, however the researchers failed to establish a consistent correlation, noting that the growth and rainfall only correlated over an 18-month period. Other indigenous studies too resulted in non-significant correlations, however all the completed studies do suggest that the potential for a successful correlation remains – going so far as to suggest alternative species, using alien/exotic species, using a greater sample size or assessing other climatic variables, such as temperature.

For this research, consideration was only given to the rainfall records in the Western Cape. Four exotic samples from three specific locations were obtained and analysed using both the principles of traditional dendroclimatology and time series-based statistical analyses. The three locations, namely Bishopscourt, Tokai and Wolseley, were selected as complete cross-sectional samples could be obtained. The samples were analysed by means of both conventional dendroclimatology software, namely TSAP-Win, and a more theoretical, statistical, time series centred approach. The TSAP-Win, log-return and ARMA analyses all, however, failed to deliver successful correlations between the rainfall and ring width series with the best

correlation occurring for the Tokai chronology, at 20.4%. Given that the correlations were statistically insignificant with the limited data sets, it was deemed necessary to attempt to reconstruct a rainfall record with a greater, validated width chronology. The “Die Bos” chronology is an original, validated chronology for the Western Cape and was therefore selected as the final sample that would be analysed through the time series analyses. The results of this, however, were poor with the best correlation of 40.1% therefore negating the possibility of a reliable historic extension. The procedure of how historic rainfall would be determined is, however, included in this research.

This research concluded that alternative methods be pursued for the analysis of tree and climate data in the Western Cape, perhaps giving more consideration to machine learning techniques such as random forests or multiple variable regression which allows other climatic variables to be considered. A greater sample set will also be advantageous as the results will inherently bear more statistical significance by meeting the requirements for minimum reliable sample sizes. Additionally, greater sample sizes would also help with generating more accurate chronologies. The possibility for a successful dendroclimatological analysis in the Western Cape is thus still possible.

Opsomming

Watersekerheid is 'n belangrik internasionale aangeleentheid en gegee die onlangse 'Day Zero' -krisis wat in die Wes-Kaap ondervind is, is die versekering van watervoorrade en volhoubare waterbestuur nou uiters belangrik in Suid-Afrika. Die bedreiging van beperkte watervoorrade word vererger deur 'n groeiende bevolking en 'n aanduiding van klimaatsverandering wat daartoe lei dat die land warmer en droër word. Dit is noodsaaklik dat meer navorsing gedoen word rakende die gevolge van die klimaat op die Suid-Afrikaanse watervoorrade, en sodoende ondersteuning van beter, meer volhoubare watergebruik en bestuur te verseker.

Eene oue reënvalrekords is veral nuttig om robuuste klimaatmodelle te ontwikkel, aangesien dit insig kan bied in die seisoenaliteit en siklusiteit wat in die klimaat van 'n streek voorkom. Suid-Afrika het egter beperkte betroubare reënvalrekords, met slegs 'n paar wat honderd jaar oorskry, wat baie ruimte laat vir verbetering in betroubare modelle sowel as die ontwikkeling van robuuste, voorspellende klimaatmodelle.

Dendroklimatologie is suksesvol gebruik om klimaatsrekords in dele van Asië, Europa en Noord-Amerika aan te vul, en bied die geleentheid om langer reënvalrekords af te lei. Dendroklimatologie, 'n vertakking van die groter dissipline van dendrochronologie, is die studie en gebruik van bome se jaarlikse groei ringe vir datering en om sodoende klimaatsinligting, soos reënval, af te lei. Die vermoë om klimaatsinligting uit die jaarlikse groei-ringreeks te verleng, is moontlik omdat die groei van 'n boom nie net deur ouderdom of eksterne faktore soos kompetisie gedryf word nie, maar ook deur klimaatsfaktore. Om die effek van die klimaatfaktore op die groei te isoleer, moet die jaarlikse groei-ringreeks egter ondersoek word deur 'n statistiese proses wat bekend staan as standaardisering en kruisdatering. Sodra die ringreeks gestandaardiseer en gekruisdateer is, kan 'n nabygeleë klimaatrekord gebruik word om die verband tussen die betrokke klimaatveranderlike en die boom se groei te bepaal, waardeur die effek van die klimaat op die groei gekwantifiseer kan word. As daar 'n goeie korrelasie is, kan daar agtertoe óf vorentoe in tyd geprojekteer word om sodoende die klimaatrekord te verleng.

Daar was voorheen nie veel sukses met die toepassing van dendroklimatologiese beginsels in Suid-Afrika nie - meestal as gevolg van die geringe aantal inheemse spesies wat die steekproefgrootte beperk het, en dus die akkuraatheid en betroubaarheid van die resultate. Die belangrikste studie wat in Suid-Afrika onderneem is, ten minste ten opsigte van 'n groter belangstelling in dendroklimatologie, was die "Die Bos"-studie wat in die laat 1970's deur LaMarche en Dunwiddie onderneem is. "Die Bos"-studie het gefokus op die gebruik van inheemse *Widdringtonia cedarbergensis (wallichii)* met die hoop om 'n beduidende korrelasie tussen reënval en die boomgroei te kwantifiseer, maar die navorsers kon nie 'n betroubare korrelasie bewerkstellig nie, met die opmerking dat die groei en reënval slegs oor 'n siklus van 18 maande ooreenstemming getoon het. Ander inheemse studies het ook tot nie-noemenswaardige korrelasies gelei, maar al die voltooides studies dui daarop dat die potensiaal vir 'n suksesvolle korrelasie bestaan. Verskeie navorsings-voorstelle word gemaak, soos die gebruik van alternatiewe boomspesies, die gebruik van eksotiese spesies, 'n groter steekproef of die ontleding van ander klimaatsveranderlikes, soos temperatuur.

Vir hierdie navorsing is slegs oorweging geskenk aan die reënvalrekords in die Wes-Kaap. Vier eksotiese boom monsters van drie spesifieke plekke is verkry en ontleed deur gebruik te maak van beide die beginsels van tradisionele dendroklimatologie en tydreëks-gebaseerde statistiese ontledings. Die drie

plekke, naamlik Bishops court, Tokai en Wolseley, is gekies omdat volledige dwarsnit-monsters verkry kon word. Die monsters is ontleed met behulp van sowel konvensionele dendroklimatologiese sagteware, naamlik TSAP-Win, asook 'n meer teoretiese, statistiese, tydreeksgesentreerde benadering. Die TSAP-Win-, logaritmiëse data ("log-return")- en ARMA-ontledings kon egter nie daarin slaag om suksesvolle korrelasies tussen reënval- en ringwydte-reeks te lewer nie, met die beste korrelasie wat vir die Tokai-chronologie voorkom, n.l. 20.4%. Aangesien die korrelasies statisties onbeduidend was met die beperkte datastelle, is dit nodig geag om te poog om 'n reënvalrekord te rekonstrueer met 'n groter, bevestigde breedte chronologie. Die "Die Bos" -chronologie is die oorspronklike, bevestigde chronologie vir die Wes-Kaap en is daarom gekies as die finale steekproef wat deur die tydreeksanalises ontleed sou word. Die resultate hiervan was egter swak, met die beste korrelasie 40.1%, wat die moontlikheid van 'n betroubare historiese uitbreiding van 'n datastel beperk. Die prosedure van hoe historiese reënval bepaal sou word, is by hierdie navorsing ingesluit.

Hierdie navorsing het tot die gevolgtrekking gekom dat alternatiewe metodes vir die ontleding van boom- en klimaatdata in die Wes-Kaap nagestreef moet word, en stel voor data daar oorweging geskenk word aan masjienleertegnieke soos ewekansige bos-generasie ("Random Forest") of meervoudige veranderlike regressie, waardeur ander klimaat veranderlikes oorweeg kan word. 'n Groter steekproefstel sal ook voordelig wees, aangesien die resultate inherent meer statistiese betekenis sal hê deur aan die vereistes vir minimum betroubare steekproefgroottes te voldoen. Boonop sal groter steekproefgroottes ook help om meer akkurate chronologieë te genereer. Die moontlikheid vir 'n suksesvolle dendroklimatologiese analise in die Wes-Kaap is dus steeds moontlik

Acknowledgements

The author wishes to acknowledge the following, without whom this thesis would be incomplete:

- My supervisor, Prof du Plessis, who supported this process from the outset and assisted me throughout my research;
- The Department of Forestry and Wood Science, particularly Mr Anton Kunneke and Dr Brand Wessels, who assisted with the obtaining and interpretation of the samples used in this study;
- The Centre for Statistical Consultation at the University of Stellenbosch, particularly Prof Daan Nel, who assisted with the selection of statistical techniques;
- My family, who took on the roles of financial aid, proof-readers, technical advisers and emotional support throughout my entire two-year masters – grateful only begins to describe it;
- My friends, who bore through two years of trials, tribulations and joy – for their support I am thankful, as Stellenbosch would not be the same without them

Table of Contents

Declaration.....	ii
Abstract.....	iii
Opsomming.....	v
Acknowledgements.....	vii
Table of Contents.....	viii
List of Figures.....	x
List of Tables.....	xii
List of Acronyms.....	xiii
Glossary.....	xiv
1. Introduction.....	15
1.1 Background.....	15
1.2 Problem Statement.....	16
1.3 Research Objectives.....	16
1.4 Research Scope and Constraints.....	16
1.4.1 Scope.....	16
1.4.2 Constraints.....	17
1.5 Research methodology.....	18
1.6 Document Outline.....	19
2. Literature Review.....	20
2.1 Definition of Dendrology.....	20
2.1.1 History of dendrochronology.....	20
2.2 Definition of Trees.....	21
2.2.1 Characteristics of a tree.....	21
2.2.2 Classification of trees.....	25
2.2.3 Growth behaviour.....	27
2.3 The Dendro-process.....	29
2.3.1 Principles of dendrochronology.....	30
2.3.2 Obtaining samples.....	34
2.3.3 Preparation of samples.....	37
2.3.4 Reading/recording of sample data.....	37
2.3.5 Calculation methods.....	38
2.4 Completed studies.....	43
2.4.1 South African studies.....	43
2.4.2 Greater continental studies.....	45

2.5	Climatic Patterns in South Africa	46
2.5.1	Western Cape climate.....	47
2.5.2	Microclimates.....	49
2.6	Literature summary and conclusion	49
3.	Methodology.....	51
3.1	Data Collection.....	51
3.1.1	Tree ring samples	51
3.1.2	Rainfall data	61
3.2	Analysis techniques.....	62
3.2.1	TSAP-Win.....	62
3.2.2	Time series analysis.....	66
4.	Results.....	68
4.1	TSAP-Win Moving Average results.....	70
4.2	Time series analyses results.....	73
4.2.1	Stationarity validation.....	73
4.2.2	Log-return results.....	73
4.2.3	Lag results	76
4.2.4	Regression and ARMA model results.....	90
4.3	Application of statistical methods on existing chronology.....	93
4.3.1	Lag results	94
4.3.2	Regression and ARMA results	96
4.3.3	Historic extension of rainfall	97
4.4	Results summary.....	99
	Recommendations	101
5.1	Recommendations	101
	Summary and Conclusion	103
6.1	Summary of research	103
6.2	Findings, conclusions and lessons learned	103
6.3	Limitations and future work	104
	References	105
	Appendices	111
A.1	Ring measurements	112
A.2	Excel sheets – TSAP-Win	122
A.3	Excel sheets – log-return.....	132
B.1	Correlation function results.....	142
B.2	Regression results	146

List of Figures

Figure 1: Relative positions of sample locations within the Western Cape (Google Earth, 2018)	17
Figure 2: Components of a tree (Genders, 2018).....	22
Figure 3: Cross-section of a typical tree's stem (Stokes & Smiley, 1968)	23
Figure 4: Typical cross-section of a gymnosperm (Stokes & Smiley, 1968).....	24
Figure 5: Gradual early-to-latewood transition vs sharp early-to-latewood transition (Kozłowski, 1971)	25
Figure 6: Cross-sectional comparison of gymnosperm & angiosperm (Lilly, 1977).....	26
Figure 7: Discontinuous rings ("wedging rings") seen in <i>Sequoia sempervirens</i> (Fritz & Averill, 1924).....	28
Figure 8: Formation of compression wood due to inclination (Schweingruber, 1971).....	29
Figure 9: Sensitivity of ring series (Stokes & Smiley, 1968)	31
Figure 10: Rinntech 4452-P Resistograph (Rinntech, 2018)	34
Figure 11: A typical Swedish increment borer (Forestry Suppliers, 2018)	35
Figure 12: Increment core being extracted from the borer (Haglof, 2018).....	36
Figure 13: Lintab Set-up (Rinntech, 2018)	38
Figure 14: Lintab's hand crank (Rinntech, 2018)	38
Figure 15: Western Cape cumulative rainfall behaviour	48
Figure 16: Location of <i>P. pinaster</i> in Bishopscourt (Google Earth, 2018).....	52
Figure 17: Locations of <i>S. sempervirens</i> and <i>C. lusitanica</i> in Tokai Park (Google Earth, 2018)	53
Figure 18: Location of <i>E. cladocalyx</i> in Wolseley (Google Earth, 2018).....	54
Figure 19: <i>Pinus pinaster</i> sample (Bishopscourt).....	55
Figure 20: <i>Sequoia sempervirens</i> sample (Tokai)	56
Figure 21: Section of <i>Cupressus lusitanica</i> sample (Tokai)	56
Figure 22: Section of <i>Eucalyptus cladocalyx</i> (Wolseley) with some marked years.....	56
Figure 23: Growth rings as seen beneath the microscope	58
Figure 24: TSAP-Win header tab	59
Figure 25: TSAP-Win set-up with complete recordings	59
Figure 26: Distance between H1E002 and the <i>E. cladocalyx</i> sample site (Google Earth, 2018)	62
Figure 27: TSAP-Win set-up for detrending with an exponential function	63
Figure 28: Comparative plot of TSAP generated residuals and raw chronology - Bishopscourt	64
Figure 29: Comparative plot of TSAP generated residuals and raw chronology - Tokai	65
Figure 30: Comparative plot of TSAP generated residuals and raw chronology - Wolseley	65
Figure 31: Bishopscourt chronology vs rainfall.....	68
Figure 32: Tokai chronology vs rainfall	69
Figure 33: Wolseley chronology vs rainfall	69
Figure 34: Wolseley chronology vs rainfall ("Zoomed" in on period where both have records)	70
Figure 35: Plot of Bishopscourt residuals and rainfall	71
Figure 36: Plot of Tokai residuals and rainfall.....	71
Figure 37: Plot of Wolseley residuals and rainfall.....	72
Figure 38: Plot of Bishopscourt log returns	74
Figure 39: Plot of Tokai log returns.....	74
Figure 40: Plot of Wolseley log returns.....	75
Figure 41: Plot of Wolseley log returns ("zoomed" in over period where both have records).....	75
Figure 42: Plot of the autocorrelation function - Bishopscourt.....	77
Figure 43: Plot of the partial autocorrelation function – Bishopscourt.....	78
Figure 44: Plot of the cross-correlation function – Bishopscourt	79
Figure 45: Plot of the autocorrelation function - Tokai	80
Figure 46: Plot of the partial autocorrelation function – Tokai	81
Figure 47: Plot of cross-correlation function – Tokai.....	82
Figure 48: Periodogram, smoothed with Parzen filter, of width chronology – Tokai	83
Figure 49: Plot of the spectral analysis, smoothed with Parzen filter, of width chronology – Tokai	84

Figure 50: Plots of autocorrelation and partial autocorrelation function - Tokai (logged)	85
Figure 51: Plot of cross-correlation function – Tokai (logged).....	86
Figure 52: Plot of autocorrelation function – Wolseley.....	87
Figure 53: Plot of partial autocorrelation function – Wolseley	88
Figure 54: Plot of cross-correlation function – Wolseley.....	89
Figure 55: Periodogram, smoothed with Parzen filter, on width chronology – Wolseley	90
Figure 56: Plots of the autocorrelation and partial autocorrelation functions – Die Bos	95
Figure 57: Plot of cross-correlogram - Die Bos	96

List of Tables

Table 1: Summary of sample species and locations	51
Table 2: Summary of average GLKs for selected chronologies	60
Table 3: TSAP-Win calculated optimised regression parameters	64
Table 4: Results of moving average and rainfall record correlations per location	72
Table 5: Summary of ADF results	73
Table 6: Results of log return of width and rainfall record correlations, per location	75
Table 7: Summary of Bishopscourt ARMA model results	91
Table 8: Summary of Tokai ARMA model results - original	92
Table 9: Summary of Tokai ARMA results - logged	93
Table 10: Summary of Wolseley least squares regression results	93
Table 11: Summary of Die Bos ARMA results	97
Table 12: Substitution values for historic extension	98
Table 13: Calculation of growth estimation error	98
Table 14: Summary of results	100
Table A1: Raw ring measurements - Bishopscourt	113
Table A2: Raw ring measurements - Tokai	116
Table A3: Raw ring measurements - Wolseley	119
Table A4: TSAP-Win results - Bishopscourt	123
Table A5: TSAP-Win results - Tokai	126
Table A6: TSAP-Win results - Wolseley	129
Table A7: Log-returned data – Bishopscourt	133
Table A8: Log-returned data – Tokai	136
Table A9: Log-returned data – Wolseley	139
Table B1: Autocorrelation function results from <i>Statistica</i> – Bishopscourt	143
Table B2: Partial autocorrelation function results from <i>Statistica</i> – Bishopscourt	144
Table B3: Autocorrelation function results from <i>Statistica</i> – Wolseley	145
Table B4: Partial autocorrelation function results from <i>Statistica</i> – Wolseley	146
Table B5: <i>EViews</i> regression results - Bishopscourt	147
Table B6: <i>EViews</i> regression results – Tokai	147
Table B7: <i>EViews</i> regression results – Tokai (logged)	148
Table B8: <i>EViews</i> regression results – Wolseley	148
Table B9: <i>Eviews</i> regression results – Die Bos	148
Table B10: <i>EViews</i> ARMA results - Bishopscourt	149
Table B11: <i>EViews</i> ARMA results – Tokai	149
Table B12: <i>EViews</i> ARMA results – Tokai (logged)	151
Table B13: <i>EViews</i> ARMA results – Die Bos	152

List of Acronyms

ACF	Autocorrelation Function
ADF	Augmented Dickey-Fuller (Test)
AR	Autoregressive Process
ARMA	Autoregressive Moving Average Process
DAFF	Department of Agriculture, Forestry and Fisheries (South Africa)
ENSO	El Niño Southern Oscillation
GLK	Gleichläufigkeit
ITRDB	International Tree Ring Database
MA	Moving Average Process
PACF	Partial Autocorrelation Function
SST	Sea Surface Temperature
WK	Waldkante

Glossary

Cross-dating	The process of comparing a recorded set of widths against a well-validated and dated chronology from the region to minimise the effect of error and flaws within the recorded data set
Dendrochronology	The science of dating objects or events using the patterns within the annual growth rings of a tree
Dendroclimatology	Sub-science of dendrochronology, which uses annual growth ring patterns to identify climatic events/circumstances and extend (or reconstruct) relevant climatic records
Limiting factor	A factor, such as soil nutrients or amount of rainfall, which can strongly influence, and thus limit, tree growth
Standardisation	The process of removing persistent trends, such as age, to isolate climatic variables to generate a stationary, climatically dominated ring series

1. Introduction

The objective of this chapter is to introduce the research undertaken through a brief description of the background, as well as the research's objectives and limitations.

1.1 Background

Water security and reliability of supply, for both agricultural and domestic means, remains a pressing issue globally. South Africa is a particularly water-scarce country with a rapidly growing population with a diverse set of social and economic issues aside from issues relating to water surety and quality (Dennis & Dennis, 2012). Compounding these obstacles is the threat to water resources posed by climate change, with literature supposing that the South African climate landscape is expected to get hotter and drier in the coming years (Easterling, et al., 2000; Mason, 2001; Donat, et al., 2013; Jury, 2018). The Intergovernmental Panel of Climate Change's (IPCC) CMIP5 climate change model predicts that areas of South Africa – particularly the Western Cape – will be drier as soon as 2030 (Applied Centre for Climate and Earth Systems Studies, 2017), which corroborates with the reality faced by South Africans when considering the recent plight of the Western Cape's "Day Zero" crisis.

Associated with increasing temperatures is also prolonged dry-spells or severe droughts. Severe droughts do not only affect South Africa households' domestic use, but also consequently result in reduced yields of crops – particularly for life-sustaining crops such as maize and export crops (Cane, et al., 1994; Benhin, 2006; Ortegren, 2008). An understanding of what drives these climatic conditions, as well as confirmation of any inherent climatic cycles or seasonal patterns, is thus vital to ensuring better management and use of the limited water resources South Africans do have access to.

There have been previous studies completed examining the influence of climatic variables such as the El Niño Southern Oscillation (ENSO) and sea surface temperatures (SSTs) on South African temperatures and rainfall variability. Short climate records remain an issue as many of South Africa's recording stations, gauges and measures have fallen into disrepair thereby limiting the sources of accurate data for analysis (Therrell, et al., 2006) – which is crucial to develop accurate robust and predictive models, and for identification of any cyclicity or seasonality within the climate.

Additionally, most instrumental environmental records, however, are generally limited to a range of 150 years and thus cannot accurately record the vast range of variability found within the Earth's natural processes (Black, et al., 2016). It thus falls upon state bodies, water resource professionals and academic institutions to derive the means to generate and analyse significantly longer records in the hope of identifying natural cycles and seasonality, as well as extremes and other key climatic characteristics. Of such methods, the use of proxies for climatic records has been successfully used in various locations across the globe – with the use of tree rings being a particularly useful proxy for temperature and rainfall, capable of generating rainfall reconstructions for upwards of thousands of years (given that the tree samples are old enough) (Diaz, et al., 2001; Shao, et al., 2005; Yang, et al., 2014). As such, as posited by Gebrekirstos et al. (2014), using tree rings as a proxy for constructing and extending rainfall records may thus hold boundless opportunities within South Africa, helping contextualise and supplement the existing records and providing indication of the climate in regions where records are not freely available.

1.2 Problem Statement

As highlighted in section 1.1, it is imperative that a clearer understanding of South Africa's climatic behaviour be achieved for more accurate and robust predictive models, in addition for the use of the planning, development and management of water resources. The main question posed in this study is thus:

Can a Western Cape regional rainfall record be extended, with climatic behaviours highlighted, through dendroclimatology/the use of annual growth rings of trees within the same region?

1.3 Research Objectives

This research aims to quantify any potential correlation found between the annual growth rings of alien trees found within the Western Cape province of South Africa and the regional rainfall. With a successful correlation, this research could then deliver comments on any cyclicity or seasonality found within the Western Cape's annual rainfall. Successful identification of cyclicity, seasonality or even noticeable characteristics within a rainfall record will support the extension of rainfall records, the development of predictive models, as well as decision-making, planning and management of water resources for both domestic and agricultural purposes.

The core objective is thus quantifying the correlation (if any) between rainfall and tree growth, which, if successful, can then be used to better understand any cyclicity, seasonality and extreme or characteristic events within the Western Cape's climate with respect to rainfall. To achieve this objective, significant data collection, modelling and analyses are required which necessitates engaging with individuals with the requisite domain knowledge. Thus, to achieve the latter, it is necessary to understand both the forestry and statistics fields.

1.4 Research Scope and Constraints

1.4.1 Scope

This research is limited to the Western Cape and, more explicitly, to three primary locations related to where tree samples could safely and legally be obtained. These locations are:

- Tokai
- Bishopscourt
- Wolseley

These locations and relative positions are denoted by Figure 1: Relative positions of sample locations within the Western Cape:

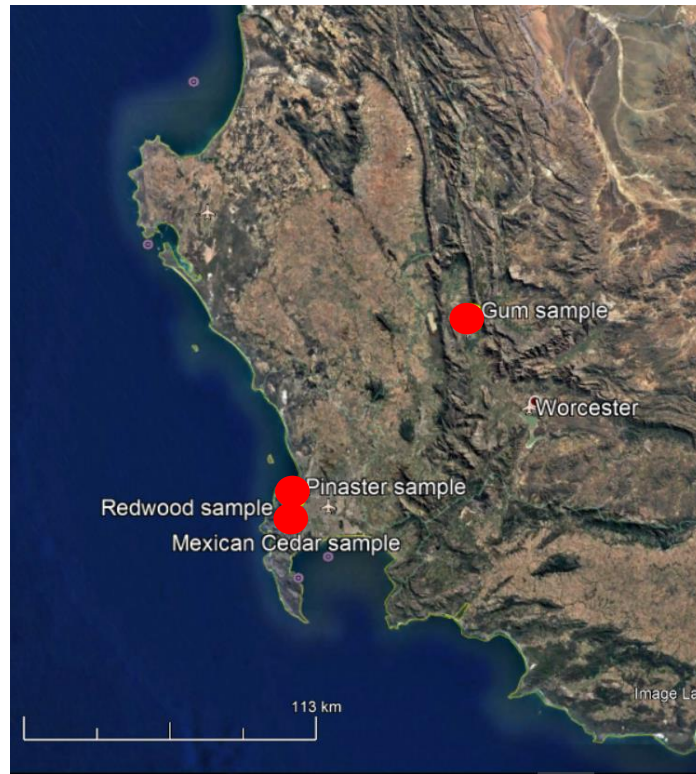


Figure 1: Relative positions of sample locations within the Western Cape (Google Earth, 2018)

Furthermore, this research aims to provide commentary on any discernible correlations and trends with respect to tree growth and rainfall, as well as on the viability of dendro-methods as a means to predict and extend records, but due to the limited number of samples a complete, statistically sound prediction and complete extension of all the records fall beyond the scope of this research – the process of extension will, however, be illustrated in full. Complete commentary on the greater Western Cape region thus, too, falls beyond the scope of this research. The nature of this research is thus more of an exploratory investigation of the potential of extending a Western Cape rainfall record by means of dendroclimatology.

1.4.2 Constraints

One of the greatest constraints was related to safely and legally obtaining the tree ring samples; tree ring samples were provided by the University of Stellenbosch's Department of Forestry and Wood Science.

For the research to be significant, tree ring samples had to be old enough (or at least longer than rainfall records for the region) so that the correlation could be validated and that the results could actively extend the rainfall record. As such, trees older than 100 years were ideal although indigenous species of such a great age are not only uncommon, due in part to the mass felling of trees across the Western Cape, and greater South Africa, for expansion during and post-colonial era (Department of Agriculture, Forestry and Fisheries, 2014) but also as most indigenous trees are protected by the South African legislation under the National Forests Act of 1998 (South African Department of Agriculture, Forestry and Fisheries, 2011). Furthermore, many indigenous and alien trees which are of a significant age (100 or older) have been declared "Champion" trees (South African Department of Agriculture, Forestry and Fisheries, 2016), rendering the possibility of obtaining core samples a near-impossible task. This research is thus constrained to alien (exotic) species which could legally be cored or felled without the additional task of

obtaining a permit or subject to external approvals.

Another constraint to the research was the limited field of knowledge, techniques and equipment available within the Western Cape. Fortunately, the Department of Forestry and Wood Science at the University of Stellenbosch could provide the standard ring recording and chronology constructing equipment from Rinntech, namely the Lintab and TSAP-Win suite. The most significant constraint to this research, however, was the limited number of samples available which makes robust data analysis and conclusions a challenge.

1.5 Research methodology

To quantify if there is any correlation between Western Cape rainfall records and tree growth the following steps were identified for execution:

1. A comprehensive literature review pertaining to the following:
 - a. Definition of dendrology and its associated branches (dendrochronology and dendroclimatology)
 - b. Definition of trees and their growth, inclusive of drivers of growth, dominating factors and defects
 - c. Definition of the dendro-process, inclusive of its principle concepts and techniques
 - d. Clarification on how samples are obtained and processed
 - e. Clarification of analysis techniques, which includes statistical time series analyses
 - f. Discussion on previous studies completed both within South Africa and the broader continent
 - g. Definition of the broader South African and Western Cape climate
2. Define, within the methodology, the process undertaken for:
 - a. Obtaining the growth ring data (including obtaining the tree samples)
 - b. Obtaining the annual rainfall data
 - c. Processing the growth ring data
 - d. Processing the annual rainfall data
 - e. Comparing, correlating and analysing both the growth ring and annual rainfall data
3. Obtain the samples and rainfall data, as well as construct the annual growth ring width chronologies
4. Analyse both the annual growth ring width chronologies and rainfall datasets, seeking any characteristic events within the dataset only
5. Investigate correlation between tree growth and rainfall by evaluating the correlation between the datasets
6. Critically evaluate the results and provide possible, contextual commentary on the results
7. Critically evaluate the usefulness of this research and provide recommendations for future work

Once the necessary literature has been reviewed, and the requisite understanding and concepts clarified, the data capture and analysis can be completed. The rainfall data was not explicitly captured as the annual rainfall was obtained from the South African Department of Water and Sanitation's rainfall record database as well as from the National Centre of Atmospheric Research's rainfall record database. The tree ring samples were obtained with assistance from the University of Stellenbosch's Department of Forestry and Wood Science, and the annual ring width variations were recorded by means of a Rinntech Lintab and TSAP-Win suite, also provided by the Department of Forestry and Wood Science.

These datasets, which are essentially time series, are then evaluated for cyclicity, seasonality and characteristic events in addition to quantifying the correlation between the rainfall and tree growth. The analysis is primarily done by means of statistical methods for time series analysis, with the chosen analysis techniques being the use of log-returns, regression by least squares, and ARMA models which were completed in Microsoft *Excel*, TIBCO *Statistica* and *EViews*.

Following the statistical analyses, recommendations and comments can be made with respect to the viability of using dendroclimatological methods as a means to extend or as a proxy for rainfall records in the Western Cape. Comments can also be made on the appropriateness of such techniques and the climatological patterns seen within the Western Cape. Should a significant correlation be found, of which the level of what is significant has been defined through the literature review, the rainfall record may also then be extended, and a longer period of climatological data may be available for evaluation.

1.6 Document Outline

This report is structured as follows:

Chapter 1: Introduction

Chapter 2: Literature Review

Chapter 3: Methodology

Chapter 4: Results

Chapter 5: Recommendations

Chapter 6: Summary and Conclusions

2. Literature Review

Presented in this chapter is more detail on the concepts required to successfully complete dendroclimatological, time series-based analyses. The chapter includes a discussion on the origin and procedure of dendroclimatological analyses as well as statistical methods that can be used to analyse time series. Additionally, the definition of the classification of trees as well as the drivers of tree ring development is also defined in this chapter. Lastly, this chapter also defines the drivers of Western Cape climate and the average precipitation experienced in the study locations.

2.1 Definition of Dendrology and Dendrochronology

Dendrochronology and associated dendroclimatology are both derived from the general study of trees known as dendrology. Within the scope of dendrology, trees are defined as being unique from other woody plants such as shrubs – in quantitative terms, a tree is defined as a woody plant that, when mature, is larger than 6 metres (20 feet) with a single trunk, unbranched for several metres above the ground, and has a reasonably defined crown (Harlow, et al., 1978).

Dendrochronology, the origins of which are discussed in greater detail in the succeeding section, is the more specific study of the aging of trees and how the age reflected in a tree's growth rings can be used to date artefacts or create historical time series. These time series can be used for a multitude of purposes – one of which is evaluating environmental and climatic patterns, which is the purpose of dendroclimatology.

2.1.1 History of dendrochronology

Formally pioneered by Andrew. E. Douglass, an astronomer at the Arizonan Lowell Observatory interested in solar cycles and sunspots, in the early 20th century, dendrochronology is the technique of dating artefacts and environmental change with the patterns of annual growth rings of living trees and timber products (Robinson, 1989). Whilst Douglass' now standard cross-dating technique was first employed in his 1911 dendrochronological study in Flagstaff, Arizona, the concept of dendrochronology was hardly new – the potential cross-correlation of separate samples' ring widths was first mentioned in an 1827 by Alexander C. Twining, whilst the notion that annual growth rings could reflect climatic history was postulated as early as the 1500s by famed polymath Leonardo da Vinci (Fritts, 1976).

Following on the observations of the annual nature of tree ring growth made by Aristotle's student Theophrastus of Erusus in 300 B.C., Leonardo da Vinci noted that "rings in the branches of sawed trees show the number of years and, according to their thickness, the years which were more or less dry" (University of Arizona, n.d.). Over two centuries later, in 1737, the next bout of interest in dendrochronology and its applications arose following investigations into the "inequality in [ring] thickness" by French academics Henri-Louis Duhamel du Monceau and the Comte de Buffon which was then succeeded by Twining in 1827, English mathematician Charles Babbage in 1838 and German forester Jacob Kuechler in 1859 (Fritts, 1976).

Following formulating the more formal and academic definition of dendrochronology, Douglass, the "father of dendrochronology" (Fritts, 1976), established the first focused research centre – namely the University of Arizona Laboratory of Tree Ring Research. Established in 1937, Douglass' laboratory currently

boasts one of the largest sample archives with approximately 2 million wood research samples and their associated records, as well as facilities and equipment that support carbon dating, X-ray densitometry and physical sample processing (University of Arizona Laboratory of Tree Ring Research , 2018). The laboratory was also instrumental in helping establish the International Tree Ring Data Bank (ITRDB), which holds approximately 4250 data sets from 66 countries across 6 continents (US National Centre for Environmental Information, 2018). Datasets stored in the ITRDB are regularly updated and includes information of the tree ring study including the investigator name, study title, location coordinates and tree species sampled.

2.2 Definition of Trees

The growth of a tree is dependent on a multitude of limiting factors, both internal and external. The intensity of the effect of internal limiting factors, however, is often related to some external factor which was dominating at a point in time (Fritts, 1976).

As dendroclimatology works with the annual growth rings of trees, defining some of the limiting factors is important as it will aid with identifying their effects in the samples. For example, periods of stress often result in missing rings or multiple rings growing in one period (if growth was disrupted) which can affect the integrity of a sample. However, before the limiting factors can be discussed, a general overview of the anatomy of trees and their growth must be defined; this can be found in the following sections.

2.2.1 Characteristics of a tree

Holistically, a tree is comprised of its roots, stem or trunk and crown, as illustrated by Figure 2.

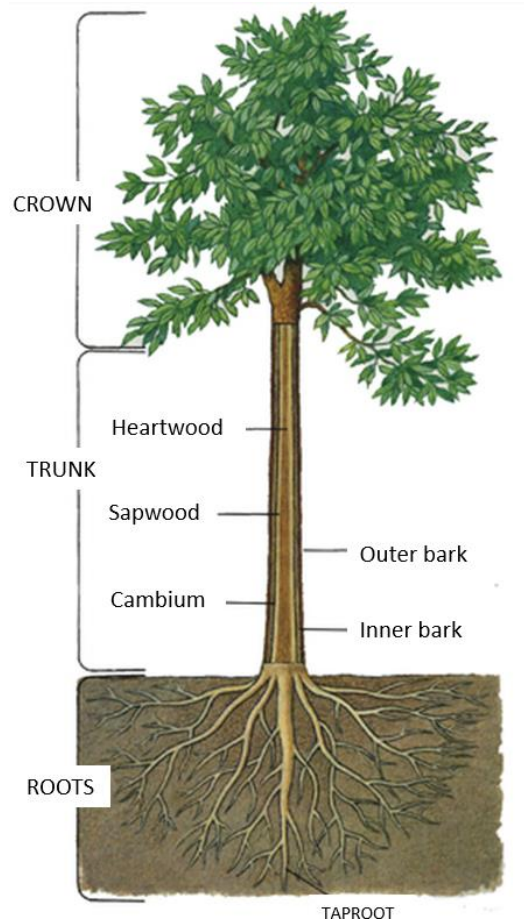


Figure 2: Components of a tree (6enders, 2018)

The roots support the uptake of water and nutrients, which supports the growth and development of a tree as well as providing structural stability for the tree. The depth of the root system of a tree is, however, dependent on the species. The upper reaches and leaves of the crown provide shade as well as expose the leaves to the sun and other climatic variables to support photosynthesis and evapotranspiration (North Carolina Forestry Association, 2018).

The trunk of a tree comprises of sub-elements, namely the outer bark which protects the xylem (sapwood), cambium, inner phloem and heartwood. The bark protects the more delicate structures found within and is formed from older phloem cells. The phloem, found beneath bark but above the cambium, supports the transportation of nutrients to the crown's leaves through the form of sap (North Carolina Forestry Association, 2018).

The expansion of a tree's width largely occurs in the cambium due to meristematic activity occurring within this region. The cambium is a sheathing and cylindrical meristem found between the stem, branches and major roots' xylem (woody part of the tree) and phloem (just outside the cambium). A typical cross-section of tree's stem is illustrated in Figure 3, where the pith is the centre of the tree and the woody exterior is identified as the bark. The cambium, visible only through a microscope, lies between the dark banded phloem and the woody xylem.

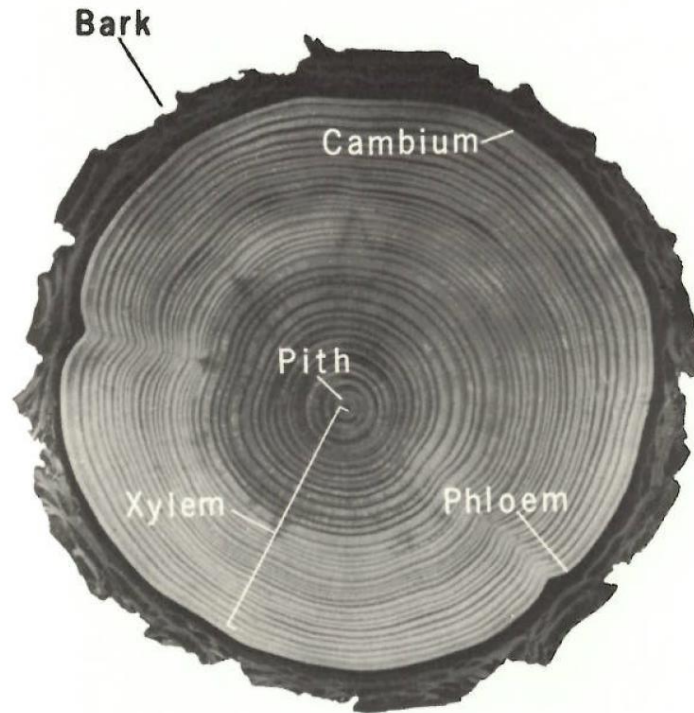


Figure 3: Cross-section of a typical tree's stem (Stokes & Smiley, 1968)

One of the main activities that occurs within the cambium is cell division, which results in either the production of secondary xylem and phloem (additive tangential division) or the increase in the cambium's circumference (multiplicative radial division). It has been shown that in temperate zones, where there is a distinctive growth period within a year, the cambial activity is "strongly periodic" (Lilly, 1977). The additive division that occurs in the cambium of trees from temperate zones following winter dormancy allows the newly formed annual xylem and phloem increments to be inserted between old layers - which results in the thickening of the stem, branches and major roots (Kozłowski, 1971). Trees in temperate zones thus typically form one growth ring a year (Schweingruber, 1988).

The growth ring thus constitutes the cells formed during the entire growing season, however the period in which the cells that forms dictates the size and form of these cells. The change in size between the cells formed in the beginning and end of the growth period results in a border that allows annual growth rings to be visible without the aid of a microscope's magnification whilst additional structures, such as resin ducts or rays, may only be visible with microscopic magnification (Stokes & Smiley, 1968). The different sized cells which form the respective borders of the annual growth ring are known as early- and latewood (as per their growth period). A typical gymnosperm (which is more clearly defined in section 2.2.2) cross-section demarcating an annual growth ring within such cell borders is shown in Figure 4.

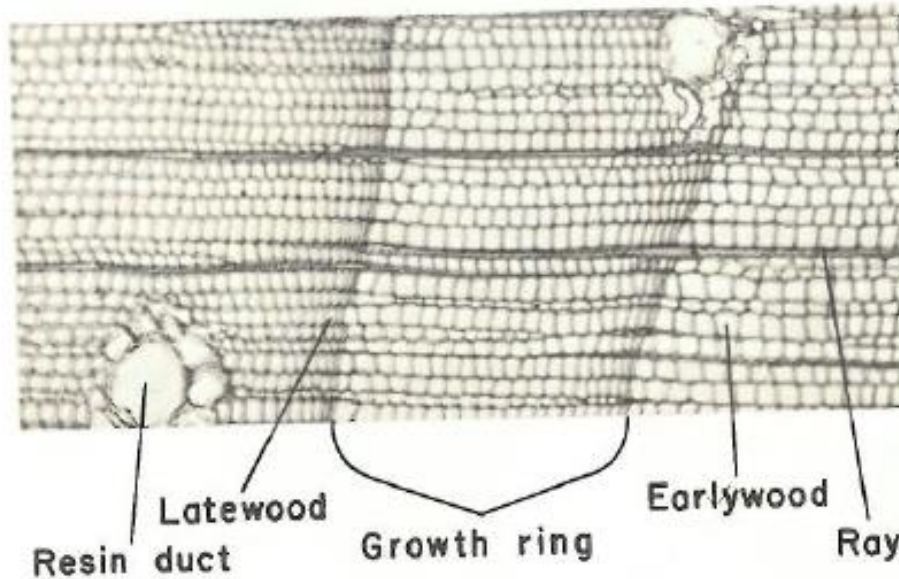


Figure 4: Typical cross-section of a gymnosperm delineating the early- and latewood borders and annual growth ring (Stokes & Smiley, 1968)

Earlywood, by definition, is low density wood, which is produced during the early season of growth, whilst latewood is defined as being the higher density wood which is produced in the later portion of the growing season. The boundary between the early- and latewood of a sample can be gradual or very distinct and sharp, as illustrated by Figure 5 where the larger, thin-walled cells form part of the earlywood and the smaller, thick-walled cells form the latewood (Kozlowski, 1971).

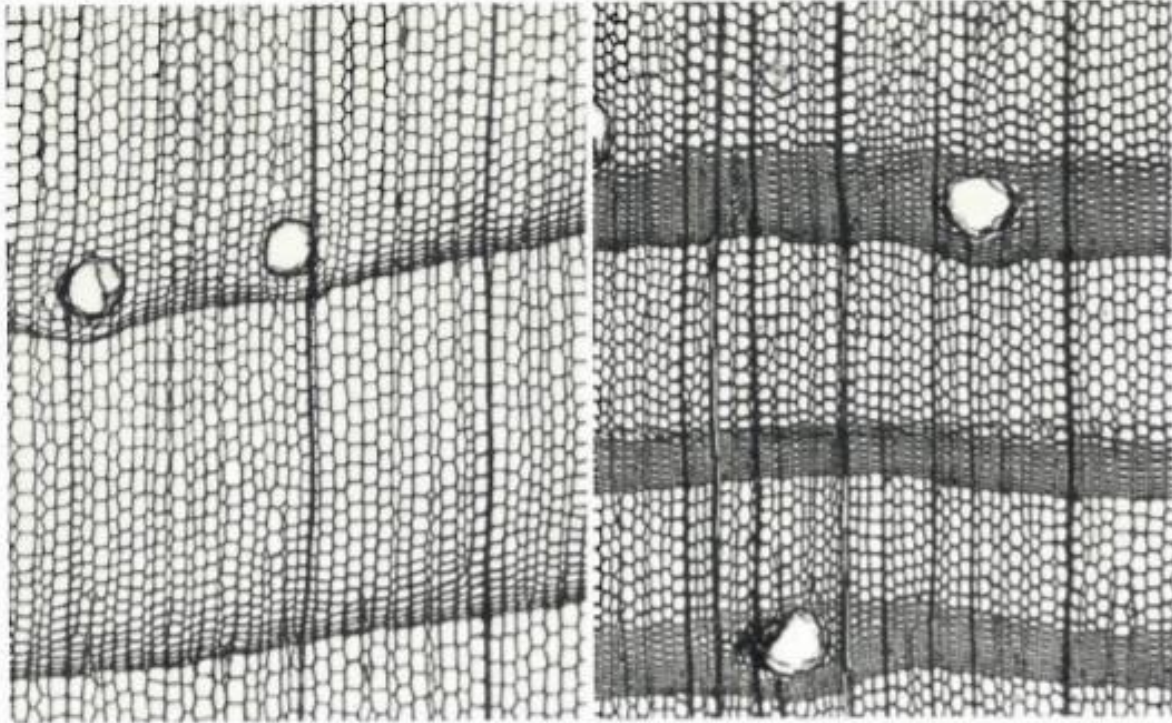


Figure 5: From left to right; gradual early-to-latewood transition vs sharp early-to-latewood transition in gymnosperms (Kozlowski, 1971)

As per Kozlowski (1962), latewood production is influenced by both internal and external (environmental) factors, where water supply often has a distinct effect on the production of the latewood. The relationship between latewood production and water supply has, in fact, been the subject of many investigations – some as early as 1899 (Schwarz, 1899) – where it has been proven that irrigation schemes and water surety increase the amount of latewood produced whilst (summer) drought periods have resulted in less latewood. Dobbs (1953) further noted that rainfall after a drought period results in the formation of thick-walled cells that appear as distinct lines on the cross-section. As water stress causes cell walls to shrink and thicken, the latewood bands of a tree experiencing water stress tend to be narrower than trees with ample water supplies (Fritts, 1976).

2.2.2 Classification of trees

As per collaborative research conducted in 2017, there are 60 065 unique tree species across the globe (Beech, Rivers, Oldfield & Smith, 2017) – each of which can also be more broadly classified as being a gymnosperm or angiosperm. Whilst the more general terminology, such as early- and latewood, is common to both the definition of such terms is dependent on the classification of the tree.

Gymnosperms, more commonly known as softwoods or evergreens, are unisexual trees that have distinctive “needles” or “scales” as leaves with their reproductive seeds stored in conical structures that are transferred only through mechanical actions such as wind. These ancient trees first appeared during the Carboniferous era, approximately 359 to 299 million years ago, and can be sub-classified in four groups namely *Coniferophyta* (conifers such as *Pinus*), *Gnetophyta* (*Welwitschia* and *Ephedra*), *Gingkoophyta* (*Gingko*) and *Cycadophyta* (cycads) (Biology Dictionary Editors, 2017).

Angiosperms, typically referred to as hardwood or deciduous trees, are flower-bearing trees which house their reproductive seeds within its fruits. Most like the *Gnetophyta* sub-class due to the shared presence of xylem tissue, angiosperms transfer their pollen through both mechanical actions like wind as well as vectors such as birds and insects – thus making angiosperms the more reproductively successful, which in turn lead to angiosperms becoming the dominant species over the ancient gymnosperm after the Mesozoic era, approximately 251 to 65.5 million years ago. As of 2017, it is estimated that of all flora on earth, 80% can be classified as angiosperms (Biology Dictionary Editors, 2017). Angiosperms come in a range of sizes, from small shrub-like trees to those exceeding 90 metres in height, and also have a range of life cycles with some angiosperms completing their lifecycles within weeks or even a single year (known as annuals) (Harlow, et al., 1978).

When comparing the anatomical structure of trees within these classifications, most of the anatomical differences arise in their respective reproductive structures, however there are some differences within the wood of the trees themselves. Gymnosperms are commonly known as softwoods due to the multiple vertical and horizontal resin canals that exist within the wood and bark tissue. These resin canals protect the tree from fungal infection as the resin will fill any wound hole within the wood or bark (Schweingruber, 1993). Gymnosperms also have tracheids and medullary rays which support the transport of water and production of sap, as well as supporting the regularity of the radial rows of cells that develop during growth meaning that when viewed under a microscope there are no visible pores – which results in growth rings being more clearly delineated when compared with the cross-section of an angiosperm (Schweingruber, 1993). Gymnosperm xylem is also more uniform, which is indicative of the fact that changes in the cell wall thickness (and thus ring thickness) are more closely correlated with any changes in xylem density, whereas angiosperms' changes in xylem density is dictated by the proportion of cell types present (which in turn is related to species and season) in addition to the thickness of the cell wall (Kozlowski, 1971).

Figure 6 is the labelled transverse cross-sectional comparison of gymnosperms and angiosperms, highlighting the porous appearance of angiosperms as well as demarcating both the early- and latewood borders (growth margins).

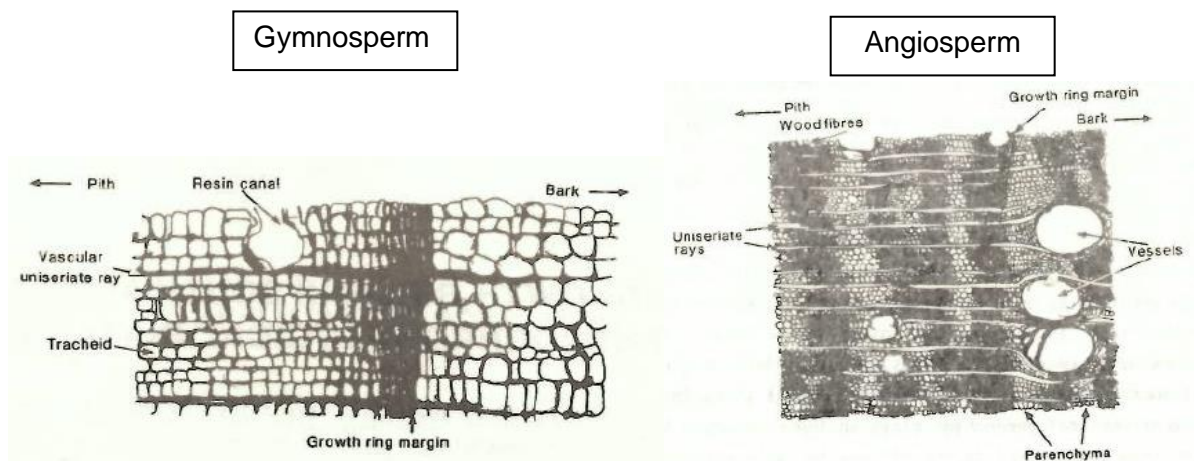


Figure 6: Cross-sectional comparison of gymnosperm (*Pinus resinosa*) & angiosperm (*Pterocarpus angolensis*) (Lilly, 1977)

Figure 6 illustrates the longitudinal vessels which appear as pores in angiosperms making the rings of angiosperms less uniform and thus harder to use in dendrochronological analyses than the clear division of a gymnosperm, as the “pores” distort the radial alignment of the cells within the cambium (Lilly, 1977).

2.2.3 Growth behaviour

Whilst cambial growth is largely generic as it is regulated by the transfer of products that have been synthesised in the crown, particularly hormonal growth regulators and carbohydrates, cambial activity is variable. There is thus always the possibility for variations in the annual growth rings of any sample.

The expansion of total leaf areas, which relate to the supply of hormones and carbohydrates, are often related to the weather of the previous year. As researchers have previously established, it is thus evident that the weather of the previous and current year affects the cambial growth although an “abrupt change” in the environment does not affect all the trees within a stand in the same manner as trees within a stand may differ in the physical (crown size, root depth, exposure) and inherent growth characteristics (Kozlowski, 1971).

As cambial growth is largely regulated by product transfer the increment of annual xylem is generally influenced by the physiology of the crown in a reasonably predictable manner based on the species. The distribution of the crown, its leaves’ metabolic activity and surfaces are, however, directly impacted by environmental variations, site characteristics, competition (Schweingruber, 1993) and extreme occurrences such as wildfires or premature defoliation (Kozlowski, 1971). Environmental variations which affect cambial growth pertain to the supply of light, minerals and water in addition to the temperature, soil properties and composition of the environment (Kozlowski, 1971). Thus, as per Fritts (1976), the four main factors which bear the greatest limiting factor on cambial growth are:

1. Concentration of growth regulators
2. Amount of “food” (carbohydrates) and mineral salts
3. Water availability and stress within the tissue
4. Temperature of growing tissue

Trees which are subject to stress due to a lack, or surplus, of any of these limiting factors have been proven to have localised effects resulting in physical defects such as missing, multiple or discontinuous growth rings. Additionally, other abiotic factors such as exposure to wind or snow, and soil stability also impact the uniformity of annual growth rings (Schweingruber, 1993) and also have been known to cause physical defects such as reaction wood or wedged rings.

Furthermore, xylem production is also noted to be variable in thickness and structure at different heights or sides of a tree and thus, whilst it is true that the cambial activity is largely generic, it would be a gross assumption that a single sample from a single tree is representative of the whole tree’s growth. It is thus essential that for a chosen tree, multiple cores should be taken to generate a more accurate representation of a tree’s growth behaviour (Kozlowski, 1971). The succeeding section (2.2.3.1) defines the possible physical defects and effects of limiting factors in greater detail.

2.2.3.1 Variations in growth behaviour

This subsection defines some of the commonly occurring physical defects of annual growth rings in greater depth.

2.2.3.1.1 Missing rings

Growth rings may be “missing” during certain periods of scarcity or due to the species’ growth behaviours, such as *Pinus palustris* which only begins developing growth rings and increasing in height approximately 15 years after first sprouting (Kozlowski, 1971). Fritts (1965) determined that periods of water stress particularly effect the growth of xylem rings, with semi-arid conditions resulting in noticeable increases in the number of missing xylem rings. Missing rings are problematic for readings as they might invalidate the statistical results of a study (Schweingruber, 1988).

2.2.3.1.2 False and multiple rings

As the cambium is very responsive to variations in the environment, particularly variations related to water supplies (such as water shortages), the cambium’s growth is not uniform. Due to environmental conditions, such as droughts and associated drought recovery, the cambium can grow multiple times in short bursts within one year meaning there will be multiple “false” rings occurring within one calendar period (Phipps, 1985). Typically, only one ring is duplicated in such conditions (i.e. only two rings for one period rather than one) although more repetitions are possible. False rings in gymnosperms are usually identifiable by their relatively indistinct and gradual early- to latewood transition in addition to the presence of a narrow latewood section close to a thicker latewood section which demarcates the actual annual growth ring border (Kozlowski, 1971). As for angiosperms, according to Vasiljevic (1955) the diameters of vessels within are typically narrower than the vessels found within a typical gymnosperm growth ring.

Furthermore, according to Tingley (1936), injury to a tree caused by fungi, insects or fire is also known to result in multiple rings, whilst heavy fruiting in angiosperms may result in multiple growth rings. False rings are problematic for dendrochronology, as the number and thickness of the rings are used for dating and modelling purposes, respectively.

2.2.3.1.3 Discontinuous and partial rings

Discontinuities are defined by annual growth rings missing from some of the samples’ radii but appearing at the same relative age on radii taken at a different orientation (though at the same height) (Phipps, 1985). In cross-sections it is thus visible as an incomplete ring, as illustrated by Figure 7, where the xylem ring appears to run into the older growth ring – which is why discontinuous rings are occasionally also known as “wedging rings”.

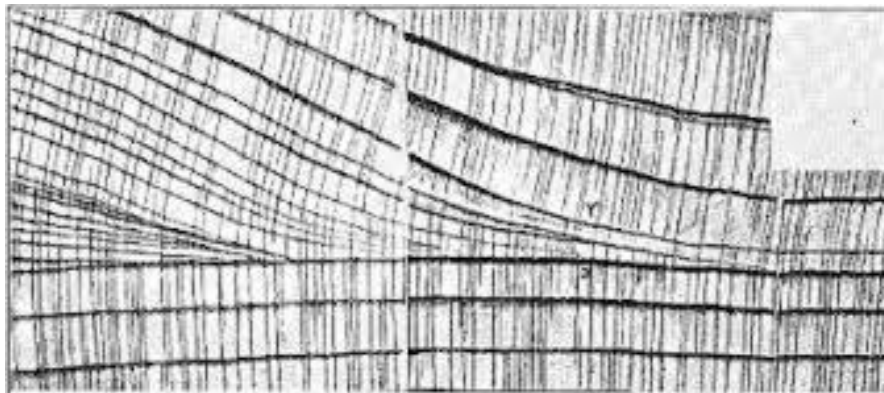


Figure 7: Discontinuous rings ("wedging rings") seen in *Sequoia sempervirens* (Fritz & Averill, 1924)

Discontinuous rings occur when the annual growth occurs unevenly across the tree, as is common for trees which have been defoliated, grow in arid regions or for which growth has been suppressed. For more

tropical regions, however, ring wedging has been found in trees which experience high levels of competition and little sunlight (Worbes, 2002). It is thus recommended that, when possible, samples should be taken at greater heights as discontinuities, whilst uncommon, are more likely at the base of a tree as one-sided dormancy in the cambium is more pronounced due to the downward transfer of growth hormones (Kozlowski, 1971).

2.2.3.1.4 Miscellaneous physical defects

Another “defect” that may be present in cross-sections and negatively impact the ability to accurately analyse the sample includes reaction wood. Reaction wood typically forms as a physical response to a tree being inclined or leaning and is known as compression wood in gymnosperms and tension wood in angiosperms (Kozlowski, 1971). This eccentric growth and presence of compression wood is illustrated for various inclinations in Figure 8:

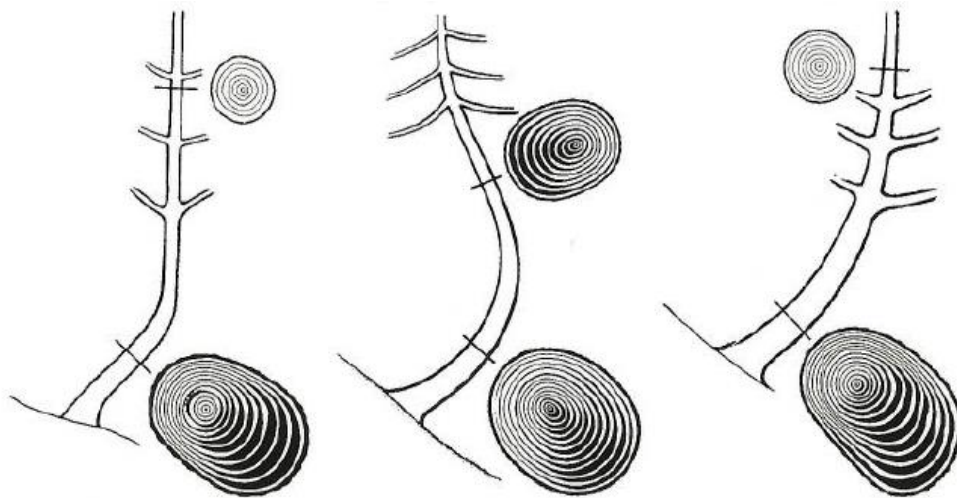


Figure 8: Formation of compression wood due to inclination (Schweingruber, 1971)

Lastly, changes to the environment in which trees grow is also known to affect the cambial growth, however the effects are not necessarily consistent across the entire tree resulting in the growth appearing defective. The effects are also different for different periods of growth, thus making it difficult to attribute a singular event to a particular defect, and generalise, without knowing the complete growth behaviour as the internal controls involved in cambial growth variate for the growth stages (Kozlowski, 1971).

2.3 The Dendro-process

The annual growth rings of trees are often seen as the direct manifestation of a tree’s growth cycles, which incorporates both the growth periods (e.g. spring and summer) and the dormant periods. However, as mentioned in section 2.2.3, the environment is not the only factor which impacts cambial growth, but annual growth rings do provide a climatological history when a suitable sample is analysed (Phipps, 1985).

To account for all the possible defects in the dataset due to the environmental or internal stress, nine dendrochronological principles were defined by Fritts (1976) in his seminal work “Tree Rings and Climate”. The succeeding subsection (2.3.1) defines these principles, upon which all calculation and processing is based, in depth.

2.3.1 Principles of dendrochronology

The following subsections define the core principles of dendrochronology in depth.

2.3.1.1 Uniformitarian

Conceptually, the uniformitarian principle applies to any biological or physiological process which impacts a given tree's growth. According to this principle, the impact of any limiting factor which affects the aforementioned processes must be seen in other trees within the stand, and that any process which is related to environmental processes impacting the growth must have been present throughout the past (Suresh, 2012). It is thus implied that only the locality, frequency and intensity of a limiting factor may be different between two samples for this principle to be satisfied. Furthermore, all data must be verified and any extremes that occur within the data must be logically verified and represented in the post-processed, calibrated data (Fritts, 1976).

2.3.1.2 Limiting factors

As previously mentioned in section 2.2.3, there are various possible limiting factors which may affect the growth of annual rings within a tree thus influencing the thickness of the annual growth ring, the site that should be selected and the sensitivity of the sample (Fritts, 1976). The matter of site selection is, in fact, its own determining principle of dendrochronology just like sample sensitivity. Both principles are thus discussed individually in depth within their own subsections.

2.3.1.3 Ecological amplitude

An ecological amplitude is defined as the range of habitats that a species is, depending on its phenotypical hereditary factors, able to grow and reproduce within. It is thus closely related to the location of a sample and thus which limiting factor will be dominant in the growth of the tree (Fritts, 1976).

2.3.1.4 Site selection

The amount of latewood produced, as well as the clarity of the early-latewood border, are directly related to the amount of rainfall and seasonal distribution within an environment (Fritts, 1976) meaning that the environment where samples are selected also plays a role in the success of a study. Selecting the correct site also helps eliminate other variables which can contribute to growth, for example with studies that are seeking patterns in the rainfall the samples should be retrieved from areas where the trees are water stressed such as talus slopes, cliff faces and non-irrigated environments (Fritts, 1976). Competition must also be a consideration as the effects of competition on the annual growth rings tends to overshadow and skew any climatic influences thereby weakening the climatic signal. Furthermore, samples where there has been significant defoliation are considered ill-suited for dendroclimatological studies, and as such sites where defoliation has occurred due to disease or insect infestation must be avoided (Harlow, et al., 1978). It is thus evident that selecting the correct site is critical for the success of the correlation as the site must support the production of sensitive rings (Suresh, 2012).

The collective samples' sites proximity also needs to be considered when designing the study. If the study aims to provide comment on a greater region's climatic behaviour, the samples need to come from sites within reasonable proximity to one another as the further the samples stray from each other, the weaker the commonality will be between the resulting chronologies and potential climatic signals. Samples from multiple, distant sites are only able to be successfully cross-dated if there is a significantly long enough record and if there is known to be a strong climatic influence across both regions dominating the sample trees' growth – although such knowledge would render climatic study of the region somewhat redundant (Phipps, 1985).

2.3.1.5 Sensitivity

The sensitivity of a sample, which is closely linked to a sample's ability to cross-date (defined in succeeding subsection 2.3.1.1.6), is defined as the sample's ability to accurately reflect and record climatic variability

in its growth (Mathias, 2012). A highly sensitive sample is thus one where the growth behaviour strongly mirrors the regional climatic variability, resulting in a chronology that correlates well with climatic time series.

“Sensitive” trees are typically found at extreme growth sites, where growth is severely limited by temperature or moisture, resulting in the ring widths to vary greatly and accurately reflect the climatic trends over the growth period. Complacent sites are those sites with more benign temperatures and enough moisture thus reducing the noticeable variations in ring width. Examples of both a sensitive and complacent ring series is illustrated by Figure 9.

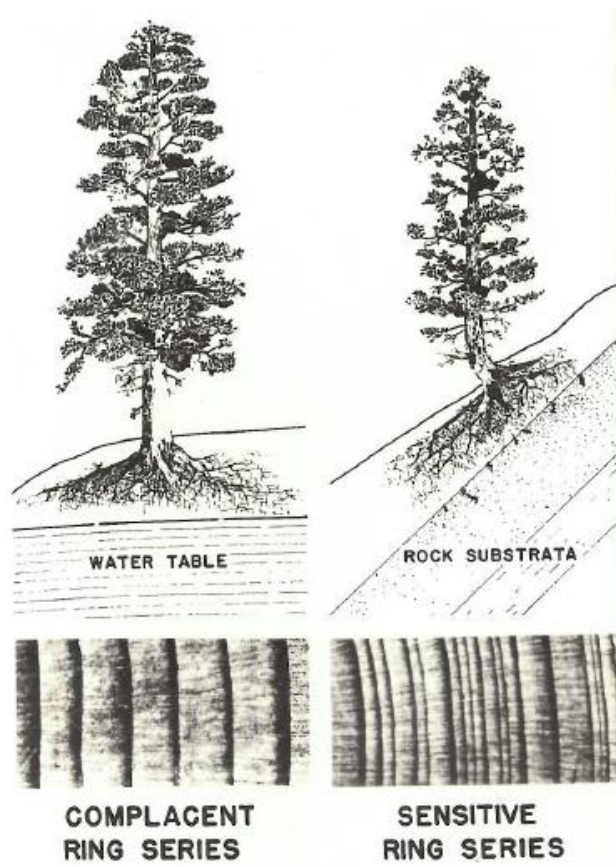


Figure 9: Sensitivity of ring series (Stokes & Smiley, 1968)

The variations in the rings, particularly from sensitive sites, will correlate over large regions that are dominated by similar climate variations; therefore, tree samples within same climatic regions can be cross-dated to make an average chronology for the climatic region (defined as the homogeneous climatic region) (Ortegren, 2008).

Sensitivity is closely linked to the two previous principles, site selection and limiting factors, as these three principles influence the decision of the others and all three minimise non-climatic influences whilst enhancing the macroclimatic components (Lilly, 1977).

2.3.1.6 Cross-dating

Cross-dating is a process of hypothesis testing and experimental control, expressly developed for dendrochronological purposes, that allows irregularities in datasets to be identified and any analysis results to be quantified and easily replicated by other researchers. The process assumes that at least one critical limiting factor is acting over a sufficiently long period and large enough area so that the factor generates a coincidental pattern, or “growth barcode”, amongst the species within the locale (Black, et al., 2016).

Simply defined, cross-dating compares the time series generated from a sample’s ring widths to a well-dated master chronology, or to other samples from the same tree or trees within the region, to ensure accurate data, free of missing rings or errors (Sheppard, 2010), however there are various ways to perform the comparison. In the case where a well-dated master chronology is not used, the resulting cross-dated chronology is known as a “floating” chronology as the age of the samples will be relative to the other samples in the study (i.e. relative dating) (Phipps, 1985).

Historically, so-called “skeleton plots” which compare only extreme values were popular as this form of comparison could easily be done by hand. This method, however, fell out of favour with the development of technology and computational power leading to approaches such as the W-statistic, product-moment correlation and graphical methods supported by software, such as TSAP-Win and COFECHA, becoming more popular (Maxwell, et al., 2011). The W-statistic approach, developed by Eckstein and Bauch (1969), relates to a percentage difference between agreements and disagreements whilst, additionally, the t-test can be used to adjust the product-moment correlation coefficient for overlap between the sample and master datasets as per Baillie and Pichler’s (1973) suggestion. TSAP-Win supports analysis through various statistics, most notably generating the Gleichläufigkeit (GLK), which is a measure of similarity between two series. All four mentioned methods, however, filter out the low frequency data found within the time series developed from the tree ring widths which is essential as it allows high-frequency, dominating climate effects to be isolated from the other processes which contribute the tree growth (such as age or soil). For dendroclimatological analyses, GLK should be a minimum of 50 to ensure complete independence although a GLK of 60 or greater indicates a highly successfully dated series. To obtain such high GLKs, however, require the master series to be a known and dated series; values above 50 are thus considered acceptable (Bretting, 2014). Removing the low frequency data is also essential to eliminating the influence of autoregression, and the consequent autocorrelation, as low frequencies are strongly linked with autoregression with low frequency variations appearing as autocorrelation (Wigley, et al., 1987).

Cross-dating also results in obtaining the absolute dates for the rings, however for cross-sectional tree samples where the date of the felling is known, the age of the terminal ring is known, making the process of obtaining an absolute date possible without cross-dating. Cross-dating will still, however, be required to remove the effects of false or missing rings as these are not always easily visually identified – especially to the untrained eye (Phipps, 1985).

When cross-dating, it is often preferred that at least two separate parties, or technicians, perform the analysis and process of cross-dating to best ensure that any defects or faults are detected thereby resulting in a more accurate resulting chronology. In the scenarios where a second human technician is not possible, the computer aided results function as a proxy to a second technician’s results when compared with visual assessments, thus ensuring accuracy even if there is only one researcher available on a study (Maxwell, et al., 2011). Additionally, care must be taken to only use samples of significant age

as juvenile samples (less than five years old) show record of different responses to climatic variance (Worbes, 2002).

2.3.1.7 Repetition

As with most scientific studies, repetition is required for validation and the maximisation of a signal by minimising noise (Suresh, 2012). For dendroclimatological studies, repetition validates the results post cross-dating and aids in the generation of an average chronology. Average chronologies are preferred for dendroclimatological studies as they tend to provide a clearer signal of potential climatic variation (Fritts, 1976).

The principle of repetition is also applied in that it is recommended that at least two samples are obtained from each tree selected for study. Multiple samples from a single tree, ideally taken perpendicularly or at different heights from each other, are preferred as a single sample is often not representative of an entire tree's growth. Additionally, the single tree can be cross-dated within itself and a more accurate result is obtained (Worbes, 2002).

2.3.1.8 Standardisation

Standardisation is the process by which climatic variables are isolated from the chronology, thereby allowing the influence of internal processes and age to be removed from the final ring width series. Standardisation thus allows younger, faster growing wood to be compared to the older wood as it also removes the autocorrelation and autoregression found within the growth process (Fritts, 1976). The process transforms nonstationary ring-widths into new stationary, relative tree-ring indices which are centred about a constant mean, often one or zero, and exhibit no linear trend (have a constant variance) (Woollons & Norton, 1990).

There are multiple methods to standardise the data, of which differencing methods and function fitting to generate residuals are both viable options. Fritts (1976) recommends using an exponential, polynomial or linear function, as per the data's requirements, whilst Monserud (1986) explicitly recommends the use of a negative exponential, multiplicative power function or a quadratic polynomial. Lastly, as per Briffa and Cook (1990), smoothing splines can also be used although the splines should be stiff in order to prevent an overestimated fit. Caution, however, must be given when using automatic detrending as automatic process are prone to removing elements of the trend data that may be considered significant in analysing the variations (Monserud, 1986; Monserud & Marshall, 2001). It is thus preferred to use simple, sparing and robust methods to ensure that only the non-climatic trends are removed without altering inherent variations (Woollons & Norton, 1990).

Once the series is standardised and stationary, stochastic processes may be used to model and analyse the chronologies and correlations further. Autoregressive (AR), moving average (MA) or combination (ARMA) process models are the most common choices for analysing the stationary residuals (Cook, 1985; Woollons & Norton, 1990; Monserud & Marshall, 2001). A more detailed discussion of these methods is presented in section 2.3.5.

2.3.1.9 Aggregate growth model

This principle is founded upon the notion that the growth of any tree is dependent on a host of factors, of which age, climate, random processes and various disturbances within both the stand and surrounds form part of. It is thus derivative upon all the preceding principles, as the growth model is developed through the incorporation of the preceding principles.

A series of standardised ring widths is thus generally regarded as a time series comprised of multiple randomly varying components that are statistically dependent upon each other due to naturally occurring

cycles or trends. The components that contribute to determining a given ring width includes the persistent age trend (A_t), exogenous disturbances within the locale (D_t), climatic environmental signals (C_t) and miscellaneous disturbances (E_t) – all of which can be approximated by a linear aggregation model created by Cook (1989):

$$R_t = A_t + C_t + \delta D1t + \delta D2t + E_t \quad \text{Equation 1}$$

From this linear equation, the age trend and noise can be removed through standardisation and calibration (as previously discussed), thus allowing climatic variables, such as temperature and precipitation, to be extrapolated from annual growth rings through statistical methods such as regression, correlation equations, and transform- and response-functions (Fritts, 1976; Cook & Kairiukstis, 1989; Speer, 2010). The ring width variation due to climatic conditions is therefore analogous to a signal whose strength relies on the sample size, sample site topography and the general sample life expectancy.

2.3.2 Obtaining samples

To complete the analyses and construct a chronology, cross-sectional or core samples where the annual growth rings are clearly visible are required. Cross-sections are, however, harder to obtain as this requires cutting from the tree or having a tree felled. For living samples, the use of an increment borer is thus more suitable, however the use of resistographs have steadily become favoured as it is less invasive than taking cores with an increment borer, as the remaining opening from sampling never exceeds 3 mm (Szewczyk, et al., 2018).

Resistographs, unlike the bulkier increment borers, make use of a needle and record the resistance of the wood against the needle to determine a sample's wood density, quality, and age. A typical resistograph is battery operated, lightweight and can drill up to depths of 50 cm; Figure 10 illustrates Rinntech's latest model resistograph, the *4452-P Resistograph* (Rinntech, 2018).



Figure 10: Rinntech 4452-P Resistograph (Rinntech, 2018)

The Swedish increment borer is still, however, commonly used in practice due to it being a cheaper equipment and more easily accessed than resistographs. Whilst the increment borer does leave a hole in

the tree, the hole is typically small enough to not cause detrimental damage to the tree – especially when proper boring procedure is followed. Based on the increment borers currently available on the market, the hole left (and thus the diameter of the core) can range between 4.3 and 12 millimetres (Haglof, 2018). When boring, the increment borer must first be fully sterilized before inserting it into the tree to avoid the spreading of unfamiliar bacteria or foreign elements into the tree. The borers are fitted with sharp cutting edges which forms part of a large, threaded double helix screw mechanism which is inserted into the tree through rotations of the shaft's handles (Schweingruber, 1988). It is recommended that the borer be lubricated, usually by organic compounds such as beeswax, as this aids the insertion of the borer and limits metal fatigue caused by friction between the borer and tree (Phipps, 1985). A typical increment borer is illustrated by Figure 11.



Figure 11: A typical Swedish increment borer (Forestry Suppliers, 2018)

Also forming part of the shaft is the extractor tray, which is used to pull the cylindrical core sample from the tree once the boring is complete. Figure 12 illustrates the core being removed via the extractor tray of the shaft:



Figure 12: Increment core being extracted from the borer (Haglof, 2018)

To obtain an adequate core sample, the borer must be angled towards the estimated pith of the tree to ensure a complete set of growth rings (Stokes & Smiley, 1996). The angle at which the branches of a tree are orientated is typically indicative of the position of the pith – particularly for conifers on hills, where the pith is often located towards the slope of the hill (Schweingruber, 1988). For dating purposes, the pith is required, and it is preferred that the sample has a defined bark end included known as a “waldkante” (WK), i.e. the terminal ring.

To support cross-dating, at least two core samples from each tree should be taken when possible. In accordance with Phipps (1985), the two cores are recommended to be taken 90° apart, at the same height and boring-angle to reduce any possible slope bias.

To remove the borer from the tree without damaging the core, the borer should be rotated counter-clockwise (opposite direction to insertion). Following this, the cores can be removed from the borer through the extractor tray and left to air dry. The cores, once dried, should be stored in tubing, like a plastic straw, to prevent further moisture or disease damaging the sample. Cores should also be labelled immediately after extraction (Schweingruber, 1988). Once all the required cores are extracted and labelled, they are prepared for analysis (Suresh, 2012).

Alternatively, ring samples can be obtained by a cut log, transversal cross-section or sourcing antique artefacts such as beams or tables that have not been heavily reworked. Logs and cross-sections are usually only obtained at active logging plantations or from invasive alien species which have been felled by conservation schemes, thus making such samples less common.

2.3.3 Preparation of samples

Preparation is required for analysis of any sample, regardless of whether the sample is a core, or partial or complete transversal cross-section. Preparation of the cores and partial transversal cross-sections is similar, where complete cross-sections are handled differently, due to their size, although the purpose for fundamental preparation processes such as sanding, buffing and smoothing, remain the same. Partial cross-sections are handled in a fashion like cores as they are similar in size and proportion as a partial cross-section is a single rectangular element cut from a complete cross-section's centre line (i.e. the partial cross section contains a portion or marker of the pith and bark).

Cores and partial sections, unlike complete cross-sections, need to be mounted for preparation and analysis purposes. The mounting for cores is typically a grooved wooden block, where each tree's set of cores is placed on a single mount which is then labelled accordingly whilst partial sections can be fixed to any wooden block long enough. To fix the samples to the mounting, the grooves are filled with wood glue (or hot glue from a glue gun) upon which the dried cores are placed with the wood grain perpendicular to the mounting block. Rubber bands, weights or clamps can be used to fix the cores in position until the glue cools or dries (Phipps, 1985).

Once mounted, the samples must be sanded down and cleaned to expose as much detail of the growth rings as possible. This step is required for all the potential sample types, being both complete cross-sections and cores. For angiosperms, slicing with a razor blade or surgical scalpel is the preferred method for exposing the rings as this prevents sawdust from entering the porous vessels typical in angiosperms (Phipps, 1985).

For the preparation of gymnosperms samples, the surface is smoothed by sanding the vertical faces to better highlight the darker latewood growth borders as the fine dust settles in the lumen of the sample. The surfaces are sanded with increasingly finely graded sandpaper, beginning at 100 and then typically moving through 200, 320, 400, and 600-grade paper before finishing with 1000 or 1200 grade paper. If the samples' rings are, however, visible during the first few rounds of sanding the surface needn't be subjected to a higher-grade sand (Schweingruber, 1988).

If partial cross-sectional samples are obtained, it is important that readings are taken along a non-eccentric face (i.e. the side without reaction wood). As discussed in section 2.2.3.1.4, trees tend to exhibit eccentric growth due to growth on inclined surfaces or external influences such as snow- or landslides (Witsuba, et al., 2013). Readings should also not be taken on samples that have distinct knots, displaced ring boundaries, reaction wood or hazel wood (Schweingruber, 1988).

Years where narrow rings are formed are referred to as "pointer years" as these are characteristic of a distinct climatic event such as a drought. A collection of successive pointer years may be referred to as a "signature" whilst a chronology with multiple signatures is "sensitive" and indicative that the tree was influenced by climatic variables (Schweingruber, 1988).

2.3.4 Reading/recording of sample data

To record the ring widths, the Department of Forest and Wood Science at the University of Stellenbosch was able to provide access to a Rinntech Lintab and TSAP-Win software. Lintab, illustrated in Figure 13, supports accurate data capture by allowing ring widths to be clearly seen beneath a microscope. The microscope, which has a resolution of 1/100 mm, allows the annual borders of the cross-sectional (or core) sample resting on the Lintab's illuminated examination table to be clearly seen with each width

being recorded by moving the examination table along, by means of the Lintab's hand crank (Figure 14), until the microscope's crosshair is aligned with the succeeding latewood border. Once the border has been identified, a foot pedal is used to record and store it in the TSAP-Win software.



Figure 13: Lintab Set-up (Rinntech, 2018)

TSAP-Win is designed to work in conjunction with Lintab and is capable of instantaneous statistical synchronization on the computer's monitor, linking to SQL databases and has a comprehensive mathematical library built into the software (Rinntech, 2018). TSAP-Win is thus capable of performing all the tasks typically undertaken in tree ring analyses, from recording the width measurements to the mathematical evaluation of the generated chronology, including standardisation through the "Math" function. For the statistics calculated by TSAP-Win, acceptable levels are defined by literature, for example the GLK associated with various confidence levels is defined by Eckstein and Bauch (1969).



Figure 14: Lintab's hand crank (Rinntech, 2018)

2.3.5 Calculation methods

As the rainfall data and the measured ring widths are considered to be analogous to chronologies, the data can additionally be analysed as time series. A time series is defined as a set of chronological observations of a quantitative characteristic, such as the widths or annual rainfall in this study, taken at regular intervals (Montgomery, et al., 2008).

Of the fundamental concepts related to time series analysis, the following were considered for the analysis of both the growth ring width- and rainfall series:

2.3.5.1 Fundamental time series concepts

2.3.5.1.1 Autoregression

Autoregression is present in time series when the series' y_t value is a function of the previous value and the related stochastic error (ε_t), represented by (Pickup, 2015) :

$$y_t = \alpha_1 y_{t-1} + \varepsilon_t \quad \text{Equation 2}$$

where:

α_1 is a constant, scaling the process y_t

2.3.5.1.2 Autocorrelation and serial correlation

Autocorrelation is defined as the correlation between sequential observations of the same sample across a significant period, or a range of time lags and defined by the following equation for a given time series, Y_t (Pickup, 2015):

$$\text{Corr}(y_t, y_{t-1}) = \frac{E((y_t - \mu_y)(y_{t-1} - \mu_y))}{E(y_t - \mu_y)^2} \quad \text{Equation 3}$$

where:

μ_y is the theoretical mean of y_t

and E denotes the expected value where $\mu_t = E(y_t)$

Autocorrelation is thus, simplistically, when a series' succeeding value is directly dependent on the preceding value - thereby violating any assumption of statistical independence. By being dependent, the presence of autocorrelation negates the results of many standard statistical tests and biases hypothesis tests, thus necessitating procedures such as standardisation or indexing to generate residuals that can better be analysed (Monserud & Marshall, 2001). Ring width chronologies which exhibit a low autocorrelation component, high mean sensitivity and strong signal (with low amounts of noise) are typically considered ideal for climatic reconstruction (Suresh, 2012); as tree ring width chronologies are typified by an autocorrelation component, the need for standardisation is, as previously discussed, essential (Wigley, et al., 1987).

Serial correlation occurs when the error term is also autocorrelated, i.e. not a white noise process with an autocorrelation of zero. To test for white noise, the Portmanteau (Q) test by Ljung and Box (1978) can be used, which is essentially a hypothesis test conducted where the null hypothesis declares a component as white noise when the sum of the errors' autocorrelations is equal to zero (Pickup, 2015). The Ljung-Box Q-test, however, exhibits poor power for sample sizes less than 100 (Monserud & Marshall, 2001).

Furthermore, the autocorrelation within the residuals of a regression analysis may be tested by means of the Durbin Watson statistic. The Durbin Watson Test is exclusively applicable to residuals of regression analyses and may have a value within the range of 0 to 4, where a value of 2 is indicative of no autocorrelation within the residual series. Values that fall below 2 are indicative of a positive autocorrelation whilst values greater than 2 are indicative of negative autocorrelations. The test statistic, d , is defined by (National Sun Yat-sen University Department of Applied Mathematics, 2018):

$$d = \frac{\sum_{i=2}^n (e_i - e_{i-1})^2}{\sum_{i=1}^n e_i^2} \quad \text{Equation 4}$$

where:

$$e_i = y_i - \hat{y}_i,$$

and y_i and \hat{y}_i are the observed and predicted values of the response variable for a given i

Thus, the closer the calculated test value is to 2, the more independent a set of residuals is from each other, thus satisfying independence requirements and supporting more accurate calculations.

2.3.5.1.3 Stationarity

A stochastic process is considered stationary when the distribution of a time series $Y_{t=1 \text{ to } t=h}$ is identical to the distribution of series $Y_{t=1+k \text{ to } h+k}$ meaning that the behaviour of the future will be similar to that of the past (Ruppert, 2014). Stationarity thus allows the parameters of all plausible distributions to be estimated from a single Y_t value, thereby circumventing the issue that stochastic processes are only capable of “displaying” one, randomly drawn, observation at a time (Pickup, 2015).

Typically, in order to analyse trends, periodicity or structural breaks, a time series needs to exhibit stationarity and, more importantly, covariance stationarity. Covariance stationarity requires that a series’ mean, variance and autocovariances are constant over time – which is often not the case without some form of standardisation (as previously discussed).

2.3.5.1.4 Periodicity, seasonality and structural breaks

Periodicity occurs when a time series’ equilibrium oscillates in a routine cycle, up and down. When the routine cycles coincide with the seasons, the periodicity is explicitly referred to as seasonality. Seasonality is removed (to create a stationary series) by explicitly lagging the dataset variables for the seasonal period considered, for example subtracting the 12th lag of every variable in a monthly dataset (Pickup, 2015). As the tree ring and rainfall chronologies are, however, annual, the lag that can be considered to offset seasonality need only be related to other known annual climatic cycles such as sunspots or solar flaring (Schlapp & Butcher, 1995; Ineson, et al., 2011).

Structural breaks can occur in the series, as well as in the covariance of the dataset. Most easily noticed as “spikes” or noticeable plot-position changes in the plot of stationary data, structural breaks are present when the relationship between the time series’ variables changes at a given point in time (Pickup, 2015).

2.3.5.2 Common models

Linear or multiple regression are possible analysis methods for time series; however, such methods are not ideal as the extrapolated future predictions tend to be more simplistic than robust stochastic methods. The presence of autocorrelation or autocovariance may also largely skew the data, rendering the results unrealistic (University of Pennsylvania, 2018). If the Durbin Watson test statistic, however, is near 2 the use of a stochastic autoregressive or moving average model is superfluous as there is nearly no autocorrelation skewing the data.

As briefly mentioned in section 2.3.1.1.8, once standardised the stationary residuals can be evaluated by the preferred stochastic processes. The stochastic processes considered applicable are the following:

2.3.5.2.1 Fourier Spectral Analysis

Discrete, stationary time series may also be analysed by means of a Fourier Analysis (Bremaud, 2014). Fourier Analyses are commonly used when there is a potential for a cyclic signal embedded within a given time series (Carleton College, 2018), thus making it a logical choice of analysis process for annual growth ring series as most studies seek to highlight and define any cyclicity within the tree’s growth that can then be correlated to any cyclicity of climatic phenomena. Spectral Fourier Analyses can thus be used to define

the lag period of growth within a sample; however, analyses be completed on detrended, stationary ring width data to ensure the validity of the computation and results.

Fourier Spectral Analyses is also used in conjunction with a chosen filter to generate a periodogram that is smoothed for autocorrelation which improves the ease of analysis by visually highlighting any cyclicity within the time series (University of Massachusetts Dartmouth, 2005). Various filters have been developed, however most modern computational software supports a subset of filters namely the Bartlett, Parzen, Tukey-Hanning, Quadratic Spectral and Truncated filters (TIBCO Software, 2017; SAS Institute Inc., 2019).

2.3.5.2.2 Autoregressive (AR)

An autoregressive process (AR(p)) is much like a multiple regression process, however rather than using linear extrapolation, AR models derive the desired variable through regression with the previously calculated values of the desired variable (i.e. this process makes use of the presence of autoregression within a series and is essentially multiple regression with lagged y_t values). The AR model of order p can therefore be expressed by Equation 5 (Hyndman & Athanasopoulos, 2018):

$$y_t = c + \varphi_1 y_{t-1} + \varphi_2 y_{t-2} + \dots + \varphi_p y_{t-p} + \varepsilon_t \quad \text{Equation 5}$$

where:

φ_p is a constant, scaling the process y_t

2.3.5.2.3 Moving Average (MA)

A moving average (MA (q)) process is like a regression model, although there are no observations of the white noise (ε_t) variables and it makes use of previous errors from the regression-like model to generate future values. A MA model, of order q, can generally be defined by Equation 6 (Hyndman & Athanasopoulos, 2018):

$$y_t = c + \varepsilon_t + \theta_1 \varepsilon_{t-1} + \theta_2 \varepsilon_{t-2} + \dots + \theta_q \varepsilon_{t-q} \quad \text{Equation 6}$$

where:

θ_q is a constant, scaling the process y_t

A valuable characteristic of both AR and MA models is that they are, somewhat, inversely related – meaning that an AR model of order p (AR(p)) can always be written as an infinite MA model, with the vice versa also being true (Hyndman & Athanasopoulos, 2018). It is due to this invertible relationship that AR and MA models may be used in a composite manner to develop an ARMA model, which is defined in greater depth in the succeeding subsection.

2.3.5.2.4 Autoregressive-Moving Average (ARMA)

An ARMA (p,q) process is a combination of the two aforementioned stochastic processes, with the influence of the AR and MA components being denoted by the function's p- or q-value. An ARMA (p,q) process is defined by Equation 7:

$$y_t = \alpha_0 + \sum_{i=1}^p \alpha_i y_{t-i} + \sum_{j=0}^q \phi_j \varepsilon_{t-j} \quad \text{Equation 7}$$

Where the first portion represents the AR process and the second the MA process. The requirements for an ARMA process are the condensed requirements which ensure stationarity of both the AR and MA processes. Using an ARMA process thus combines the benefits of both AR and MA to create a process which best models time series dynamics of data driven by other processes. One challenge of ARMA is,

however, that there are numerous alternatives which all are capable of representing the data. As such, the Box-Jenkins approach is often used to define the applicable ARMA process and its order required to best approximate the data (Pickup, 2015). As per the Box-Jenkins approach, there are three steps to defining the ARMA model, namely identification, estimation and diagnostic checking. The identification phase aids in defining the order of the p- and q-values, primarily through correlograms (correlation plots) of the autocorrelation (ACF) and partial autocorrelation functions (PACF). The identification phase, which is the most critical, is considered to be one of the most challenging aspects of time series analysis, generally, and as such it is often recommended that only experienced and knowledgeable parties undertake the task of defining the ARMA process (Monserud & Marshall, 2001).

Furthermore, within the scope of the Box-Jenkins approach, the Ljung-Box Test can be used to test for the absence of a serial autocorrelation within the residuals of an ARMA model meaning that the null hypothesis (H_0) assumes that the data is random and that there is no autocorrelation for a given number of lag periods (National Institute of Standards and Technology (USA), 2016).

The Ljung-Box Test is dictated by the chi-square (X^2) distribution and defined by the following equation:

$$Q_{LB} = n(n + 2) \sum_{j=1}^h \frac{\rho_j^2}{n-j} \quad \text{Equation 8}$$

where: n is the sample size

h is the number of lags being tested

ρ_j is the autocorrelation at lag j

According to Woollons and Norton (1990), pure time-series based statistical analyses are not commonly applied to ecological data due to constraints, such as limited or poor-quality data however there is indication that applying a time-series analysis to ring-width and rainfall data is possible; and, indeed, successfully completed before.

Woollons and Norton (1990) successfully used an ARMA (1,1) and an AR (1) process to analyse the ring widths of *Nothofagus menziesii* and *soldari*, demonstrating the robust capabilities of time-series analysis for dendroclimatological studies. When undertaking the time-series analyses, four components of the ring width series were identified as part of the analyses, namely:

- i) A distinct, long-term trend;
- ii) Reasonably regular oscillations about the trend;
- iii) Noticeable seasonality (seasonal impact);
- iv) Presence of an irregular, random components known as the “white noise”

These components hold true in ring width series of other studies, where the critical task is to extract the climatic data by removing the long-term, persistent trends – the importance of which is previously discussed in section 2.3.1.1.8. Woollons and Norton also substantiate their choice of an ARMA (1,1) process as the ARMA (1,1) process had been successfully used by Rose in 1983, Monserud in 1986 and Biondi and Swetnam in 1987.

Furthermore, Monserud and Marshall (2001) successfully implemented two ARMA models, lagged by 1- and 2-years respectively, for a study undertaken on chronologies constructed by carbon isotopes of *Pinus ponderosa*, *Pinus monticola* and *Psuedotsuga menziesii*. Monserud, considered a leader in time series analysis of ring width chronologies, posited in 1986 that the ARMA (1,1) process very well may be the best universal stochastic model to represent tree growth (Monserud, 1986). Other studies tend to substantiate

this, although it remains mere suggestion at this point due to no concrete evidence that the ARMA (1,1) process is a truly universal fit for tree growth.

Should the time series, however, not be stationary an autoregressive integrated moving average (ARIMA) process can be applied. Functionally, the ARIMA process is the same as an ARMA process although unlike the ARMA process, the ARIMA process is capable of handling a non-stationary time series as it integrates the differences between terms to account for the non-stationarity. Alternatively, AR, MA and ARMA models could be used to forecast time series but these processes are explosive, meaning that they are limitless in their forecast and can thus be overestimations although the forecasts are still reasonably indicative of trends (Nau, 2019).

2.4 Completed studies

Although the number of dendroclimatological studies completed in Southern Africa are fewer than most of the international community due to limited samples and poor potential of many species (Bhugeloo, 2014), there have been studies completed on and about various indigenous species. This chapter discusses the various studies undertaken in the greater Southern Africa.

2.4.1 South African studies

Shortly after Fritts' publication outlining the general process for dendrochronological studies, the first detailed South African publication relating to dendrochronology was compiled by M.A. Lilly of the University of Witwatersand in 1977 and focused on assessing the dendrochronological potential of indigenous South African trees.

Within Lilly's study, several issues with using South African trees were identified of which sourcing an adequate sample is the greatest challenge. According to the South African Department of Agriculture, Forestry and Fisheries (DAFF) (2014) less than 2% of South Africa is forest land as most of the original forest land has been exploited by 1900s woodcutters and colonisers. Of the reported land covered by forests in South Africa, the DAFF estimates that approximately 1% of the total South African landmass is actively afforested whilst a mere 0.5% of South Africa's landscape is still covered in original, natural forests. This small proportion of forests is largely due to woodcutters of the colonial era randomly selecting trees which appeared to be the best, resulting in many of the larger coniferous species such as *Podocarpus* and *Widdringtonia* practically being depleted (Department of Agriculture, Forestry and Fisheries, 2014). This becomes problematic as it does not only reduce the overall number of trees available for sampling, but also led to species such as *Podocarpus* being listed as a protected species – which is a species of high conservation value, or national importance, that need to be regulated in an ecologically sustainable manner as per the South African government's discretion (Fallis, 2013).

Another issue with a large conifer such as *Podocarpus* being listed as a protected species is that the rings of large conifers have been proven to be the best climate proxies within dendrochronological studies. Internationally, various forms of *Pinus* or *Juniper* have been successfully used as conifers generally produce one growth layer in a year of which the width is largely dependent on water availability, photoperiods and suitable temperatures – meaning that droughts, short photoperiods and low temperature conditions are easily detected in the ring widths. Although *Podocarpus* and *Widdringtonia* do not develop as distinct early-latewood borders as *Pinus*, as the cell walls do not thicken as much during the cambial growth period, their latewood borders are still easily detected by the naked eye (Lilly, 1977).

As of May 2018, the ITRDB has only three South African studies recorded, of which just one is a climatic reconstruction. The first of these, and arguably the best-known South African study, was completed by LaMarche and Dunwiddie in 1980 on several *Widdringtonia cedarbegensis (wallichii)* in the Cedarberg region colloquially known as “Die Bos” (meaning the forest) (US National Centres for Environmental Information, 2018). The “Die Bos” study was challenged, as most South African studies are, with a limited sample selection however the 32 selected trees’ core samples had few defects meaning that a cross-dated chronology could, reasonably, be relied upon to be an accurate representation of the tree’s growth.

Notably, the “Die Bos” study found that the climatic record from the region bore a significant correlation to the growth of the region’s trees with 73% of the annual change in ring width being due to deviations from the norm temperatures and rainfall amounts in the 18-month period preceding and concurrent with the tree’s growing season. This correlation, however, is not consistent over all seasons within a year, with the effect of the same sort of deviations in another season resulting in opposite outcomes (Dunwiddie & LaMarche, 1980).

Furthermore, following the initial interest from the “Die Bos” study, W. Zucchini and L.A.V Hiemstra of the University of Stellenbosch published their “note on the relationship between annual rainfall and tree ring indices” in 1983. Much like the “Die Bos” study, Zucchini and Hiemstra only used a single South African site for their analysis; however, they intended to relate the results obtained from the “Die Bos” study to their Wupperthal rainfall data as they believed a larger database of dendroclimatological studies meant that the reconstruction LaMarche and Dunwiddie hoped for is, indeed, possible. Working with a patched rainfall record of the Wupperthal rainfall station, Zucchini and Hiemstra related the rainfall record to the “Die Bos” residuals and found statistically significant correlations, much like LaMarche and Dunwiddie, however the correlation was not high enough to support reliable climatic reconstructions (Zucchini & Hiemstra, 1983). Zucchini and Hiemstra’s work was thus not added to the ITRDB as the study used the chronology developed by LaMarche and Dunwiddie to seek significant climatic correlations.

Many years later, based on LaMarche and Dunwiddie’s success with creating chronologies *Widdringtonia*, Edmund C. February from the University of Cape Town collaborated with Mary Gagen from the University of Wales to assess the dendrochronological potential of the remaining two *Widdringtonia* species found in South Africa, namely *W. schwarzii* samples from the Baviaanskloof wilderness area, to which *W. schwarzii* are indigenous, and *W. nodiflora* samples from the Grootvadersbosch Nature Reserve in the Western Cape. February and Gagen however failed to even generate a chronology, nor improve upon LaMarche and Dunwiddie’s work by successfully correlating the series with rainfall. It was thus concluded that these *Widdringtonia* species were unsuitable for dendrochronological purposes, as there were persistent inconsistencies in the samples’ ring widths, converging rings and very poorly defined growth boundaries – all which prevented successful cross-dating of the sample. February and Gagen attribute these difficulties to the very nature of the species; *W. schwarzii* is ill-suited for dendrochronological study as its extensive root system ensures a supply of water through deeper groundwater resulting in false rings and poor growth boundaries, whilst *W. nodiflora* exhibits the same issues and, generally, does not live long enough to support the reconstruction of a significant series. February and Gagen, however, do go on to suggest two other coniferous species that still need to be investigated, namely *Podocarpus elongatus* and *Podocarpus henkelii* (February & Gagen, 2003).

Shortly before February and Gagen published their study on the *Widdringtonia* February supervised a study completed by John C. Midgley, then-honours student at the University of Cape Town, which investigated the dendrochronological potential of an alien species *Pinus radiata*. This investigation, a first of its kind in South Africa given that all previous studies focused on using indigenous species, used 41

samples from the Silvermine Nature Reserve in Cape Town and managed to reconstruct a simple chronology although the chronology did not correlate to seasonal rainfall or temperature patterns of the region (Midgley, 2002).

Following the relative research “boom” of the 1980s to the 2000s, the next ITRDB listed study came from the University of Bern’s Raphael Neukom in 2013. Neukom’s study is the only climatic reconstruction listed for South Africa on the ITRDB and is a 200-year multiproxy precipitation reconstruction of both the summer and winter precipitation. Neukom’s research used a combination of tree ring widths, coral samples and historical artefacts or documentation to create a unified reconstruction. The main tree rings used in this reconstruction were those sampled by LaMarche and Dunwiddie in “Die Bos”. Analysis on the unified series confirmed a strong relationship between seasonal rainfall and surrounding sea surface temperature (SST) within Southern Africa, as well as concluding that there was an overall decrease in precipitation in the summer rainfall regions whilst rainfall variability had generally increased with time (Neukom, et al., 2013).

The most recent addition to the ITRDB is the University of Pretoria’s Stephan Woodborne’s 1000-year *Adansonia digitata* carbon isotope proxy rainfall record, generated from four *A. digitata* from the upper reaches of the Kruger National Park bordering Mozambique. Woodborne’s study focused on developing an unprecedentedly long climate record that can be used to better evaluate and forecast the relationship between rainfall and oceanic conditions. To create the 1000-year record, carbon isotope measurements were used as a proxy in developing the rainfall record. Carbon isotope $\delta^{13}\text{C}$ can be used as a proxy to derive a rainfall record as the isotope ratios found within the wood are directly linked to a tree’s physiological response to water stress (Woodborne, et al., 2015).

Woodborne’s study concluded that *A. digitata* were suitable for carbon isotope analysis and yielded a high enough resolution record that commentary on the centennial and decadal rainfall cycles can be made. From the constructed record it was noted that an overall decline in rainfall had occurred from 1075 AD to 1805 AD, and that over the past 700 years El Niño Southern Oscillation (ENSO) conditions correlated with wet conditions in South Africa’s summer rainfall regions, which marks a shift away from the previously accepted correlation between El Niño and dry conditions in the same region.

Phillip Fischer, from the University of Stellenbosch, also used $\delta^{13}\text{C}$ to define water usage, however Fischer’s study involved *Pinus radiata* from the Western and Southern Cape and aimed at developing classifications on how *P. radiata* utilised groundwater – particularly when stressed in drought conditions (Fischer, 2011). Other than these two studies, there were also studies completed using $\delta^{13}\text{C}$ which resulted in complete chronologies although not all these successfully correlated. The studies focused on local trees and included KwaZulu-Natal *Mimusops caffra* (coastal red milkwood) by Hall and Woodborne (2009), *Podocarpus latifolius* also by Woodborne and Hall (2008) and *Breodonia salicina* (matumi) by Norstrom et al. in 2005.

Carbon isotope analysis is, in fact, the recommended way forward for using indigenous species in the greater Africa given that dendroclimatic reconstructions and generally climatic science in Africa is the most poorly developed in the world (Gebrekirstos, et al., 2014).

2.4.2 Greater continental studies

Much like South Africa itself, the greater African continent has not had much success with dendroclimatological studies however there have been multiple attempts and occasional successes.

Within the greater Southern Africa, Matthew D. Therrell successfully reconstructed a 200-year chronology with Zimbabwean *Pterocarpus angolensis* (African Teak or Kiaat) which correlated well with the ENSO indices in addition to substantiating 46% of instrumental rainfall variance (Therrell, et al., 2006). The decision to use *P. angolensis* was supported by both previous studies by David W. Stahle (a co-researcher of Therrell's) which found success in reconstructing short records using *P. angolensis* due to the species forming distinct rings that correlate well with rainfall records (Stahle, 1999) and knowledge that teaks are some of the limited tropical species known to develop annual growth rings (Suresh, 2012).

P. angolensis, along with the more sensitive *Burkea africana*, was also found to bear strong climatic signals in the semi-arid forests of Namibia as per research completed by Esther Fitchler et al. In Fitchler's study, it was determined that the *P. angolensis* and *B. Africana* are adequate proxies of climatological variables, providing substantiation that certain tropical trees growing in semi-arid environments correlate well, although the resulting chronologies are site specific (Fitchler, et al., 2004).

In Ethiopia, a 68-year chronology was successfully constructed by Aster Gebrekirstos et al. with various members of the *Acacia* species found in the semi-arid regions of the country's savanna woodlands. By using samples of *Acacia seyal*, *Acacia senegal*, *Acacia tortilis* and *Balanites aegyptiaca*, Gebrekirstos' study determined that there was not only an overwhelmingly positive correlation between the annual ring growth and precipitation but also between a decreased ring width and El Niño periods which, additionally, coincide with marked drought and famine periods within Ethiopia (Gebrekirstos, et al., 2008).

2.5 Climatic Patterns in South Africa

Across South Africa there are different climate behaviours. The southwestern part of the country (i.e. the Western Cape Province) experiences a decidedly different climate than the rest of the country. Most of the country experiences a more tropical "summer" rainfall, whilst the southwestern part of the country experiences a Mediterranean "winter" rainfall (Lawal, 2015; Government of South Africa, 2019). The semi-arid climatic landscape of South Africa is largely influenced by its plateauing topography, ocean currents (the Agulhas and Benguela) as well as the sub-tropical position of the country (Jury, 2018).

Rainfall in South Africa is largely controlled by El Niño and La Niña Southern Oscillations. The El Niño Southern Oscillation phase (ENSO) typically results in a decrease in rainfall and increase temperature whilst the complementary La Niña results in the inverse – an increase in rainfall and relative decrease in temperature (Fitchler, et al., 2004; MacKellar, et al., 2014). Both the El Niño and La Niña have been associated with extreme rainfall and temperature events across the globe, with South Africa, particularly in the region south of 10° S, commonly experiencing droughts because of ENSO (Lindesay, et al., 1986; Jury, 1995). According to Mason (2001), the greater South Africa has experienced below normal amounts of rainfall (within the lowest third of all record years) in the December to February (summer) period during eight recorded El Niño events, from 1950 to 1996, indicating the noticeable effect ENSO has on the country's climate environment although other research has highlighted that the effect of ENSO is better understood in the "summer" rainfall regions (Philippon, et al., 2012).

The ENSO is defined as the interaction between the ocean and atmosphere which results in cyclic fluctuations in the sea surface temperature (SST) and, thus, determines the dry or wet conditions over the period within the cycle (International Research Institute for Climate and Society - Columbia University, 2018).

Furthermore, noticeable in the collated records from 1906 to 1997, there have been bouts of extreme rainfall in the eastern parts of South Africa – particularly in the 30 years from 1961 to 1990 – related to a general increase in the intensity of the rainfall across the broader country (Kruger & Nxumalo, 2017). Kruger and Nxumalo (2017) additionally found that there has been a distinct increase in rainfall over the western region of South Africa, extending inwards to the southern interior of the country, whilst the north-eastern regions have decreased amounts of rainfall. The increase in rainfall is, however, not noticed in the south-western portion of the Cape (which encompasses the better part of the Western Cape province) although Kruger and Nxumalo, as well as MacKellar et al. (2014), do acknowledge significant decreases along the southern Cape coast. Furthermore, Kruger and Nxumalo's findings of a generally increased rainfall intensity does corroborate with work completed by Donat et al. (2013) which determined that on a general, global scale the intensity, frequency and quantity of rainfall events have increased (Donat, et al., 2013).

Conversely, Du Plessis and Schloms (2017) concluded that the southern coast of the Cape exhibits a longer rainfall season which would, generally, correlate with wetter weather. This research also commented on the noticeable shift towards a drier western portion of the Western Cape province (decreasing the Mediterranean region's rainfall) which does, indeed, corroborate with other research which supposed longer summer conditions in the regions of the Western Cape (Du Plessis & Schloms, 2017). Jury (2018) also supports this, with the results of his study determining that the Western Cape is the one region in the country which has experienced a noticeable drying trend since 1980.

2.5.1 Western Cape climate

The climate of the Western Cape, like the greater southwestern region of the country, can largely be considered as Mediterranean and is considered a "winter rainfall" region (Lilly, 1977, p. 13), meaning that the bulk of the precipitation experienced each year occurs during the winter seasons, which is to say between the months of June and August (Precop, 2007) although the rainfall may begin in the autumn season (April) and end in the early spring season (September) (Philippon, et al., 2012). The greater Cape Town region typically receives an average 788 mm of rain in a year, with June typically the wettest month and February the driest (SA Explorer, 2017). For the "winter rainfall" region of the Southwestern Cape, the amount of rainfall is largely determined by circular atmospheric patterns in addition to the relief and distance from the Indian Ocean (Lilly, 1977, pp. 13-14).

During the decade from 2003 to 2013, the Western Cape Province experienced severe flooding, triggered by "intense" rainfall, and climate which caused damage of at least R4.9 billion to both property (particularly farmlands) and infrastructure across the province (De Waal, et al., 2017). As per the research completed by de Waal et al. (2017), 63% of the rainfall stations in the Western Cape exhibited an increased 1-day rainfall extreme value for the 20- and 50-year return periods. Additionally, other studies also corroborate that there is an increased extreme 1-day rainfall across most of the country – particularly in the southern regions of the country, where the Western Cape lies. Easterling et al. (2000) found that extreme rainfall frequency, which is for rainfall events greater than 25.4 mm for the Western Cape (southwestern) region, increased by 5.5% per decade whilst Groisman et al. (2004) noted an increased frequency of heavy rainfalls during 1901-1910 and 1931-1997 over the country as a whole (Easterling, et al., 2000; Groisman, et al., 2005).

This "intense" rainfall is a product of cut-off low weather systems, which is known to bring moderate to heavy rains with 20% of all cut-off lows in Southern Africa causing heavy rainfall (Molekwa, 2013) – which De Waal et al. (2017) also hypothesised to be the reason for the increased frequency of extreme rainfall events during 2010-2013 in the Western Cape. The frequency of cut-off lows is correlated with other

atmospheric factors which includes La Niña, however it appears El Niño bears little influence on cut-off lows (Donaldson, 2009). El Niño does, however, appear to bear influence on the temperature and rainfall as droughts are more commonly aligned with El Niño periods (Mason, 2001), although this effect is not necessarily as noticeable in the Western Cape region. As per Philippon et al. (2011), the exact effect of ENSO on the Western Cape “winter” rainfall region is not easily defined although the study did conclude that ENSO phases do not result in any discernible differences in the rainfall extremes. The study did, however contrarily, determine that in the Western Cape (and particularly higher north within the province) there is an increase in the length of the wet-periods and the amount of rainfall which is reasonably correlated to ENSO.

This behaviour of extreme rainfall is rather contrary to what occurred in the year subsequent to 2013; as of 2018, the majority of the Western Cape was hard hit with drought conditions which nearly resulted in a near-system collapse in which there would be no available water, commonly referred to as “Day Zero” (City of Cape Town, 2017). As illustrated by Figure 15, the cumulative rainfall for the 2016/2017 hydrological year was well below the expected norm. The cumulative rainfall for 2017/2018 was also below the expected norm, however only marginally if compared with the preceding hydrological year. It was noted by the City of Cape Town’s official reports that whilst 2018’s rainfall was lower than average, it was still more than double 2017’s – a marked improvement (City of Cape Town, 2018). As of 2019, the rainfall for the 2018/2019 period appears to be, like the years before, below the expected rainfall with the October of 2018 only having approximately half the rainfall yield than expected (South African Department of Water and Sanitation , 2019).

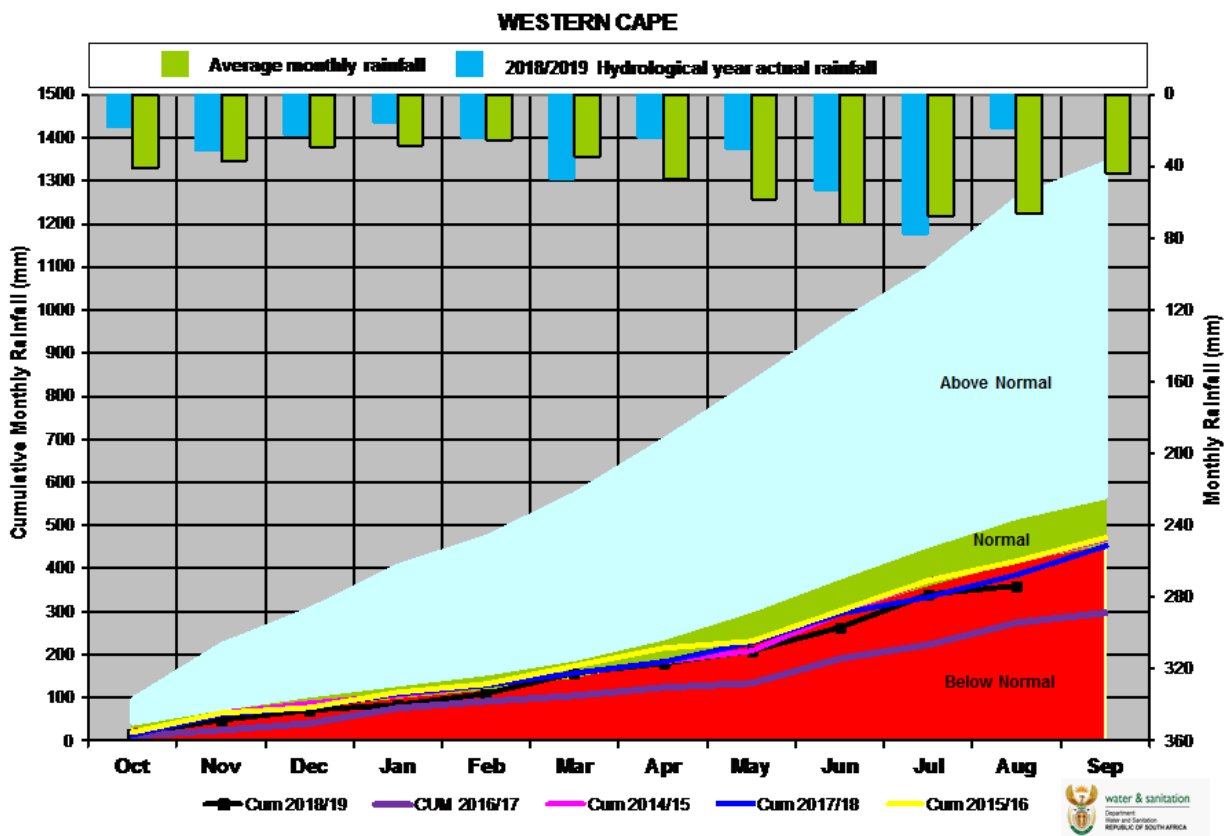


Figure 15: Western Cape cumulative rainfall behaviour (South African Department of Water and Sanitation , 2019)

It thus follows that the periods in the southern hemisphere with the most climatic influence on trees are between November and February (Brown, 1971). Lilly (1977) also reiterated that for Mediterranean climates, such as that in the Western Cape, annual growth rings tend to have sharper boundaries with minimal discontinuities as the rainfall typically occurs before the first growth-flush.

2.5.2 Microclimates

For this research, the microclimates within the Western Cape were considered. Two distinct regional microclimates were identified to be significant for the study, namely that of Tokai/Bishopscourt (Southern Suburbs) and Wolseley. These climatic locations were reviewed as they correlate to the locations of the samples used within in the study.

2.5.2.1 Tokai and Bishopscourt

Tokai and Bishopscourt are reasonably close to each other – as seen in Figure 1, the Tokai and Bishopscourt samples were sourced within a 10 km distance from each other – and thus experience similar microclimatic variations. The greater Southern Suburbs region experiences an annual average rainfall of 835 mm, thus making it a wetter region than Wolseley. The average summer temperature is, at most, 20.9°C and the winter temperature is an average of 12.8°C (Climate Data Organisation, 2018). Bishopscourt and Tokai are more distinctly south than Wolseley, thus substantiating the slight difference in microclimate.

2.5.2.2 Wolseley

Wolseley, in the Breede River Valley (more central portion of the province), also experiences a Mediterranean microclimate although receiving an average of 753 mm of rainfall per year it is drier than the Southern Suburbs region. The average temperature is 16.8°C although there is a more pronounced difference between the summer and winter periods' average temperatures than that of the Southern Suburbs with the January temperature averaging 22.8°C and the winter month of July averaging 10.9°C (Climate Data Organisation, 2019).

2.6 Literature summary and conclusion

It is evident, upon reviewing the literature, that there are multiple factors that dictate the growth and development of a tree of which only one is climate. Thus, to model climate from the annual tree rings, careful consideration must be given to the samples collected as well as the method of processing the ring width and climatic data.

Samples must therefore carefully be selected from sites where the desired climatic variable is a dominant factor in affecting the growth of the tree, for example trees growing on cliff faces or along talus slopes, as this increases the strength of the climatic signal within the width chronology. Processing must also be done in the correct manner, with additional cross-dating and standardisation being completed to result in a ring width chronology that is free from defects and usable in analyses, as the persistent age and exogenous trends are removed through standardisation. Species may also influence the resulting chronology and relationship, as different species have somewhat different growth behaviours. Species-specific analysis is thus ideal, although multiple species with similar growth behaviours may be used for regional analyses where sample size is limited.

Various studies have been undertaken in Southern Africa, the first notable being a full study on the viability of South African indigenous samples for dendroclimatological analyses by M.A. Lilly in 1977.

Subsequently, LaMarche and Dunwiddie completed the first ITRDB study colloquially known as the “Die Bos” study on a sample set of *Widdringtonia cedarbergensis (wallichii)* in 1980 with moderate success. The “Die Bos” study yielded a reliable chronology constructed from 32 samples which was then used in further dendroclimatological analyses. LaMarche and Dunwiddie concluded that 73% of the tree growth within an 18-month period could be related to temperature and rainfall amounts although this finding was not consistent across the entire series, with some seasons resulting in opposite results than expected. As such, LaMarche and Dunwiddie recommended further study into the plausibility and suitability of dendroclimatological studies within Southern Africa.

Following the results of the “Die Bos” study, researchers Zucchini and Hiemstra attempted in 1983 to further extend rainfall records through seeking correlations between the nearby Wupperthal record to the “Die Bos” chronology. Although Zucchini and Hiemstra succeeded in finding correlations between the chronology and rainfall records, the statistical significance was not great enough to support reconstructions or an extension of the rainfall record.

The two other South African studies listed in the ITRDB were completed by Raphael Neukom in 2013 and Stephan Woodborne, in 2015 although the interim local researchers February and Gagen, as well as their student Midgley, completed studies using *Widdringtonia* and *Pinus* samples. Midgley, supervised by February in 2002, completed a study assessing the viability of using *Pinus radiata* samples for climatic reconstructions however he failed to find any significant correlation. The research completed by February and Gagen in 2003 analysed the suitability of all known *Widdringtonia* within in South Africa, mainly due to LaMarche and Dunwiddie’s success with using *Widdringtonia* in their study, although February and Gagen concluded that most *Widdringtonia* specimens are unsuitable for dendroclimatological studies and suggested the (now protected) *Podocarpus* species as potentially viable samples.

Neukom’s study is the only multiproxy rainfall study, making use of a variety of samples including historic artefacts, coral and the “Die Bos” chronology. Neukom’s study concluded that there was a noticeable general decrease in precipitation in the summer rainfall regions (which comprises the greater portion of the country) whilst the variability of rainfall had generally increased. Additionally, Neukom concluded that there is a significant correlation between SST and rainfall.

Woodborne, the most recent addition to the ITRDB, moved away from conventional sampling practices and utilised carbon isotope dating techniques to infer a growth ring chronology. Woodborne’s study presented an unprecedented 1000-year record, derived from the dating of *A. digitate* and concluded that there is significant correlation between the ENSO cycles and wet periods in Southern Africa for the past 700 years. The use of carbon isotopes in dendroclimatological studies was, again, further used by Phillip Fischer, however his study focused on the correlation between the growth of *Pinus radiata* and groundwater rather than rainfall or temperature.

Furthermore, this chapter also defined the climate of the relevant regions of the study, namely Tokai, Bishopscourt and Wolseley as well as the climate of the greater Western Cape. Focus was given the average precipitation experienced in the Western Cape as well as what factors control the climate.

Lastly, the statistical methods that can be employed in time series analyses of the ring width and rainfall chronologies are also discussed in this chapter, and informed the selection of the statistical methods employed in this research – of which the exact processes that are utilised are discussed in Chapter 3.

3. Methodology

This chapter defines the methodology applied throughout this research, explicitly defining the means of obtaining and preparing data in addition to the methods applied to analyse the data.

3.1 Data Collection

This subsection defines the means by which data was obtained and is divided into two subsections as two primary datasets were obtained, namely the ring width (and resulting chronology) data obtained from the tree ring samples and the annual rainfall data obtained from rainfall stations or gauges.

3.1.1 Tree ring samples

The four samples for this study were supplied by the Department of Forestry and Wood Science at University of Stellenbosch and are as follows:

Table 1: Summary of sample species and locations

Species	Location	Approximate coordinates
<i>Pinus pinaster</i> (Cluster Pine)	Bishopscourt	33° 59' 34.62" S, 18° 26' 34.39" E
<i>Sequoia sempervirens</i> (Californian Redwood)	Tokai Forest (now Park)	34° 3' 42.90" S, 18° 24' 45.03" E
<i>Cupressus lusitanica</i> (Mexican Cedar)	Tokai Forest (now Park)	34° 3' 40.71" S, 18° 24' 46.89" E
<i>Eucalyptus cladocalyx</i> (Sugar Gum)	Wolseley	33° 25' 40.79" S, 19° 10' 49.74" E

The following subsections discuss the locations of the samples in more detail:

3.1.1.1 Locations

Bishopscourt is a leafy, upper-middle class suburb located in the Western Cape with many of the suburban homeowners planting a variety of both indigenous and alien species in the area. The *Pinus pinaster* which was obtained from the Bishopscourt area was, however, not obtained from a private garden; the sample was obtained from a *P. pinaster* that was felled between September and December of 2017 as part of a greater effort to remove domineering alien species from the region to support future rehabilitation. Figure 16 illustrates the location of the sample:

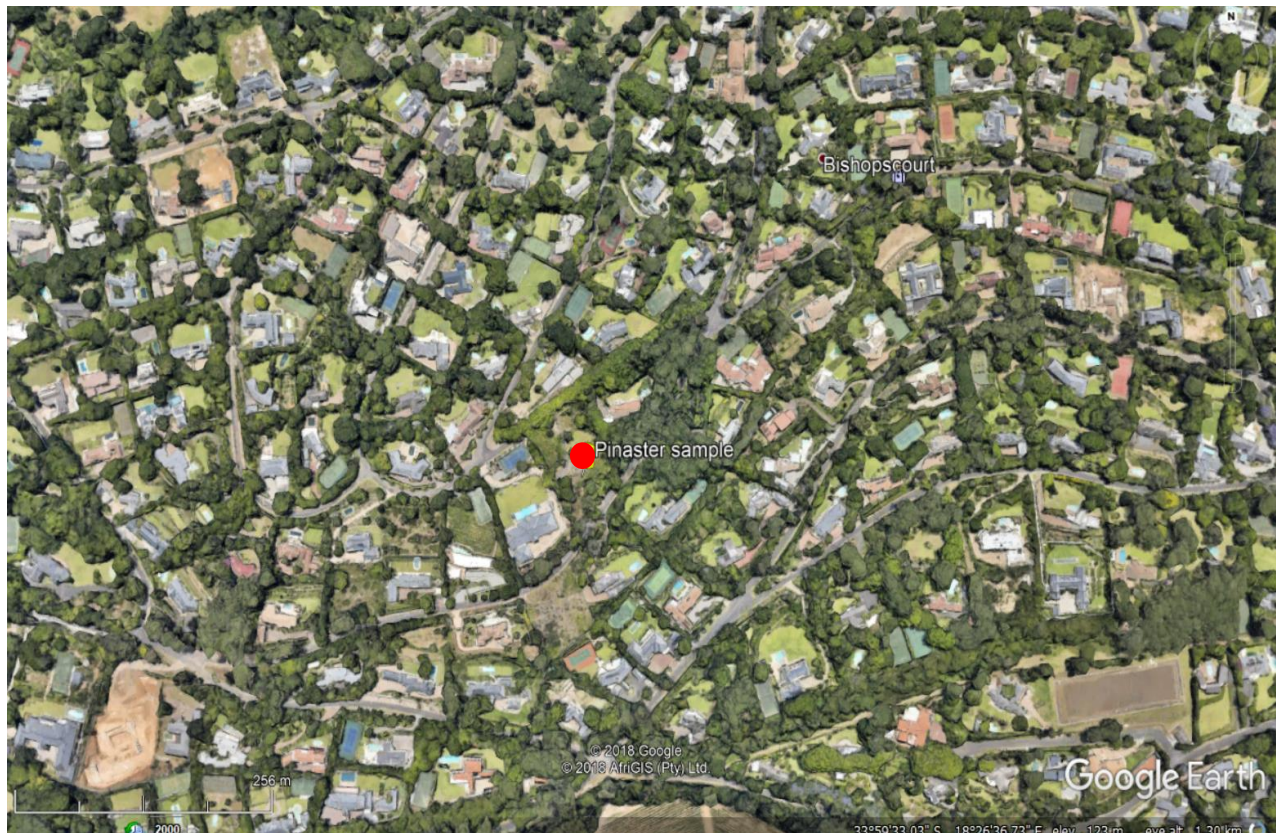


Figure 16: Location of *P. pinaster* in Bishopscourt (Google Earth, 2018)

Tokai Park (commonly referred to by its former name Tokai Forest) has been operated by South African National Parks (SANParks) since April 2005, when it became part of the greater Table Mountain National Park. Established in 1885 as a commercial plantation, the Tokai forest has been actively providing trees, cyclically, since 1920 for commercial and construction use (South African National Parks, 2019). The Tokai Park mainly comprises of alien Pine, Gum (Eucalyptus) and the occasionally Port Jackson, however the terrain also has some indigenous fynbos and other species amongst these planted. The *Sequoia sempervirens* (Californian Redwood) found in the Tokai Park is derived from the original Tokai Arboretum's alien species which were propagated by Joseph Storr Lister, the conservator of the then-Cape Colony's forests, in 1886 as part of a study to investigate which foreign species flourished in the Cape's climate and terrain (SA Venues, 2019). Whilst a noticeable portion of the alien Pine, Gum and Port Jacksons have been felled during the 2016 to 2017 period, to make way for the natural fynbos to recover and reclaim the region, some of the *Sequoia* and other alien species were also felled from the arboretum for very similar reasons (Hunter, 2016; South African Department of Agriculture, Forestry and Fisheries, 2006).

The *S. sempervirens*, and *Cupressus lusitanica* (Mexican Cedar), were both felled in December 2017 and are derivatives from the original stand of alien species brought into the arboretum. Cross-sections from a felled tree of each species were sourced by University of Stellenbosch's Department of Forestry and Wood Science, and the approximate locations of the redwood and cedar are illustrated by Figure 17.

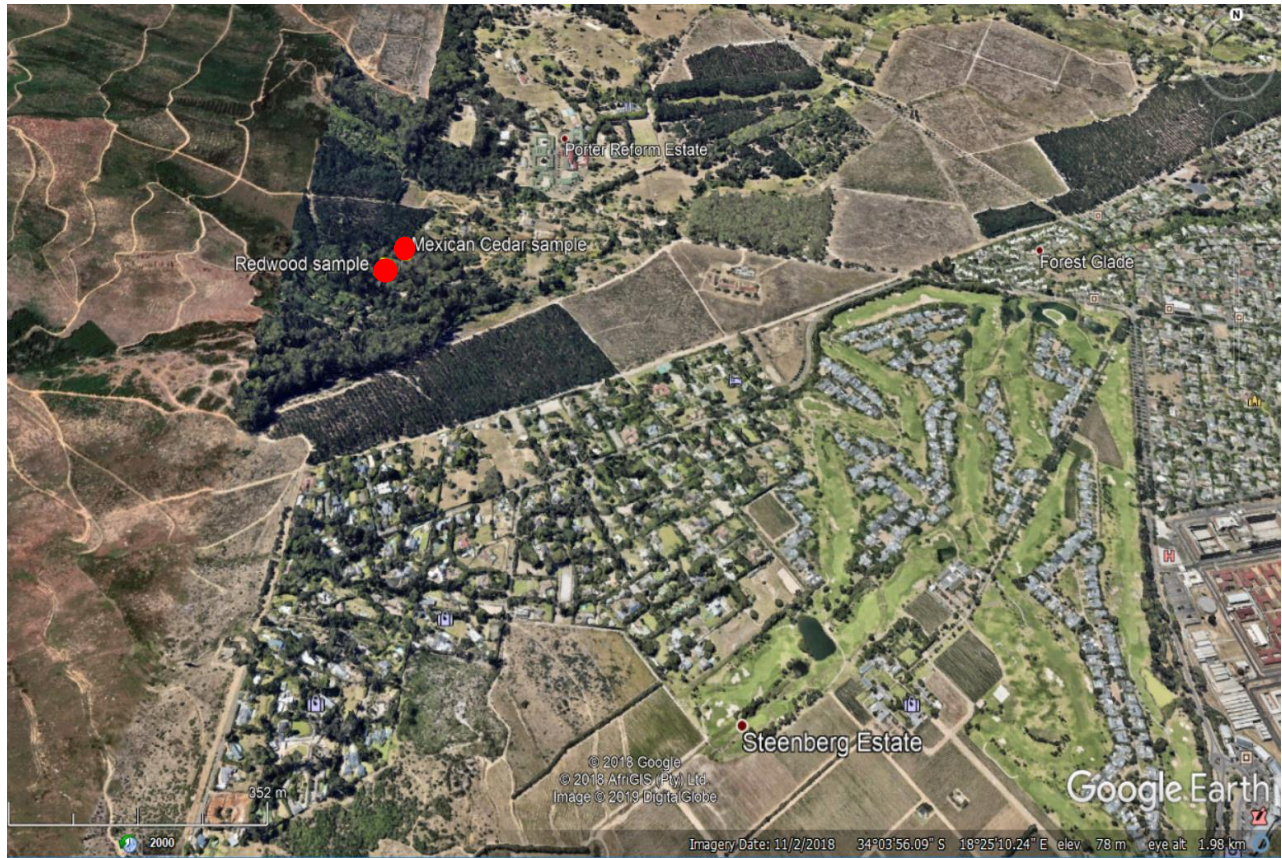


Figure 17: Locations of *S. sempervirens* and *C. lusitanica* in Tokai Park (Google Earth, 2018)

Also felled in the later period of 2017, the *E. cladocalyx* was obtained from a stand of the alien species in Wolesley, as shown in Figure 18.

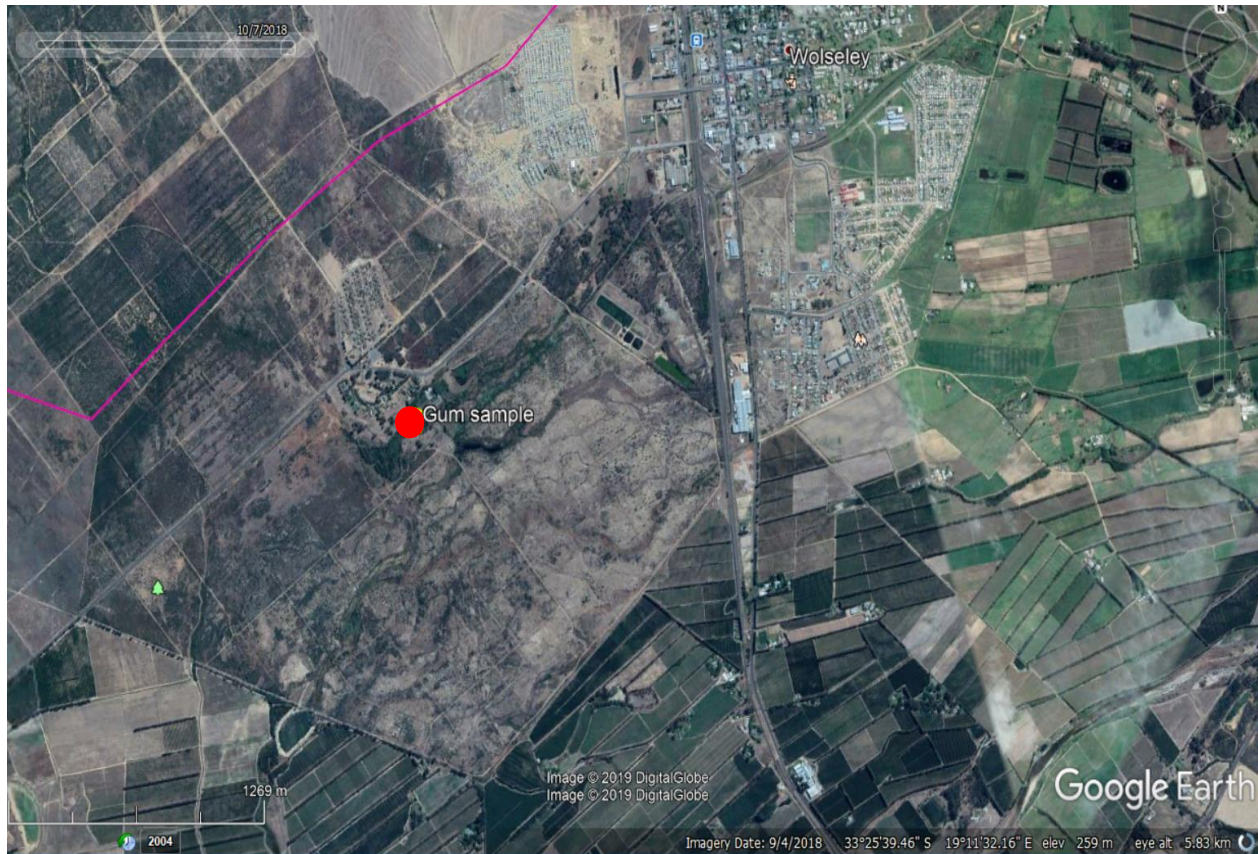


Figure 18: Location of *E. cladocalyx* in Wolseley (Google Earth, 2018)

3.1.1.2 Preparation

The preparation of the samples was largely aided by the Department of Forestry and Wood Science, with the cross-sectional strips being sawed out of the complete cross-section by a skilled party. The sawn sections were then mounted by an experienced party from the Department, as per procedure, onto rectangular wood strips for the final step of preparation – sanding. All four samples were sanded as per the standard procedure, namely beginning at a rougher grit of 150 and incrementally increasing the fineness of the grit until a final polish was done with a 1000-grit sandpaper. Lastly, the samples were visually dated for an estimate of the age range of the different samples prior to constructing the chronology by means of the Rinntech Lintab and TSAP-Win suite. Two of the samples, namely the *E. cladocalyx* and *S. sempervirens*, have particularly poor visibility of the annual growth rings for all or part of the section, thus, to better aid the readings, pencil markings of the (assumed) annual growth rings were also made on the samples prior to constructing the chronologies. Figures 19 through 22 show the final, prepared samples which includes the aforementioned boundary markings.



Figure 19: Pinus pinaster sample (Bishopscourt)

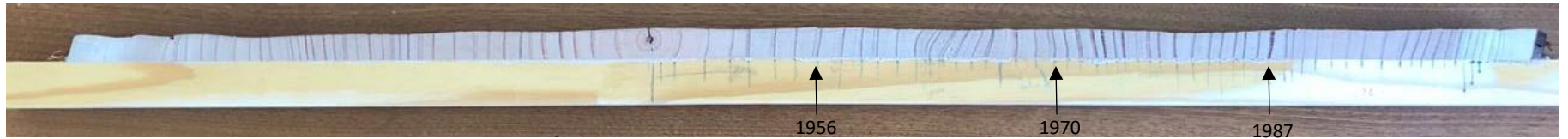


Figure 20: *Sequoia sempervirens* sample (Tokai) – saturated image, with some marked years, to highlight rings

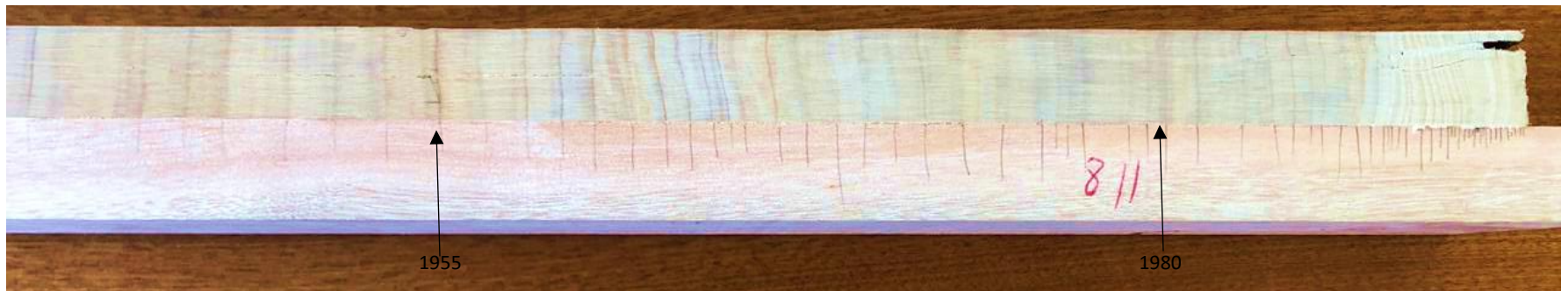


Figure 21: Section of *Cupressus lusitanica* sample (Tokai) – saturated image, with some marked years, to highlight rings

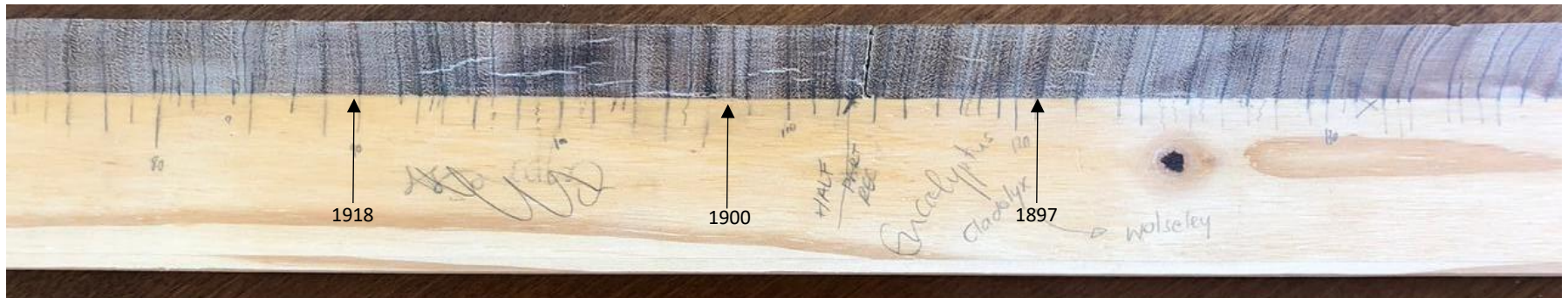


Figure 22: Section of *Eucalyptus cladocalyx* (Wolseley) with some marked years

As illustrated by Figure 19, the Bishopscourt samples exhibit the clearest growth ring boundaries, with no noticeable ring wedging or false rings whilst the Wolseley sample had the worst clarity of any of the four samples. The poor visibility of the *E. cladocalyx* rings (**Error! Reference source not found.**) was addressed through an additional pass with a finer grit sandpaper and polish as well as slightly dampening the sample (as recommended by Stokes & Smiley, Phipps, Kozwolski and others) to attempt to better highlight the darker ring borders and prevent inaccuracies. Furthermore, the borders for the Wolseley sample were also further highlighted before recording through marking the borders with pencil on the sample's mount (seen in **Error! Reference source not found.**).

The Tokai samples (Figures 20 and 21) both have moderately visible ring markings although there are noticeable missing and wedged rings. As such, the missing and wedged rings were marked before being confirmed by a second party who visually validated the estimated age of the samples and the ring markings made on the samples' mounts. Only those markings validated by the second party were recorded as per the steps in section 3.1.1.3. Furthermore, the effect of any missing or partial rings not noticed by the two-person check will be largely negated through the standardisation process.

3.1.1.3 Recording

To construct the chronologies of each sample, and subsequently create average chronologies for the greater Southern Suburbs region (the Tokai and Bishopscourt samples), Tokai (the two Tokai samples) and a general Western Cape region (combination of all four samples), Rinntech Lintab and TSAP-Win were used. Potential defects, such as those discussed in section 2.2.3.1, and the estimated length of the chronology were, however, visually estimated by both the researcher and a third party with experience (a member of the Department of Forestry and Wood Science) before the computer aided capture was completed; this was done to best mitigate any potential errors in the readings and potentially produce more accurate results, much like how skeleton plots or memorization techniques can be used to validate cross-dating results against the computer's (i.e. the "second technician's) results (Maxwell, et al., 2011).

The hard- and software used in the construction of the chronologies was supplied by University of Stellenbosch's Department of Forestry and Wood Science's Tree Ring Lab. The process of using the Lintab, and computer recording properties of TSAP-Win, is as follows:

1. Place the sample on the moving board of the Lintab
2. Adjust the dioptre of the microscope until the rings of the sample become clear beneath the crosshair – Figure 23 here shows clear rings as seen beneath the microscope

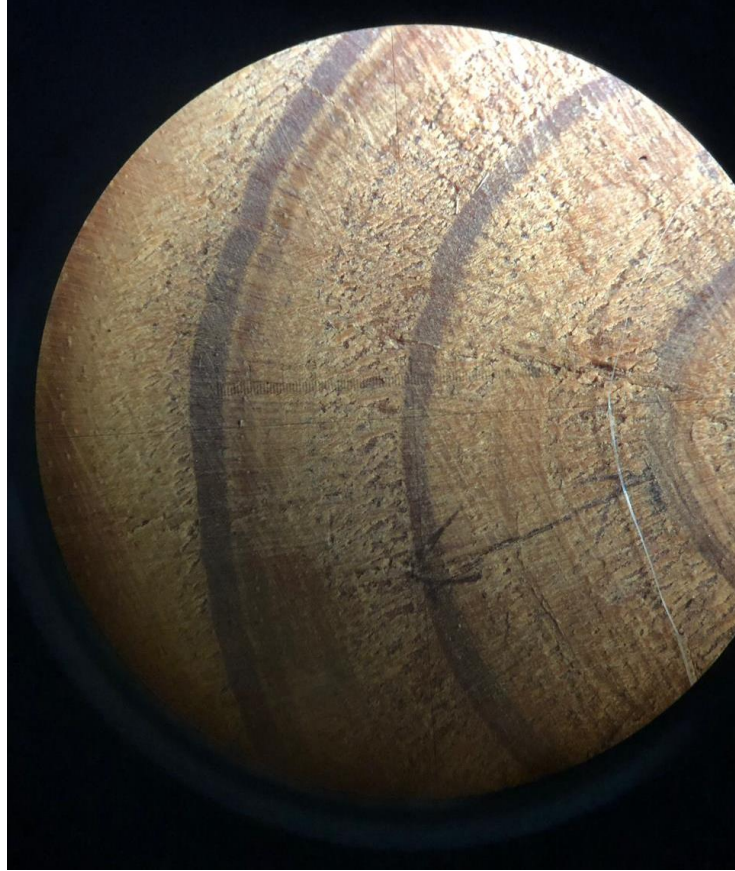


Figure 23: Growth rings as seen beneath the microscope

3. Reposition the sample so that the bark/terminal ring is beneath the crosshair of the microscope – this can be done by physically altering the position of the sample's placement or moving the board along by the crank of the Lintab
4. Once the bark/terminal ring is in position, the right mouse button is used to assign that point as "position zero"
5. Once a "zero" position has been defined, TSAP-Win brings up an editable header interface which requires detail on the sample (see Figure 24). Information on the sample's species, terminal age (if known) and transitions (early-to-latewood or vice versa) are all completed here

The screenshot shows the 'Dataset header' dialog box in the TSAP-Win software. The 'Header' tab is active, displaying various input fields for sample metadata. The fields are organized into several rows: Keycode, Project, Location, Species, Length, DateBegin, and DateEnd; Tree no., Radius no., Core no., Stem disk no., Sp. name, Pith, Sapwood, Waldkante, Data type, Unit, Series type, Series starts with, and Series ends with; and a Comment field. The 'Length' field is set to 0, and 'DateBegin' and 'DateEnd' are also set to 0. The 'OK' and 'Cancel' buttons are located at the bottom right of the dialog.

Figure 24: TSAP-Win header tab

6. Following the declaration of the sample's detail in the header, and the definition of a "zero" position, the left mouse button is used to record the latewood border of every annual growth ring encountered beneath the crosshair. The crank is used to incrementally move the sample, and thus the position marker in TSAP-Win, along
7. The sample's rings are "read" left to right and are complete once the pith of the sample is reached. Hitting the escape key on the keyboard results in the recording process terminating, bringing up the original header interface with the start and end dates now being filled in
8. Closing the header interface, the raw (unstandardized) sample chronology will be visible on the display (set-up in Figure 25), with the x-axis showing the relative dates and the y-axis the relative width fluctuations

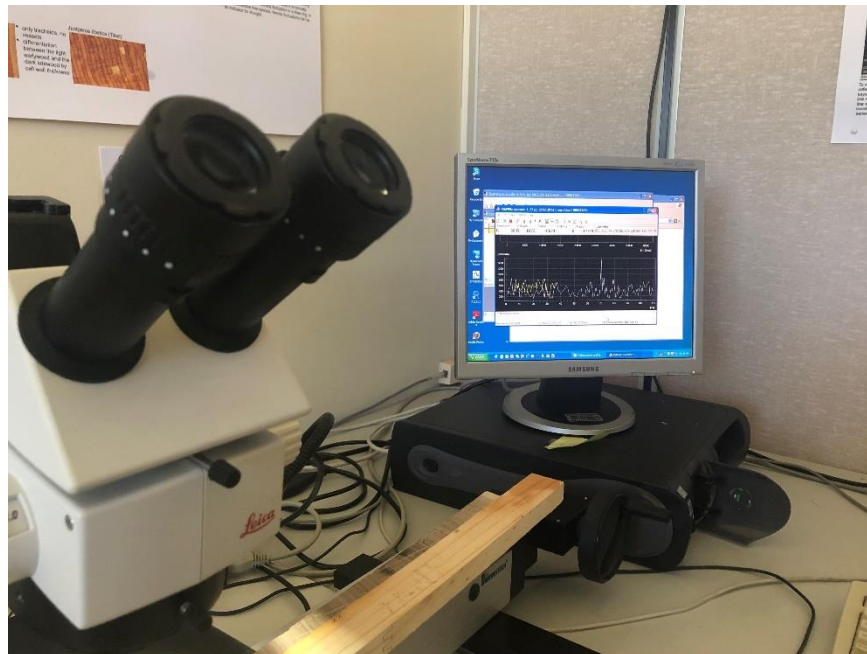


Figure 25: TSAP-Win set-up with complete recordings

3.1.1.4 Construction of chronology

Using TSAP-Win, the chronology for each sample, as well as combined average chronologies for the greater Southern Suburbs, Tokai and Western Cape region, can be constructed. The chronologies per sample are directly constructed by the recordings taken when using the Lintab. These chronologies are, however, considered raw and uncross-dated with cross-dating being completed once the four samples are recorded.

Cross-dating, a critical component of dendroclimatological study, is completed on all four samples. For *P. pinaster*, the Department of Forestry and Wood Science provided two cross sectional samples thus allowing the *P. pinaster* to be cross-dated within itself through the two samples. The other samples, however, were cross-dated with the (then already dated) *P. pinaster* sample. The sample chronologies were then either accepted or rejected based on Bretting's (2014) recommendation, with chronologies having GLKs greater than 50 being accepted. The mean GLK for the chronologies are as follows:

Table 2: Summary of average GLKs for selected chronologies

Chronology	GLK	Accepted or Rejected
Bishopscourt	58	Accepted
Tokai	54.5	Accepted
Wolseley	58	Accepted

Once cross-dated, the chronologies could be aggregated into average chronologies for the previously mentioned regions by using the built-in math function. The final, cross-dated, resulting chronologies obtained from the Lintab and TSAP-Win are thus:

1. *P. pinaster* chronology (Bishopscourt)
2. *S. sempervirens* chronology
3. *C. lusitanica* chronology
4. *E. cladocalyx* chronology (Wolseley)
5. Tokai average chronology (*S. sempervirens* and *C. lusitanica*)
6. Southern suburbs chronology (*S. sempervirens*, *C. lusitanica* and *P. pinaster*)
7. General Western Cape chronology (all samples)

The resulting raw, cross-dated chronologies are included in Appendix A.1 Tables A1 to A3.

To best represent the conditions and work with the limited samples, only three of the resulting chronologies were selected to undergo dendroclimatological and time series analyses (i.e. be standardised and cross-correlated with rainfall), which were the *E. cladocalyx* chronology (i.e. the Wolseley chronology), the *P. pinaster* chronology (i.e. the Bishopscourt chronology) and the aggregated Tokai chronology. The resulting raw cross-dated chronologies, plotted with the relevant location's rainfall data, are illustrated in Figures 31 to 34 in the Chapter 4. Three analysis approaches were used to evaluate the data, with all three standardising the data differently. These approaches are, simplistically, as follows:

1. The "conventional" dendroclimatological analysis, which involved standardising the data by means of TSAP-Win's "trend/regression" function found within the math function and then correlating it to the rainfall data;
2. A time series approach comparing the log-returns of the rainfall and ring width data;
3. A time series approach comparing the rainfall and ring width data using:
 - a. Spectral density/Fourier analyses
 - b. Least squares regression

c. ARMA modelling

These methods are discussed in greater depth in section 3.2.

3.1.2 Rainfall data

As there are three distinct areas from which the samples originate, the annual rainfall records for these locations are required to complete the analyses. The rainfall datasets used are thus:

1. Interpolated grid rainfall data at 33°75' S 18°26' E for Bishopscourt (1901-2017)
2. Interpolated grid rainfall data at 33°25' S 18°59' E for Tokai (1901-2017)
3. Wolseley Experimental Farm, H1E002 (1964-2012), obtained from the Department of Water and Sanitation's (DWAS) published records.

The annual rainfall records are required to complete the cross-correlation between the standardised chronologies and the records, as well as statistical analyses on the rainfall record themselves.

The Tokai and Bishopscourt rainfall records were sourced directly from grid data which is complete from 1901 to 2017. The grid data is compiled by the National Centre for Atmospheric Research and a composite of multiple sources thereby making it far more complete than any other single source (National Center for Atmospheric Research, 2017). The gridded data is not exactly at the same locations as where the samples were sourced from, although they are close enough that the interpolated data ensures that the latitudes are correct and thus rendering the data accurate enough for the analysis.

The rainfall record for Wolseley was obtained from the DWS and are recorded at the Wolseley Experimental Farm, which is approximately 3.9 km from the location where the sample was felled (see Figure 26). The records are monthly records for the 1964 to 2012 hydrological years, although some of the months were missing or estimates. Although, as the ring width chronologies are annual in nature, the annual (rather than monthly) rainfall values are used in both the dendroclimatological and statistical analyses. For annual periods that do not have a recorded rainfall, the missing values were filled with the calculated average, which was determined to be 599 mm.

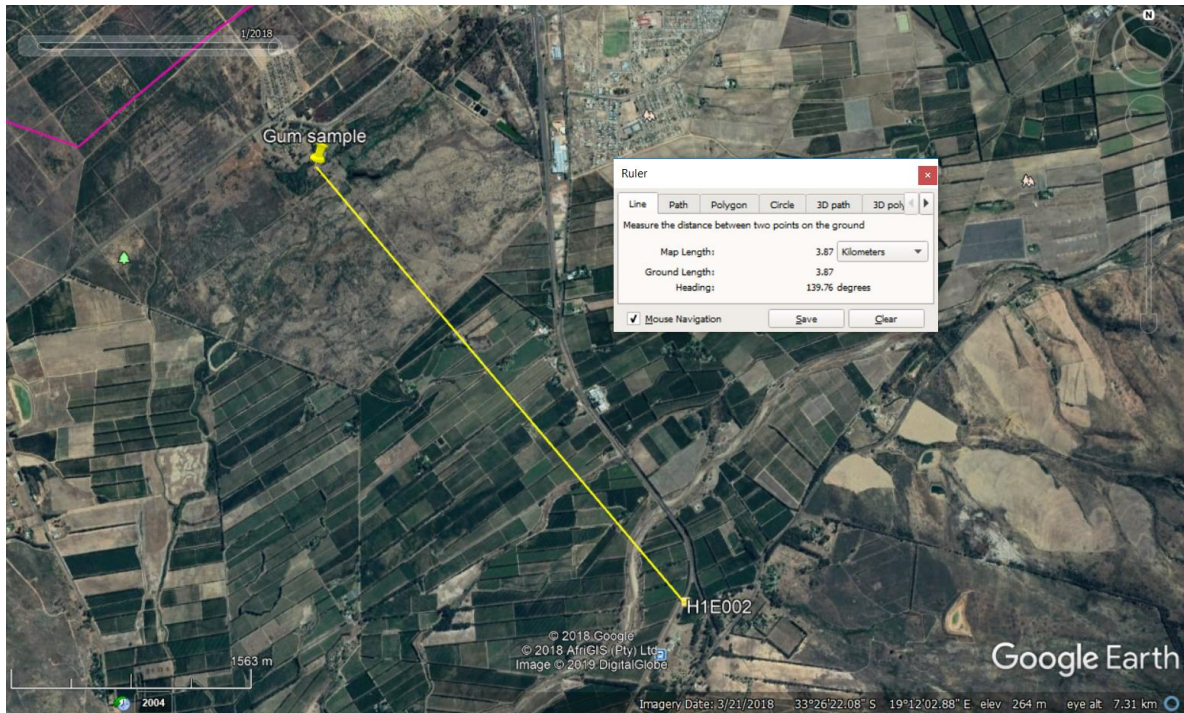


Figure 26: Estimation of the distance between H1E002 and the *E.cladocalyx* sample site (Google Earth, 2018)

3.2 Analysis techniques

The following subsections define the analysis techniques utilised in this study. Primarily, two approaches were taken namely computer-aided using TSAP-Win and a more “pure”, statistical approach of time series analysis. The statistical analyses were, however, also aided by using software, including Microsoft *Excel*, TIBCO *Statistica* and *EViews*. The results of the analyses are all discussed and summarised in Chapter 4.

3.2.1 TSAP-Win

The three selected aggregated chronologies were standardised with TSAP-Win’s built-in Math functions, which includes a detrending capability. Each of the three chronologies were detrending using three approaches, namely linear, exponential and moving average equations to detrend the time series. For each of these three approaches, TSAP-Win is able to optimise the equation and resolve the correlation coefficient (r), slope, scale and other respective parameters – an example of which is illustrated in Figure 27:

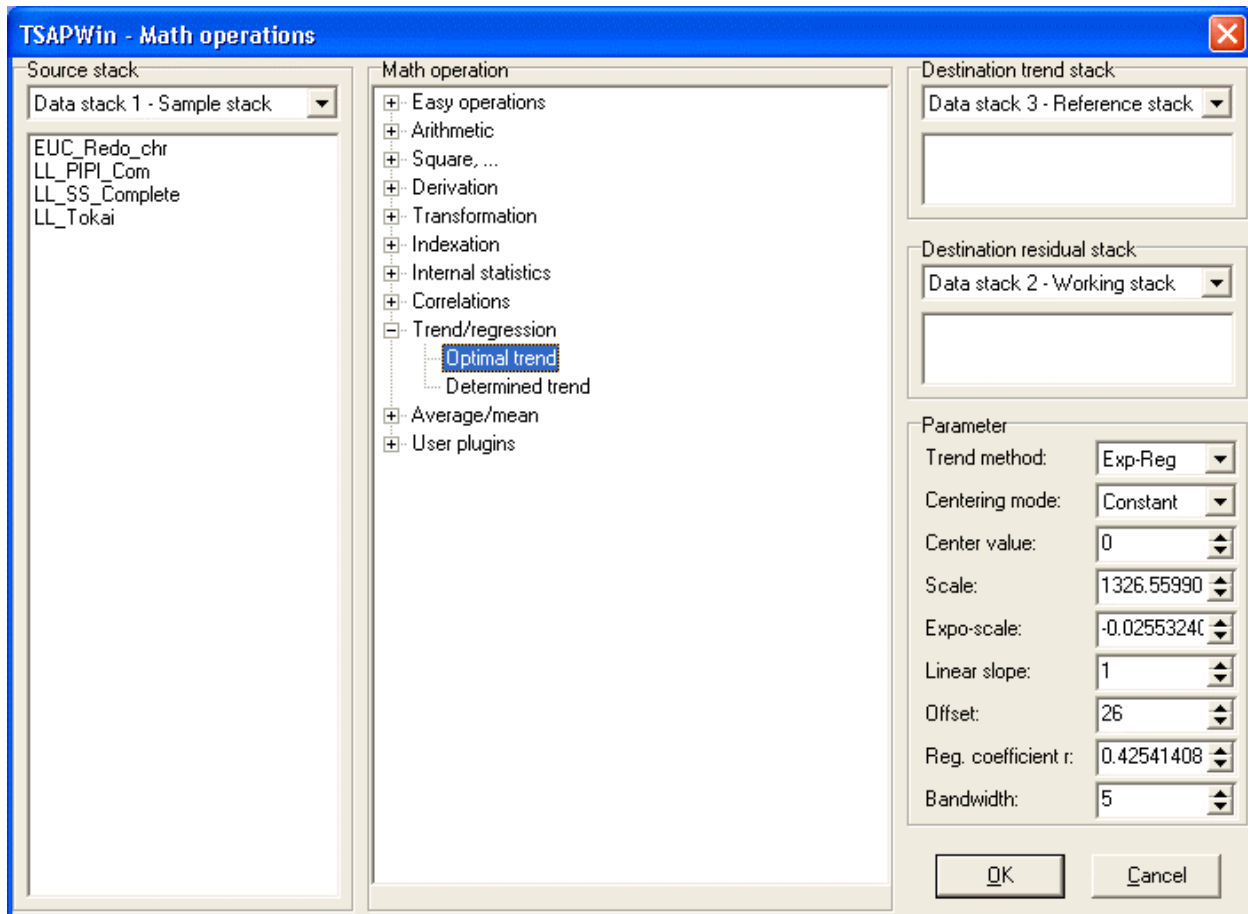


Figure 27: TSAP-Win set-up for detrending with an exponential function

Applying the detrending equations extracts the residuals, which forms the standardised chronology, as well as the overall trend found within the dataset. The equations, and their calculated optimised parameters, are calculated by TSAP-Win per method for all the same chronologies selected (i.e. the parameters are the same per detrending approach, regardless of the chronology). The optimised parameters, per approach, are summarised in Table 3:

Table 3: TSAP-Win calculated optimised regression parameters

Chronology	Slope	Scale	r-coefficient	Offset
Linear regression				
Bishopscourt	-6.0225	N/A	0.37769	848.7675
Tokai				
Wolseley				
Exponential regression				
Bishopscourt	N/A	1326.5599	0.4254	26
Tokai				
Wolseley				
Moving Average detrending				
Bishopscourt	N/A	N/A	N/A	N/A
Tokai				
Wolseley				

The resulting, detrended, standardised chronologies were then plotted and are illustrated, in comparison, with the original, raw data for each of the chronologies as shown in Figures 28 to 30.

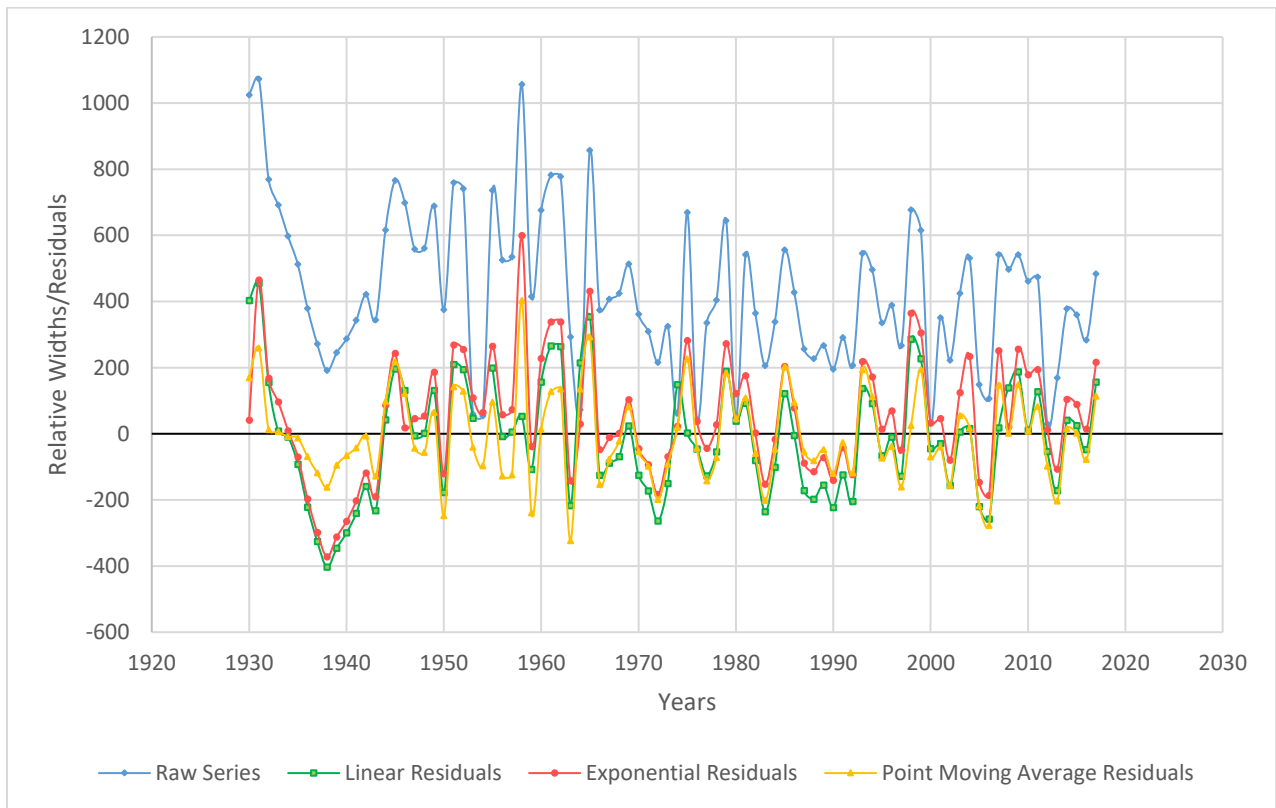


Figure 28: Comparative plot of TSAP generated residuals and raw chronology - Bishopscourt

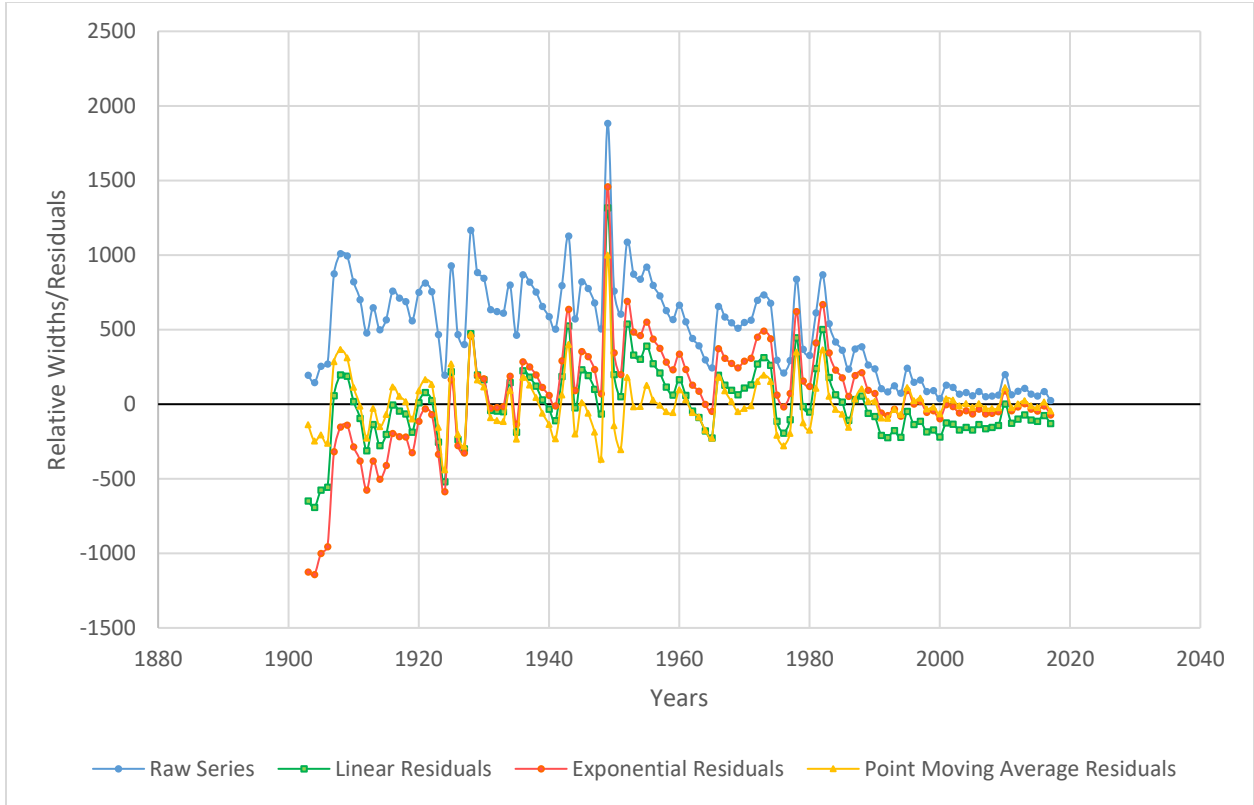


Figure 29: Comparative plot of TSAP generated residuals and raw chronology - Tokai

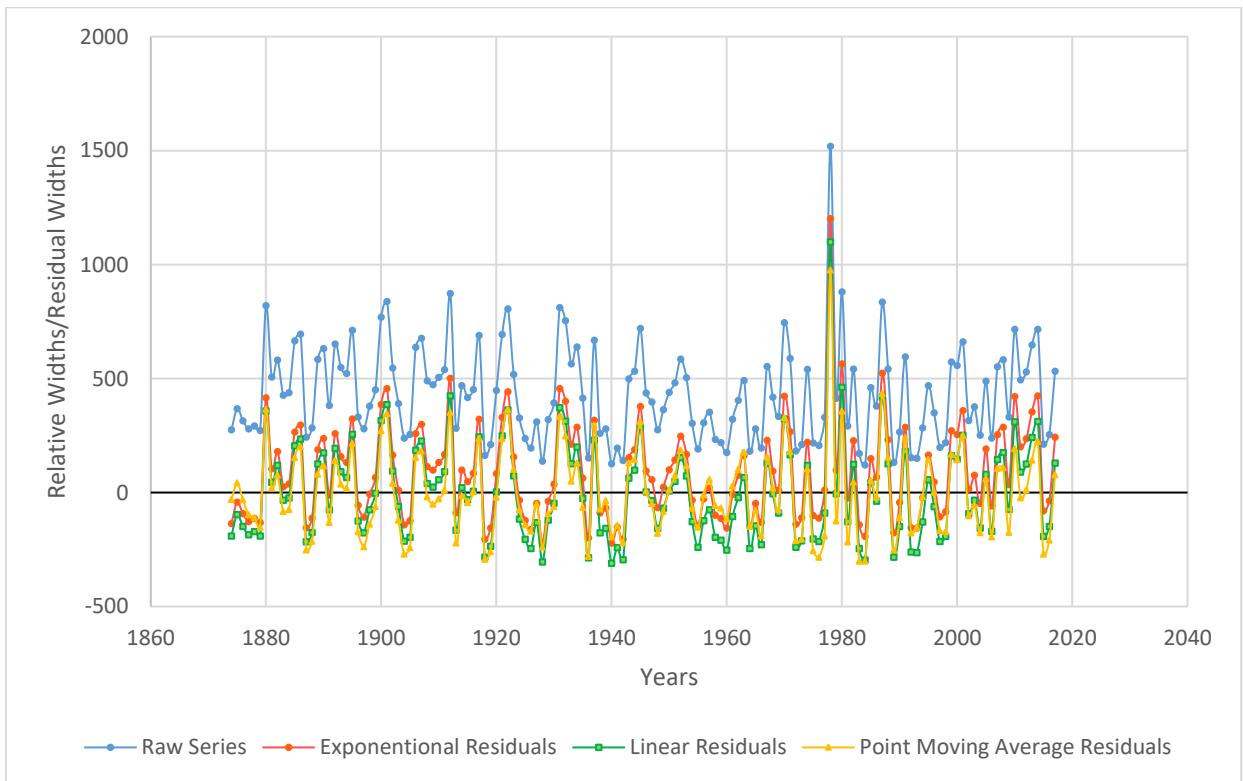


Figure 30: Comparative plot of TSAP generated residuals and raw chronology - Wolseley

When visually comparing the comparative plots above, it is evident that the moving average results in the most centralised residual chronology, which is indicative of it being the best approach to remove the persistent age trends and noise within the ring width series, thus leading the other two detrending approaches to be disregarded from here on and only the results from the moving average approach are considered when seeking the correlation.

With the moving average residuals calculated by TSAP, the “raw” rainfall series and TSAP residuals are plotted in Microsoft *Excel* and compared. The correlation between the ring width and rainfall is calculated by means of the *Excel*’s “CORREL” function.

3.2.2 Time series analysis

A time series analysis approach was applied to the data sets to best resolve any possible correlations within the data sets, where both regression and stochastic methods were employed where relevant.

3.2.2.1 Log-returns and stationarity

Before any analysis of the recorded data can occur, the stationarity of the data had to be validated. The Augmented Dickey-Fuller (ADF) test for the presence a unit root was employed in *EViews* to ascertain whether the data set was stationary or not. The null hypothesis for the ADF supposes that a unit root is present within a time series, where the larger the negative result for the test statistic is, the more confidently the null hypothesis can be rejected (Kang, 2017). If the data set accepts the null hypothesis, the data had to be made stationary through taking the log-return of the data values instead of the “raw” chronology, however for the sake of completeness the correlation between the log-returns of all three samples’ widths and rainfalls was calculated – in other words, the correlation between the log-returns was calculated regardless of whether the raw data sets were stationary, although the log-return values were only used for further time series analyses if the raw data sets were not stationary (which is the case only for Tokai).

Log-returns are independent and identically distributed and assumes a continuous compounding effect (Ruppert, 2014) – which is generally true for the behaviour of the growth of trees. The concept of log-returns, typically used for the analysis of financial and stock market data, was utilised to provide stationarity to the chronologies thereby allowing the correlation between the growth and rainfall, as well as the statistical characteristics of the chronology, to be assessed.

The log-returns are calculated, where necessary, for both the annual ring and rainfall data by the following:

$$r_t = \ln \left(\frac{x_t}{x_{t-1}} \right) \quad \text{Equation 9}$$

If the log-return values were required to be calculated (i.e. the ADF resulted in accepting the null hypothesis), a second validation of the stationarity was completed on the logged data sets – again, using the ADF test – to ensure that the data is adequately stationary for time series analyses. To complete the ADF test on the three locations’ width chronology and rainfall *EViews*, a software package equipped with a multitude of statistical, forecasting and modelling tools, was used.

Furthermore, as a form of cursory analysis the correlation between the log-returns of the width and rainfall for all localities’ chronologies (regardless of whether the ADF indicated the data required the log-return) was determined by means of Microsoft *Excel*’s “CORREL” function.

3.2.2.2 Determination of lags – autocorrelations and spectral analyses

Once determined that the data sets are sufficiently stationary, additional evaluations were completed to quantify any possible cyclicity and growth lag, as the growth of trees is not necessarily within the same year as the rainfall. To assess the cyclicity and lag, four tests were employed where a lag was considered related to the growth and development of a tree if it occurred in a regular interval (i.e. cyclical). The four tests were plotting the cross-correlations, plotting the autocorrelation function (ACF) in conjunction with the Ljung-Box test, plotting the partial autocorrelation function (PACF) and Fourier Spectral analysis (generating a periodogram) smoothed by a Parzen filter – all of which were completed in TIBCO *Statistica*.

The first three correlative plots were completed with the ring width chronologies being the lagged variable, where significant, potential lags were defined as those periods where the standard error exceeded the 95% confidence interval. For the autocorrelation function, the Ljung-Box Q was determined in addition to plotting the ACF where standard errors are assumed to be white noise estimates. Again, lags are noted when they exceed the confidence interval band. Following the ACF, the PACF, ultimately, defines the order of a potential ARMA model (where applicable) where the order is the lag period which, as before, exceeds the confidence interval.

Additionally, the presence of any cyclicity (or lack thereof) was visually investigated by means of a periodogram generated by Fourier Spectral Density analysis, where the periodogram is smoothed by means of a Parzen filter. The Parzen filter in *Statistica* functions as a weighted moving average transformation (Parzen, 1967) and allows the periodogram to be smoothed so that any cyclicity may easily be visually identified.

3.2.2.3 Regression and ARMA models

Whilst the PACF gives a strong indication of whether a ARMA model is required, an ARMA model was not immediately created for each locality – a least squares regression was computed on each ring width chronology, with relation to rain, in *EViews* where the result of the Durbin-Watson test determined, finally, whether or not an ARMA model is required. Should the results of the least squares regression's Durbin-Watson test resolve a value near to 2, an ARMA model is not required. For values less than 2, however, an ARMA model of an order defined by the results of the PACF must be generated as this results in the most parsimonious model. The suitability of the ARMA model is again validated with Durbin-Watson test statistic, where values near to 2 are the desired result. Once the final model is generated, be it a regression or ARMA model, the correlation coefficient (r^2) is the primary summary statistic of interest as it defines the extent to which the rainfall influences the growth variance within the sample.

4. Results

This chapter discusses the results of the analyses of the ring width chronologies and their potential correlation with their respective station rainfall records where each approach's results are discussed in its own subsection beginning with the "conventional" TSAP-Win approach and culminating in the time series, stochastic ARMA approach. As previously discussed in the methodology, ultimately only three standardised ring width chronologies (namely Bishops court, Tokai and Wolseley) were considered for analyses, and thus only the chosen three were assessed for correlations and discussed within this chapter.

Before the analysis could, however, be undertaken the ring width chronologies had to be completely cross-dated, as defined in section 3.1.1.4. The resulting raw, cross-dated chronologies comparatively plotted with the relevant location's rainfall are illustrated by figures 31 to 34, below, where a cursory correlation could be resolved although as the data is not entirely standardised or stationary, the result would be skewed and thus not entirely accurate.

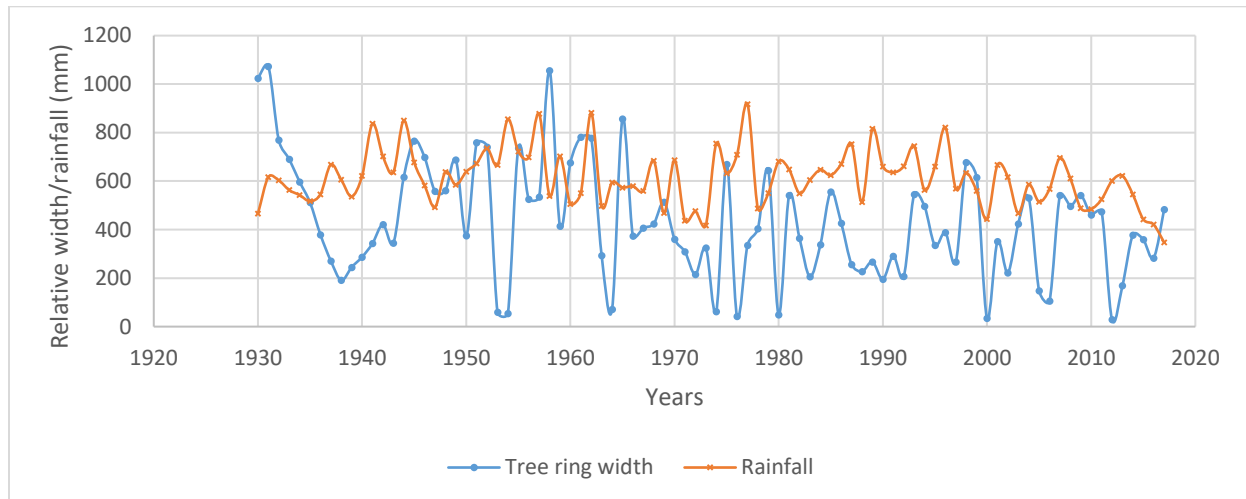


Figure 31: Bishopscourt chronology vs rainfall

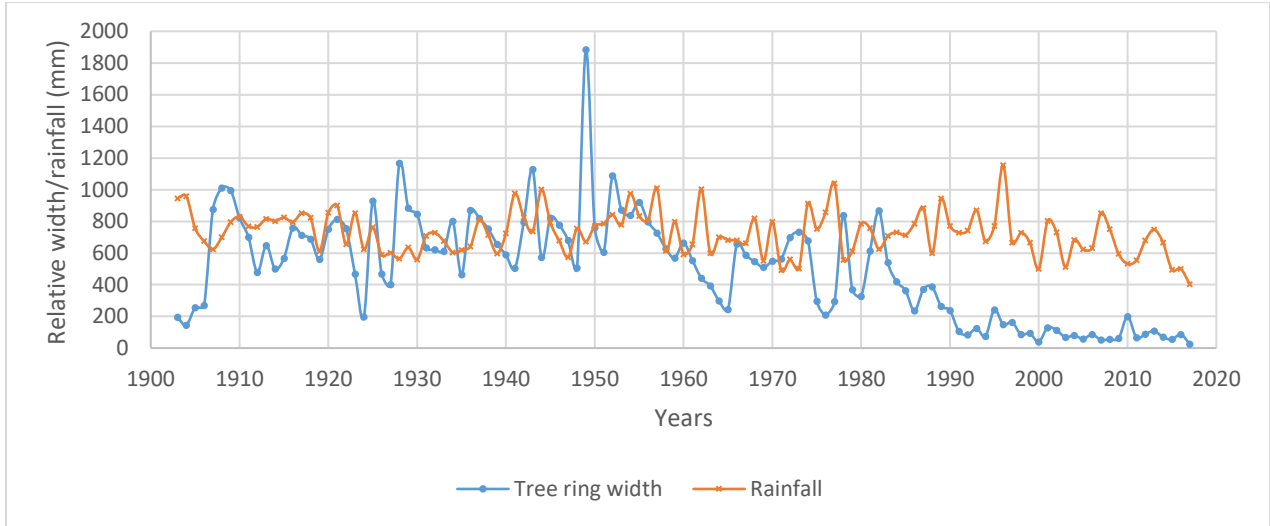


Figure 32: Tokai chronology vs rainfall

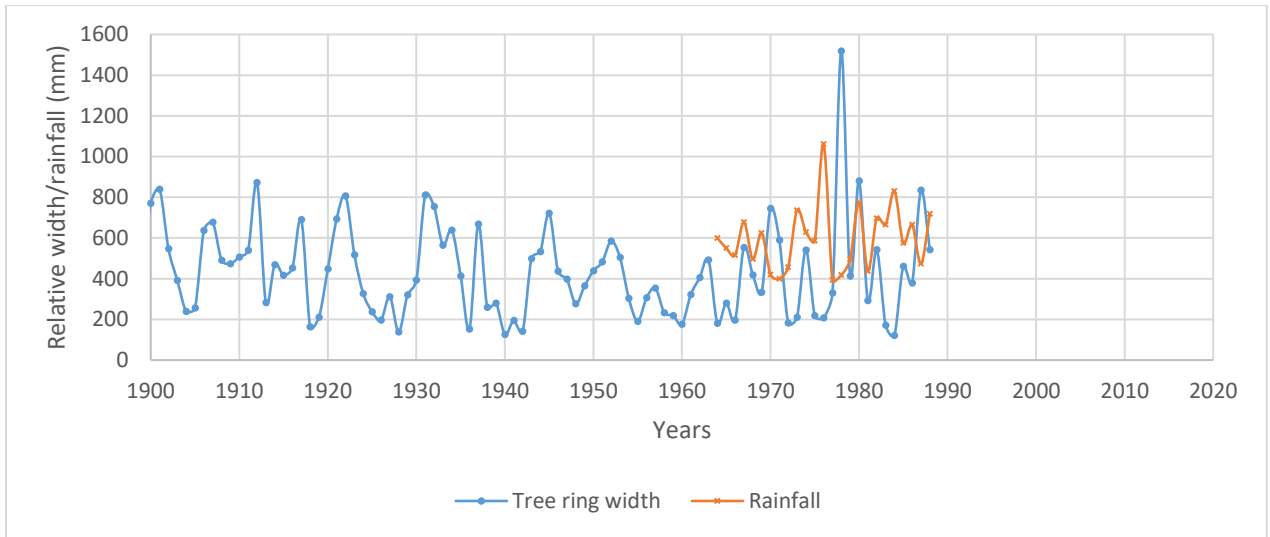


Figure 33: Wolseley chronology vs rainfall

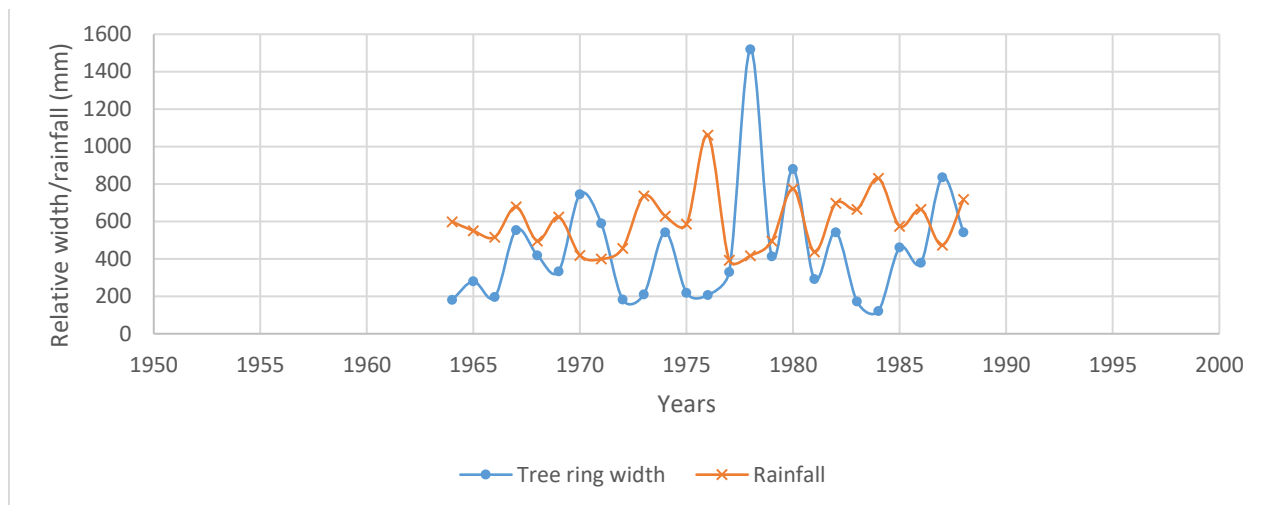


Figure 34: Wolseley chronology vs rainfall ("Zoomed" in on period where both have records)

Just visually comparing the raw plots, it would appear that the growth is most varied in the Tokai aggregated chronology (made up of the *S. sempervirens* and *C. lusitanica*), although the rainfall is not nearly as varied as the growth pattern potentially already belying the notion that purely the rainfall is influencing the growth of the Tokai samples – which would therein result in the Tokai chronology not being useful for the extension of the rainfall model. The greatest discrepancy between the rainfall and growth trends for the Tokai chronology is notably the downward growth trend from 1990 onwards. The decreased increment of growth could be due to a host factors, such as temperature, humidity, competition or disease (although there are no noticeable traces of infestation or disease on the sample, this cannot be entirely ruled out).

The *P. pinaster* sample of Bishopscourt is also highly varied in growth, although does not exhibit the substantial decrease in growth seen with the Tokai chronology. Generally, the Bishopscourt chronology appears to have the greatest similarity in pattern to its rainfall record of the three analysed locales, with many of the pits and peaks occurring in tandem with the rainfall record's pits and peaks. Nevertheless, the extreme nature of the variation in the chronology is not reflected in the rainfall record.

For the *E. cladocalyx* from Wolseley, however, the scale of the growth fluctuation is more closely reflected in the fluctuation of the rainfall record, with the periods from 1966 to 1969 and 1980 to 1982 following the same trend as the growth (visible in Figure 34). Though, despite this, the Wolseley chronology's greatest peaks and pits do not align with that of its rainfall record, with the 1978 year being a particularly clear example of this. This does, however, suggest that the effect of the rain on growth may be delayed. For this reason, any potential lag, or cyclicity, in any of the chronologies is investigated by means of a periodogram.

4.1 TSAP-Win Moving Average results

As discussed in section 3.2.1, only the moving average residuals were considered for analyses. TSAP-Win calculated the moving average residuals from the standardised chronologies, which were then comparatively plotted, along with the other residuals per location (see Figures 28 - 30 in section 3.2.1). Figures 35 to 37, below, are the plots of the moving average residuals with the location's rainfall record – which were then utilised to define any potential correlation.

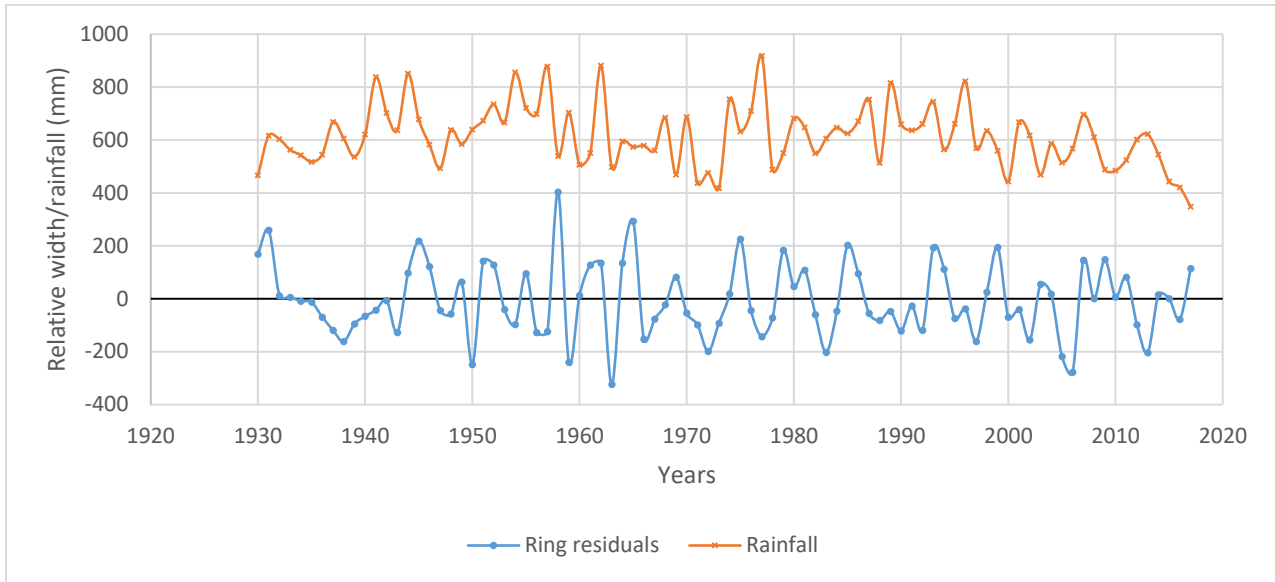


Figure 35: Plot of Bishopscourt residuals and rainfall

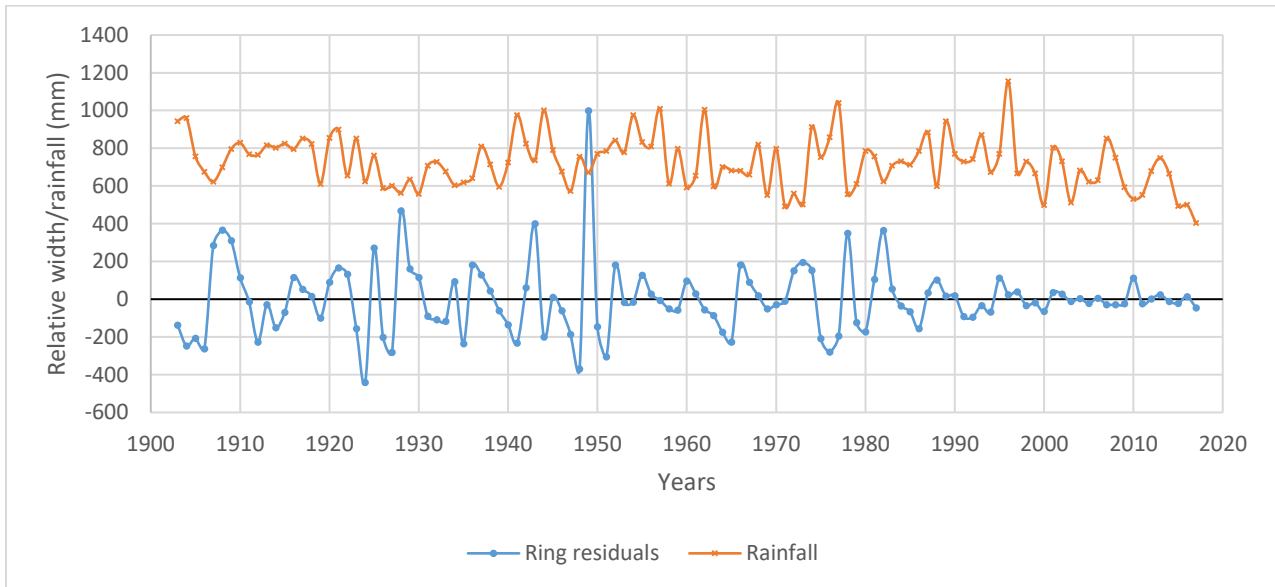


Figure 36: Plot of Tokai residuals and rainfall

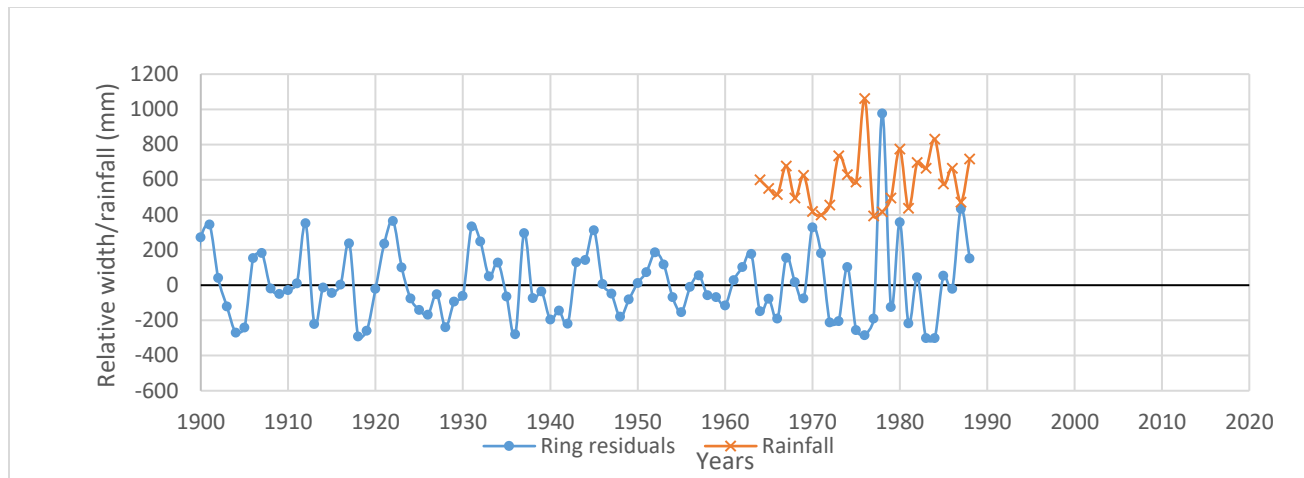


Figure 37: Plot of Wolseley residuals and rainfall

The correlations, which were resolved through the *Excel* “CORREL” function, are summarised in Table 4: Results of moving average and rainfall record correlations per location, and the complete spreadsheet of data and calculations, for all TSAP methods, can be found in Appendix A.2 Tables A4 to A6.

Table 4: Results of moving average and rainfall record correlations per location

Chronology	Calculated correlation
Bishopscourt	-0.014
Tokai	-0.138
Wolseley	-0.186

As denoted in Table 4, the calculated correlations for all the chronologies are negative – which is typically indicative of the one variable negatively influencing the other, meaning, in this scenario, that the rain would be stunting the growth of a tree. The negative correlations are, however, are near to zero meaning that the negative correlations are more likely indicative of the calculated correlation just being particularly poor and nearly non-existent.

The lack of correlation is seconded by visual inspection of Figures 35 through 37 as well as the original raw data sets’ plots (Figures 31 through 34).

In the case of Bishopscourt as previously mentioned when assessing the raw chronology’s trend, the growth trend appears to be the most similar of all the chronologies to its unshifted rainfall record, which supports that the calculated correlation (-0.014) is the “smallest” (nearest to zero). The width chronology, although not having a calculated correlation, does particularly bear the same trend as the Bishopscourt rainfall record for the 1941 to 1953 period, where after the growth appears to be one period after the rainfall (for example 1957’s rainfall increase and a 1958 growth increase). This possible lag is somewhat present in the rest of the growth chronology, although some of the smaller growth fluctuations need to be clustered together for this to hold true - for example the decreased 1988 rainfall would need to result in the decreased growth seen in 1988, 1990 and 1992. Furthermore, the extent of the variation of growth is far more extreme than that of the rainfall record; this is particularly noticeable in the growth depression in 1953-1954 (aligned with the decreased 1953 rainfall). The difference in the extent of the variation could,

perhaps, be considered plausible if there was some consistency to the scale of difference between the chronology and record, however there is not a clear and consistent multiplicative scale difference between the two series.

For Tokai, the significant decrease in the growth trend from 1992 to 2017, although stationary, is still remarkable. The outlying peak in 1949 is also still unexplained by the rainfall, as it remains notably out of scale with not only the rainfall record but also within the width residuals. As the Tokai sample is a composite of both Tokai samples, a visual reinspection of both samples is done to ascertain if there is a noticeably large ring width discrepancy in the physical samples. Whilst the *S. sempervirens* generally exhibits larger growth bands, there is a noticeably large band in the *C. lusitanica* sample occurring at the date. The large spike is thus due to the compounding of two large widths for 1949 in both samples – although it appears unrelated to the rainfall for Tokai.

Lastly, for the Wolseley chronology the lack of correlation is also apparent, particularly where the rainfall seems to decrease and the growth spike such as in 1970 and 1978. Unshifted, it appears to be the worst visual fit of all three chronologies, therein supporting the calculated results as Wolseley’s calculated correlation of -0.186 is the “most negative” (i.e. furthest from 0 and thus most distant from being correlated).

4.2 Time series analyses results

4.2.1 Stationarity validation

The stationarity of the data sets, both width and rainfall, was validated through the Augmented Dickey-Fuller (ADF) test for a unit root, completed in *EViews*. The following table summarises the results of the ADF for the three chronologies and respective rainfall records, where rejecting the null hypothesis equates to the data set being sufficiently stationary:

Table 5: Summary of ADF results

Location	Width			Rainfall		
	<i>t</i> -Statistic	Probability	Result	<i>t</i> -Statistic	Probability	Result
Bishopscourt	-7.26	0	Reject H_0	-7.708	0	Reject H_0
Tokai	-2.133	0.232	Accept H_0	-8.617	0	Reject H_0
Wolseley	-6.766	0	Reject H_0	-7.853	0	Reject H_0

As noted in the summary table, and previously in this document, the only chronology which is not sufficiently stationary is Tokai. As such, the log-return values were used in later time series-based analyses for Tokai. The resulting ADF, post taking the log-returns of the Tokai chronology, had a probability of 2.28% which was considered low enough for the resulting log-returned chronology to reject the null hypothesis and consider the chronology stationary.

4.2.2 Log-return results

For the respective locations, the log returns of the sample’s recorded widths and rainfall were calculated with *Excel*. The resulting log returns, which are stationary, could then have its correlation calculated and visually assessed through the plots of the log returns (Figures 38 through 41).

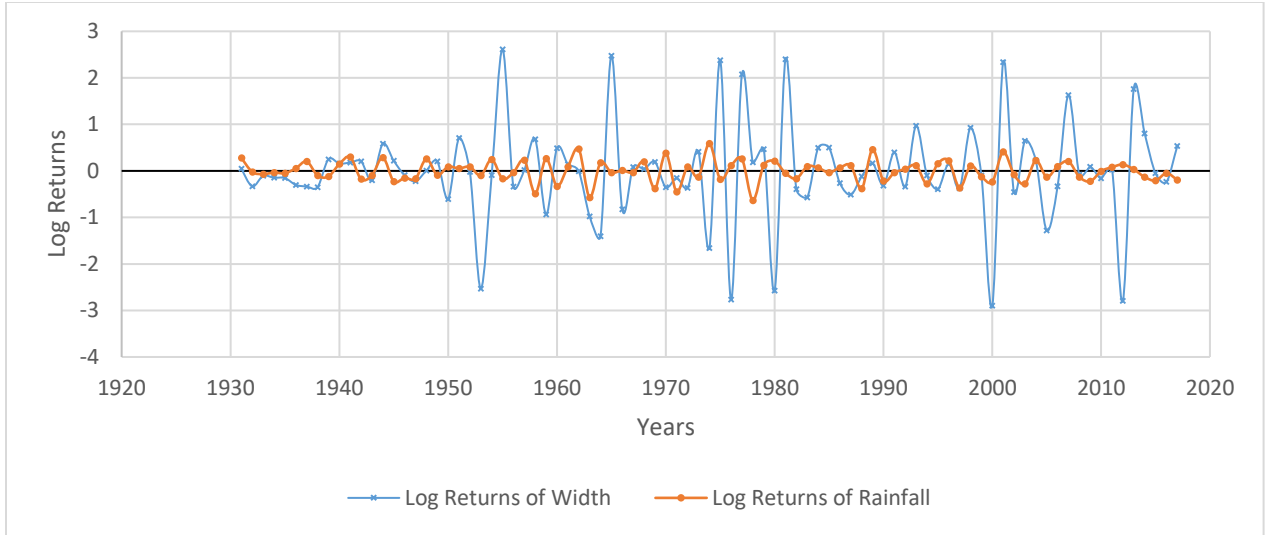


Figure 38: Plot of Bishopscourt log returns

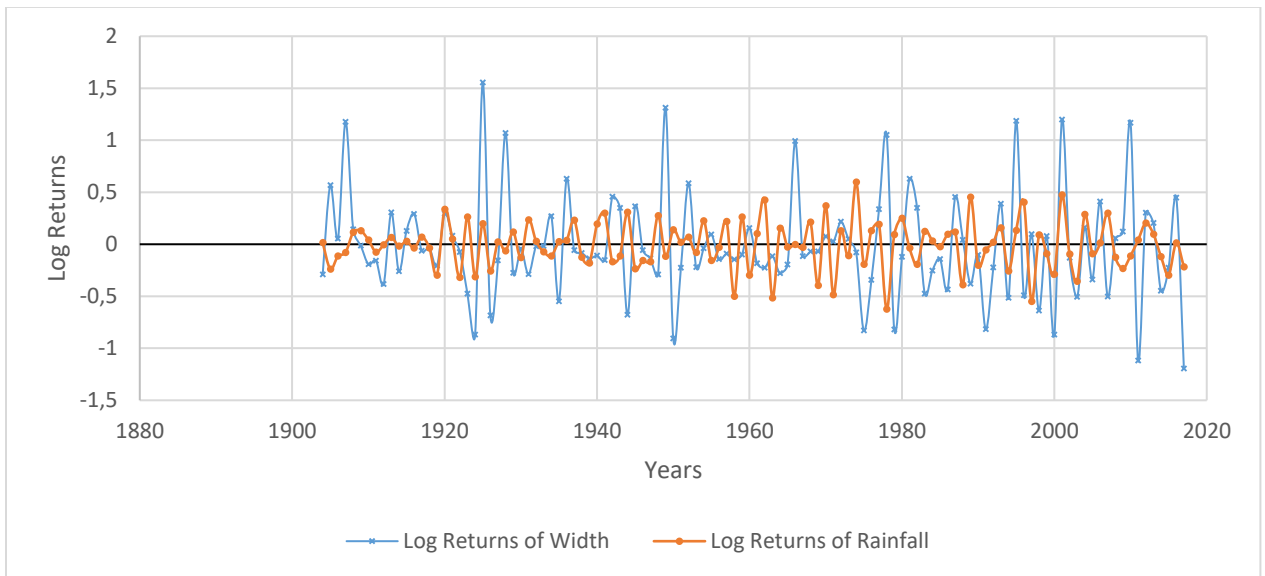


Figure 39: Plot of Tokai log returns

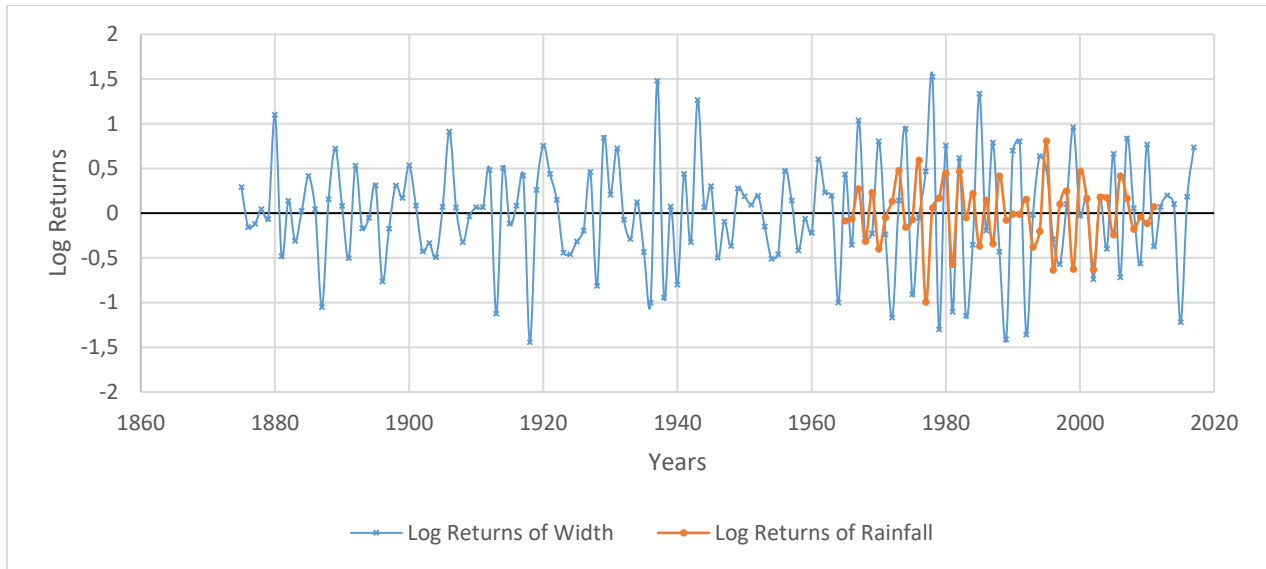


Figure 40: Plot of Wolsley log returns

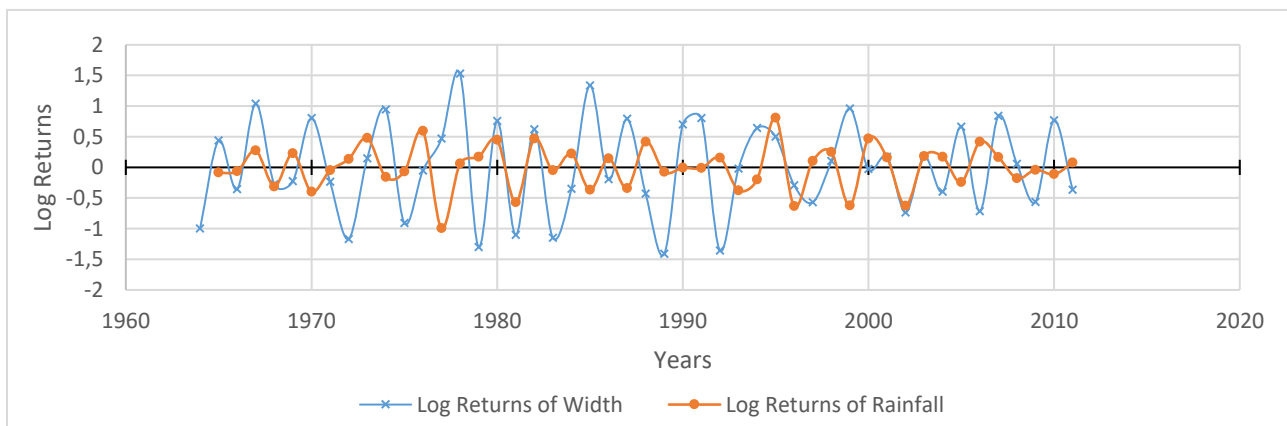


Figure 41: Plot of Wolsley log returns ("zoomed" in over period where both have records)

The calculated correlations, summarised by Table 6, once again indicate that there is not a correlation between the rainfall and tree's growth meaning that an extension of the rainfall record cannot accurately be completed.

Table 6: Results of log return of width and rainfall record correlations, per location

Chronology	Calculated correlation
Bishopscourt	-0.035
Tokai	-0.005
Wolsley	-0.034

The calculated correlations are noticeably changed from those calculated from the TSAP-Win residuals and raw rainfall record, although they all remain negative thereby indicating that there is no definable correlation between the ring width growth and the amount of rain within a given year. Both the Tokai and

Wolseley chronologies' correlations have increased in value (become closer to zero) with the greatest change occurring in the Wolseley data set where the correlation has increased from -0.186 by 0.152. The Tokai data set's correlation increased by 0.133 from -0.138 to the nearly zero correlation of -0.005. Conversely, the Bishops court correlation, which was previously the correlation nearest to zero, decreased (i.e. became more negative), decreasing by -0.021 to a value of -0.035.

Visually inspecting the generated plots, a noticeable trend across all the locations is that the rainfall's amplitude is appreciably smaller than the amplitude of the growth, however this does not necessarily negate the possibility of a correlation – although in this study's scenario it is an indicator of the lack of correlation. Once again, the Bishops court chronology appears to be experiencing a delay of a year but earlier than the 1953 date noted in the residual's plot, with the lag appearing to begin from 1949 (due to 1948 rainfall season).

The amplitude of the rainfall is somewhat more similar to that exhibited by the rainfall for the Tokai data set, however, as previously mentioned, it is still not to the same extent as what is seen for the growth. The ten-year period from 1954 to 1964 is particularly asynchronous, with the peaks in the rainfall record occurring simultaneously with a pit of the growth chronology. This suggests that the growth may be lagged, although more generally the rainfall record is synchronous with the growth chronology meaning that shifting the growth chronology along will most likely not improve the correlation. A particularly good match between the data sets can be found within the earlier years of the data set with 1919 and 1920 having a near perfect fit and 2000 to 2004 being completely synchronous. Additionally, the issue of interpreting and relating to the sharp decline in growth from 1986 onwards is resolved through the log-return process. As seen with the results of the calculated correlations for this method, the benefit of stationarity is most clearly exhibited in the reduction of Tokai's negative correlation. Nevertheless, the data is still uncorrelated and not suitable for a rainfall reconstruction in Tokai.

Although Wolseley exhibits synchronicity for 1980-1983, the logged rainfall record for Wolseley is generally asynchronous with the growth record supporting the result of the larger negative correlation calculated for Wolseley log returns. As with the other chronologies, this may suggest a lag factor resulting in a lack of correlation and, as before, the possibility of lag is to be investigated.

4.2.3 Lag results

As the TSAP and log-return analyses failed to find any correlations, consideration was given to the possibility of the chronologies needing to be lagged as the response of growth following rain may be delayed. To resolve the lag, a periodogram was plotted for each of the locations using the stationary form of all the respective data sets and the ACF, PACF and cross-correlations resolved however before the aforementioned could be resolved, the stationarity of the data had to be validated. If the data sets were not stationary, the values of the log-returns are used in determining the ACF, PACF and cross-correlations.

The data used for the ACF, PACF and cross-correlations must be stationary, thus using the results from the ADF it was determined that only the Tokai chronology's data needed to be logged, whilst the Bishops court and Wolseley samples' original chronologies were sufficiently stationary. The correlation plots of the unlogged Tokai data set are, however, included for completeness. The plots of the various correlation functions are included in the relevant subsections below, however the tabulated results, calculated in *Statistica*, for each location can be found in Appendix B.1 Tables B1 to B4.

4.2.3.1 Bishops court

The standard errors calculated for the PACF of Bishops court results in a constant across all periods, at a value of 0.1066. The consistency of the value within the PACF is to be expected as it is indicative of the data's stationarity as well as the constant noise left in the system; in other words, it confirms the success of the standardisation process as the varying influence of age has been successfully removed but suggests the need for further time series analysis methods, such as an AR, MA or ARMA model.

Visually inspecting the ACF and PACF plots (Figures 42 and 43) generated in *Statistica* for Bishops court's relative width chronology, two periods clearly exceed the prescribed confidence limits, namely period 1 and period 10. This would suggest that there is possibly a lag of either one or 10 years in the growth following annual rainfall events, however the ACF and PACF alone cannot be relied upon to draw a conclusion.

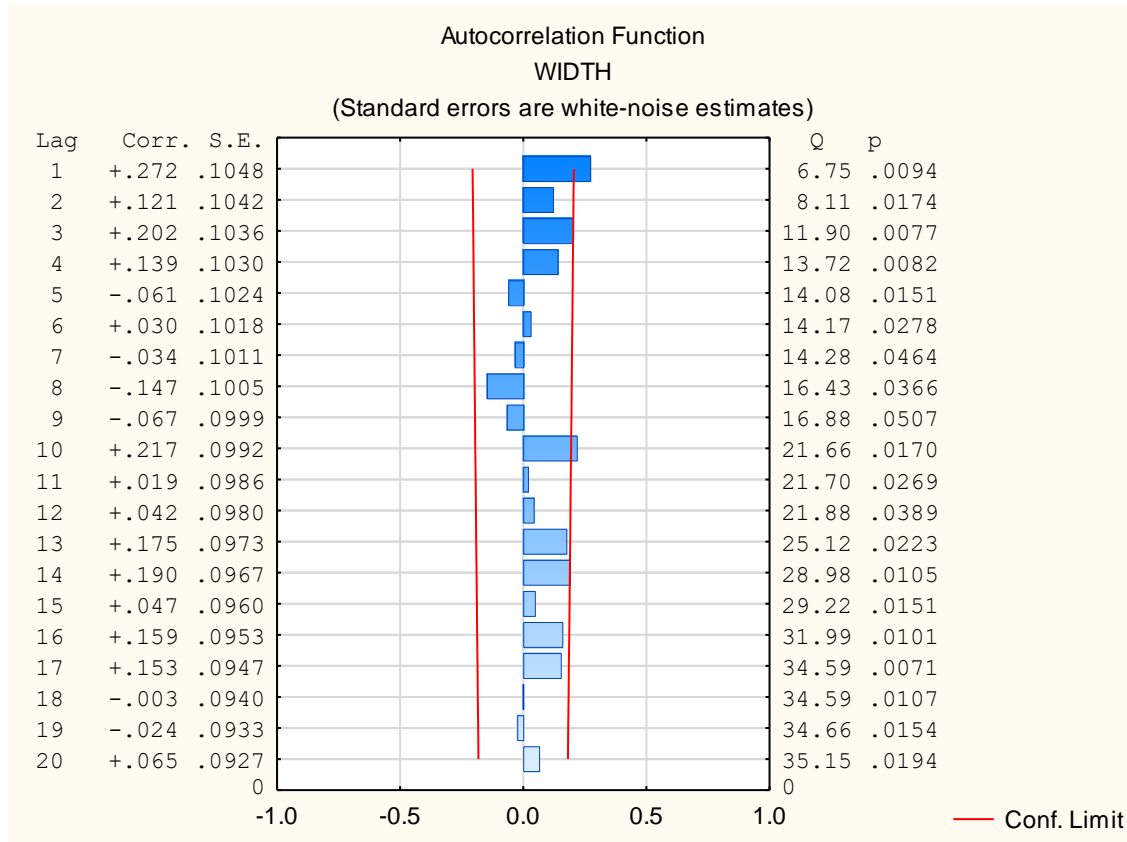


Figure 42: Plot of the autocorrelation function - Bishops court

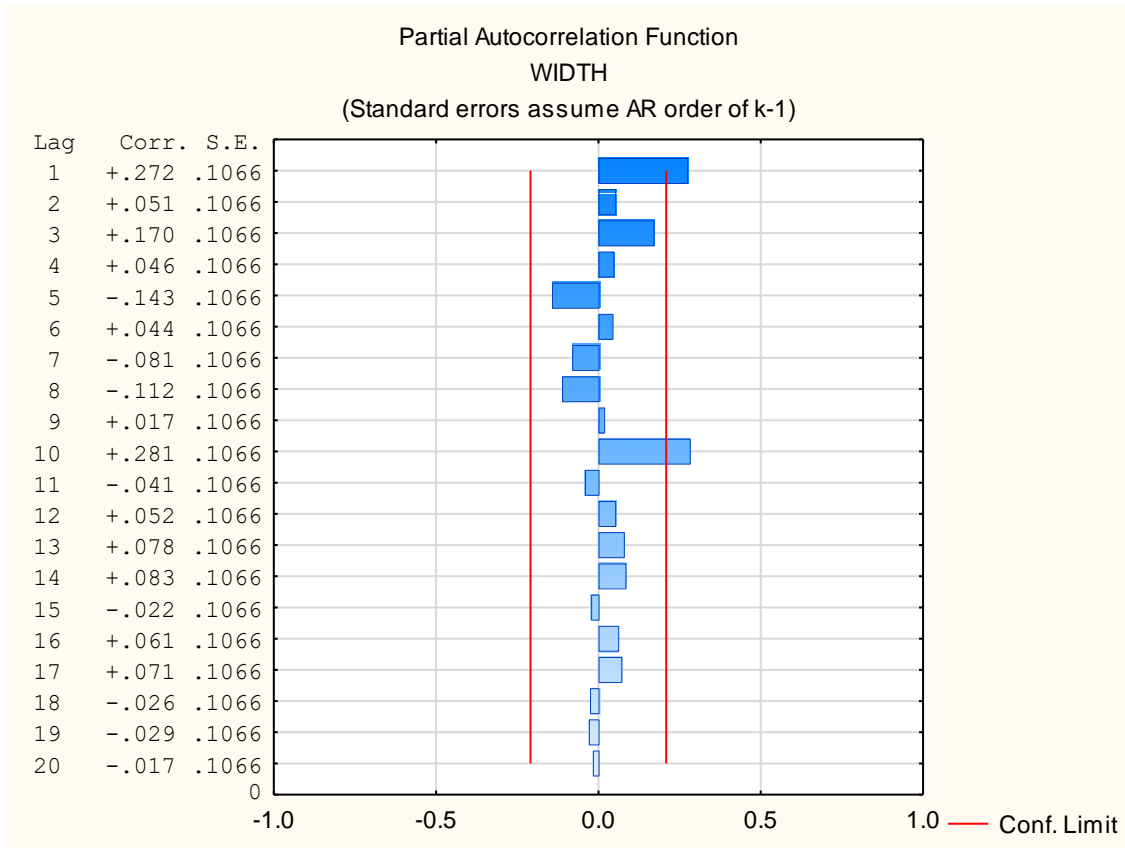


Figure 43: Plot of the partial autocorrelation function – Bishopscourt

As such, the cross-correlations are also resolved and plotted (Figure 44), wherein the 1st lag period does not present any exceedance of the confidence limits and the 10th lag narrowly falls within the confidence limit. Furthermore, as noted in Figure 44, the 4th historic lag period (the -4 period) now becomes the period to exceed the confidence limit thus suggesting the possibility of a four-year lag, however four years in the future (4th period) does not reflect the possibility of a consistent lag. Additionally, none of the identified possible lags occur cyclically, with neither factor of 10 (such as the 20th period) or one resulting in the exceedance of the confidence limit. As there is no discernible pattern within the factors, it was determined that it is, thus, unlikely that there is a consistent lag period within the chronology.

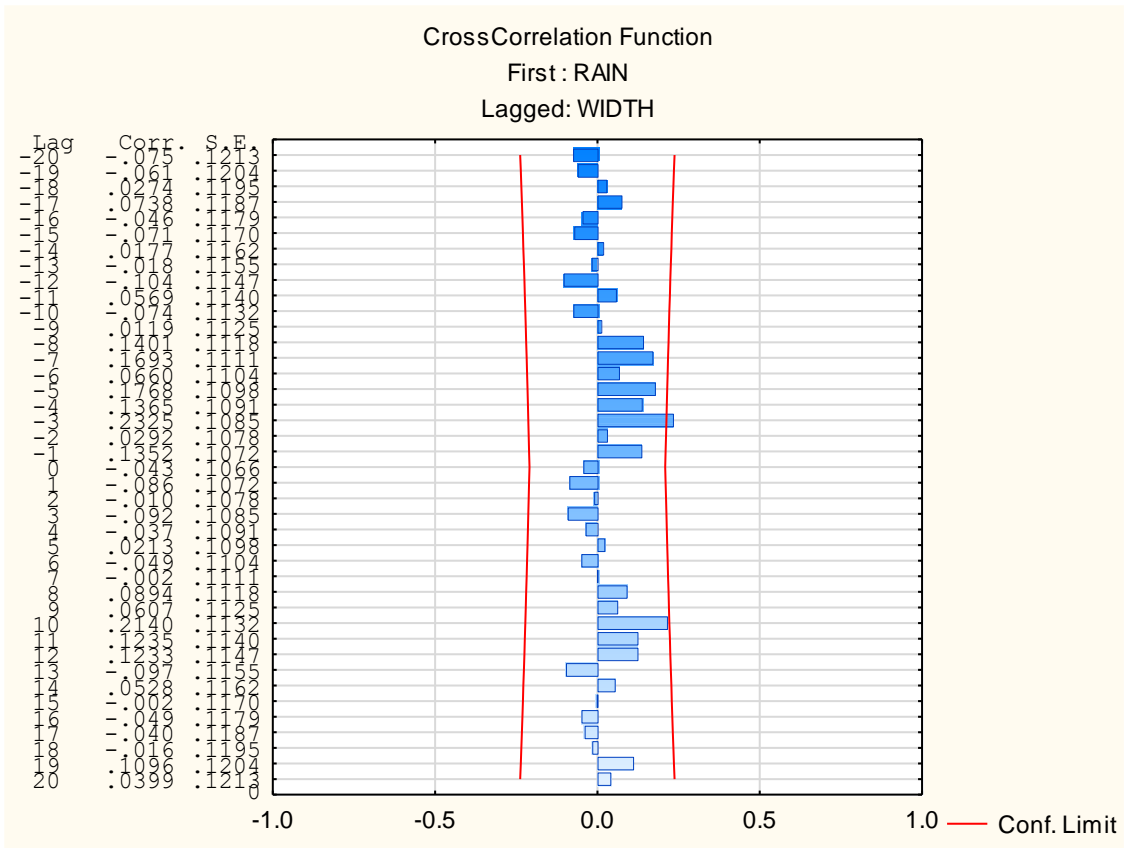


Figure 44: Plot of the cross-correlation function – Bishopscourt

4.2.3.2 Tokai

4.2.3.2.1 Original, non-stationary data set

The calculated ACF, and subsequent PACF, for Tokai indicates multiple possibilities for lag with periods 1, 2, 5, 6 and 16 all exceeding the confidence limits in the ACF (Figure 45) and periods 1, 2 and 5 exceeding the limits in the PACF (Figure 46). It thus follows that the 1st, 2nd and 5th periods are all possible lags, however due to the lack of exceedance in the other factors of these intervals (such as the 10th period – a factor of both 2 and 5) it appears unlikely that there is a regular cycle.

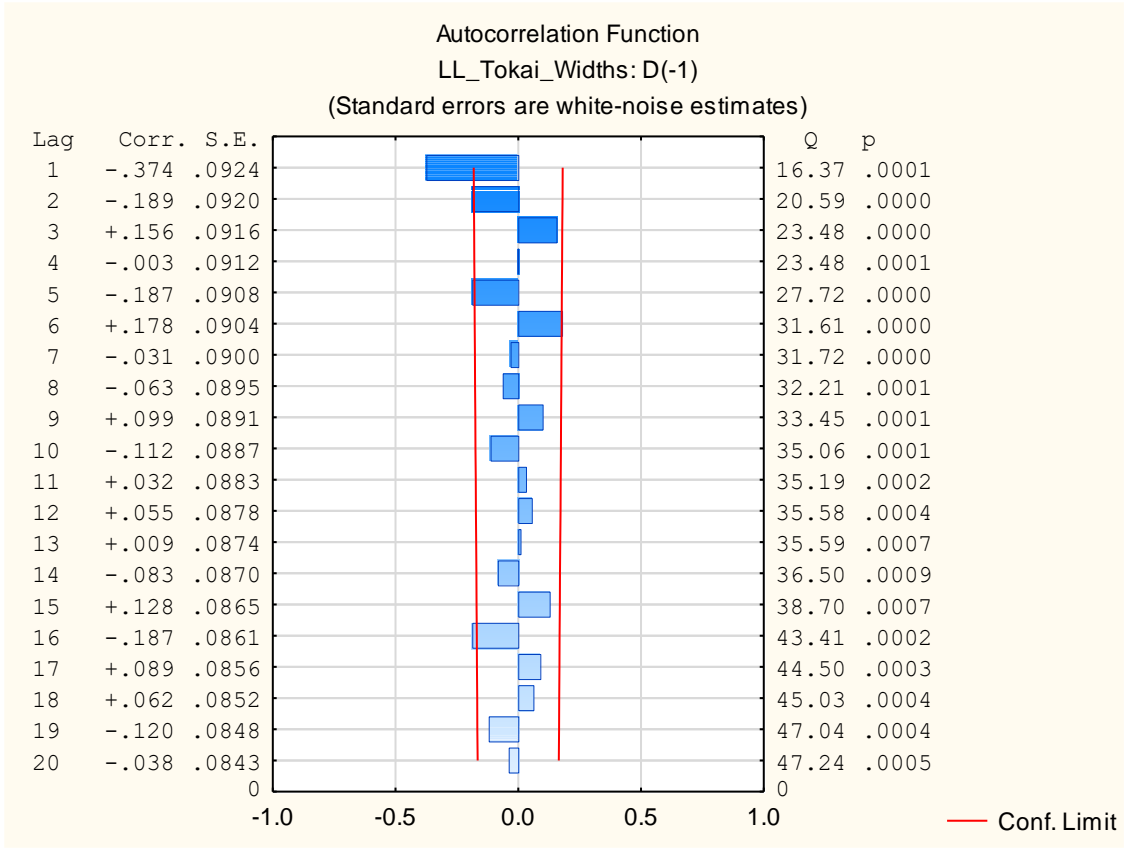


Figure 45: Plot of the autocorrelation function - Tokai

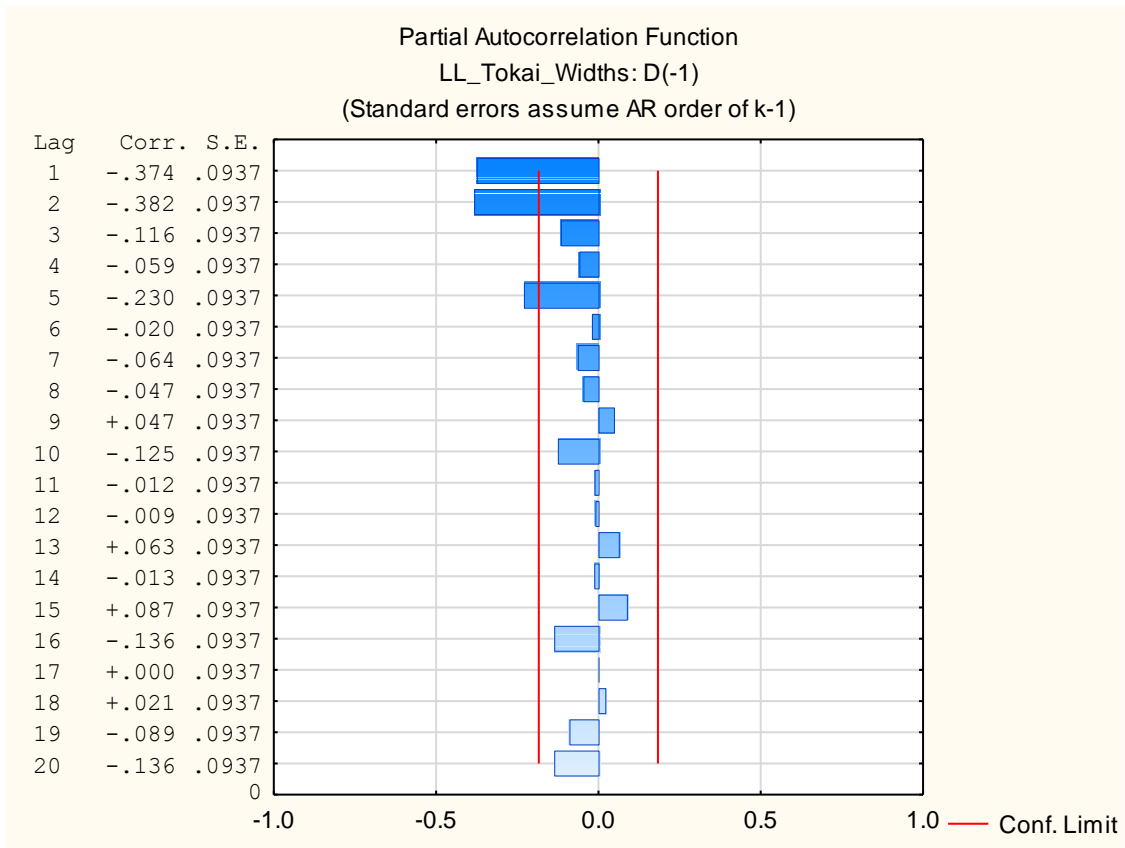


Figure 46: Plot of the partial autocorrelation function – Tokai

Upon reviewing the cross-correlation plot (Figure 47), the multiple potential lags are again noted with periods two through five and seven, eight and thirteen all exceeding the confidence limits. As with the ACF and PACF, however, none of these appear to consistently repeat across the series implying the unlikelihood of there being seasonality. The 2nd period does, however, appear as an exceeding period across all correlative plots and was thus, finally, validated for any cyclicity by means of a smoothed periodogram.

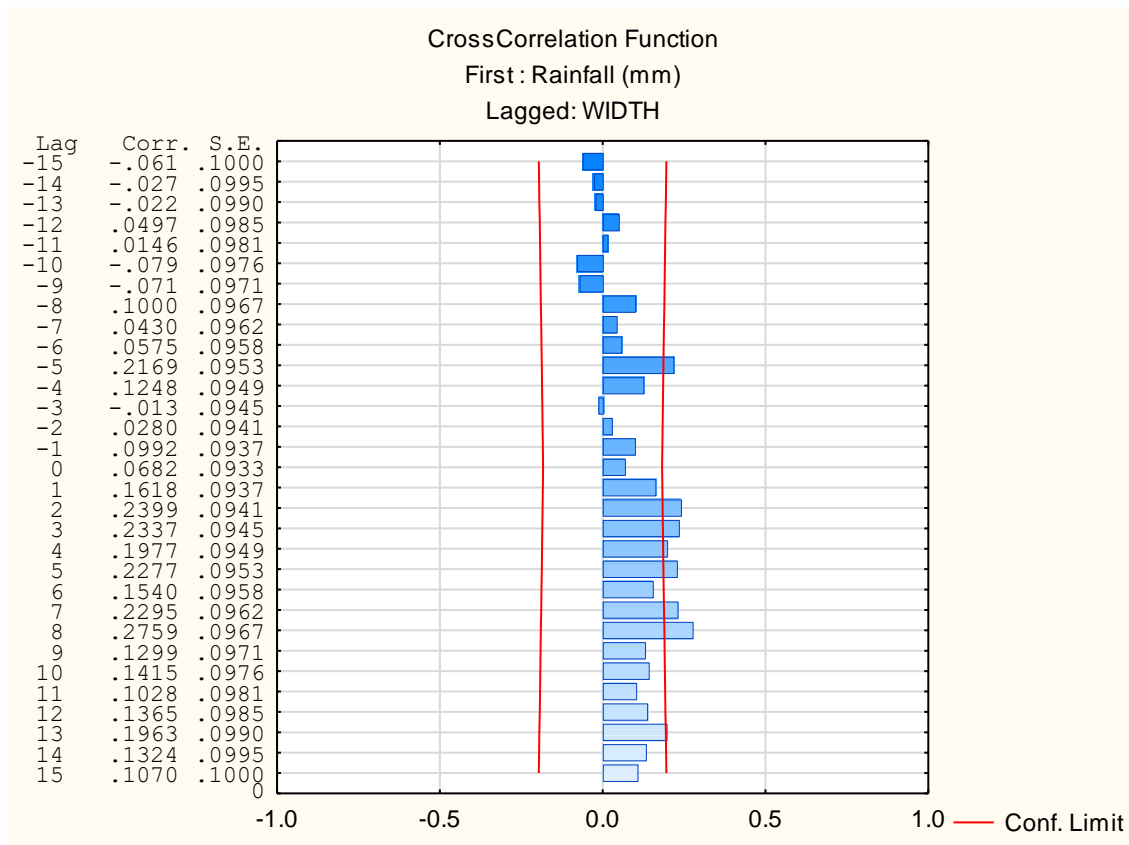


Figure 47: Plot of cross-correlation function – Tokai

Following the correlative functions being resolved and plotted, the possibility of the 2-year cycle was finally assessed by means of a periodogram (Figure 48). The periodogram, however, definitively illustrates that whilst there are fluctuations which relate to the noted possible lag periods, none of the fluctuations can be considered consistent or cyclical therefore removing the possibility of defining a consistent lag for the Tokai series. Furthermore, when reviewing the plot (Figure 49) of the spectral analysis post-filter, the lag period appears to be 38-years, which far exceeds any of the previously suggested lags and in so doing invalidates the possibility of any of the previous values being the correct lag period.

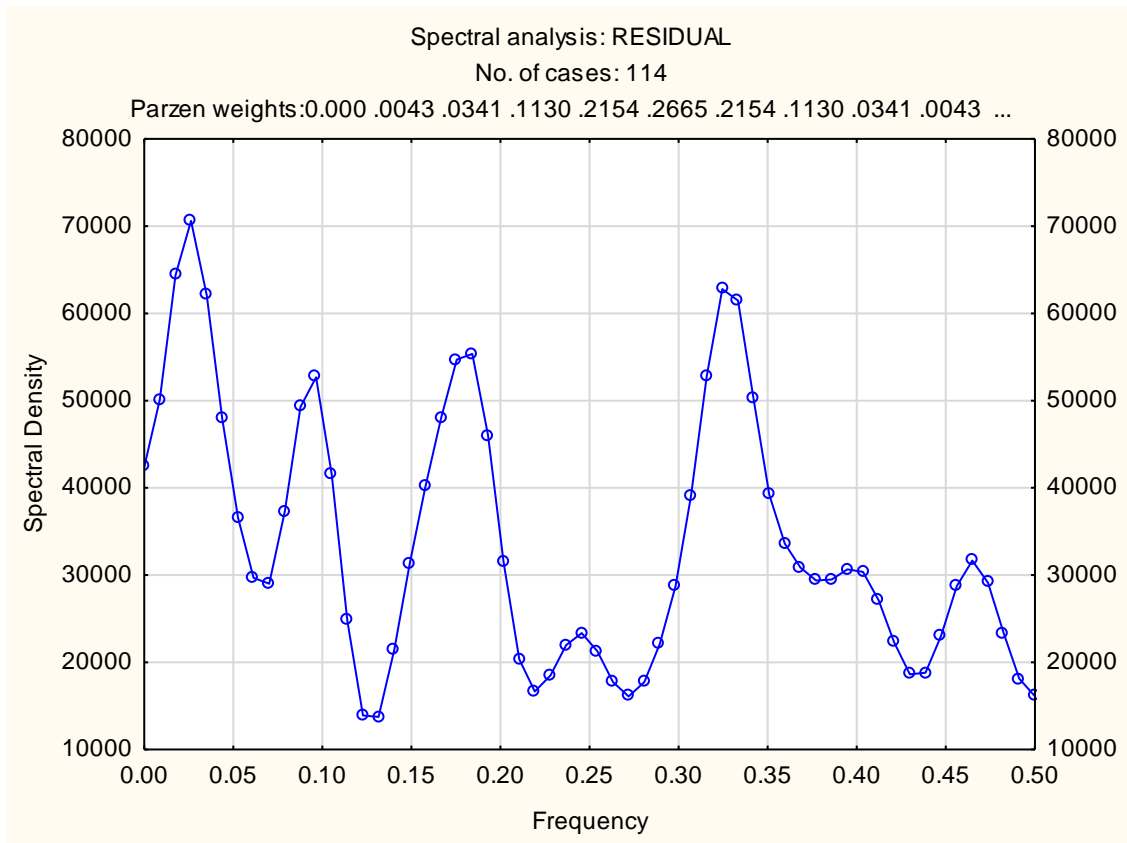


Figure 48: Periodogram, smoothed with Parzen filter, of width chronology – Tokai

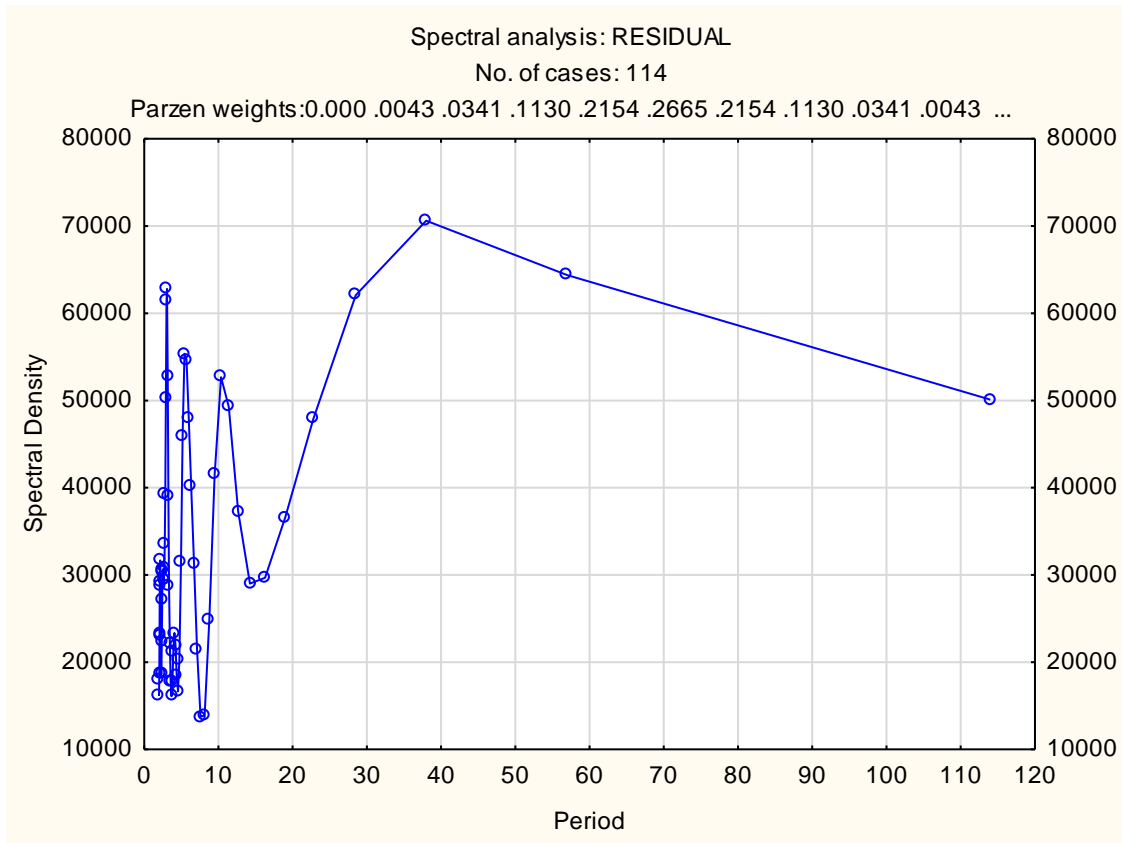


Figure 49: Plot of the spectral analysis, smoothed with Parzen filter, of width chronology – Tokai

4.2.3.2.2 Logged, stationary data set

The ACF and PACF, as seen in *EViews*, is illustrated by Figure 50 here, where it is evident that the first, second and fifth periods are again possible lag periods for the data set.

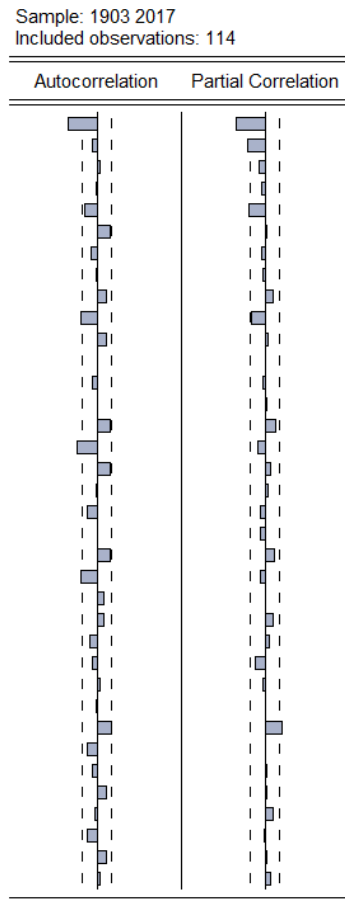


Figure 50: Plots of autocorrelation and partial autocorrelation function - Tokai (logged)

When comparing the plot with the unlogged data set, the potential lag periods are all identical to those identified previously, although the extent to which the functions exceed the confidence limits are less. Nevertheless, the same potential lag periods were validated through comparison with the cross-correlation plot (Figure 51), which, again, failed to validate the identified periods as consistent lag periods.

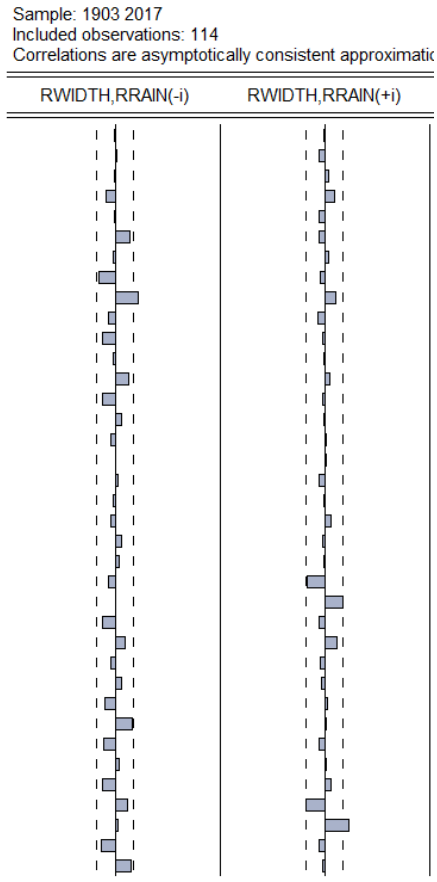


Figure 51: Plot of cross-correlation function – Tokai (logged)

4.2.3.3 Wolseley

When evaluating the results of the ACF and PACF for Wolseley (Figures 52 and 53) the possibility that there may be no need for an ARMA model becomes apparent as no single period stands out as an exclusion from the prescribed confidence intervals. Additionally, the lack of an exceeding autocorrelation value for any given period further implies that there is no cycle or noticeable lag in the Wolseley data set.

For the PACF, however, a single period narrowly exceeds the confidence limits. The sixth period, which was the closest to exceeding the confidence interval in the ACF, exceeds the 90% confidence prescribed by the PACF and, as such, could be considered when evaluating for the possibility of lag.

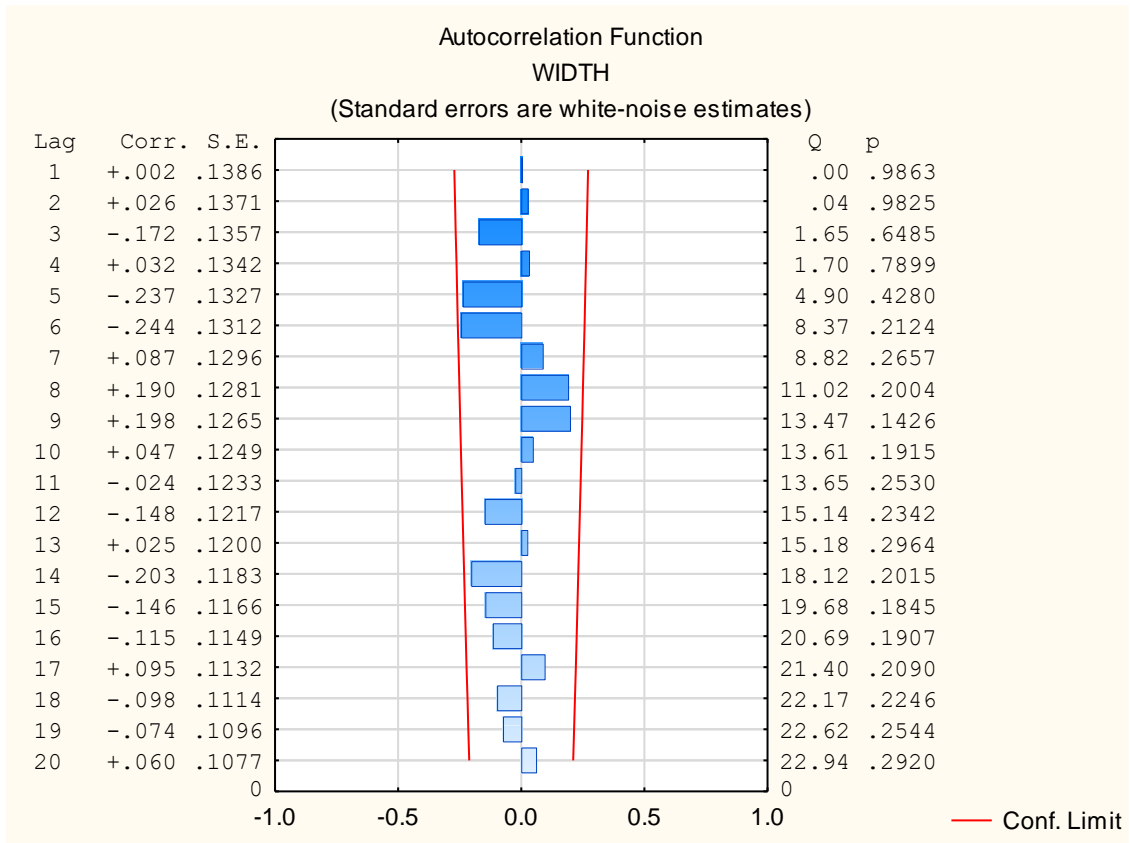


Figure 52: Plot of autocorrelation function – Wolseley

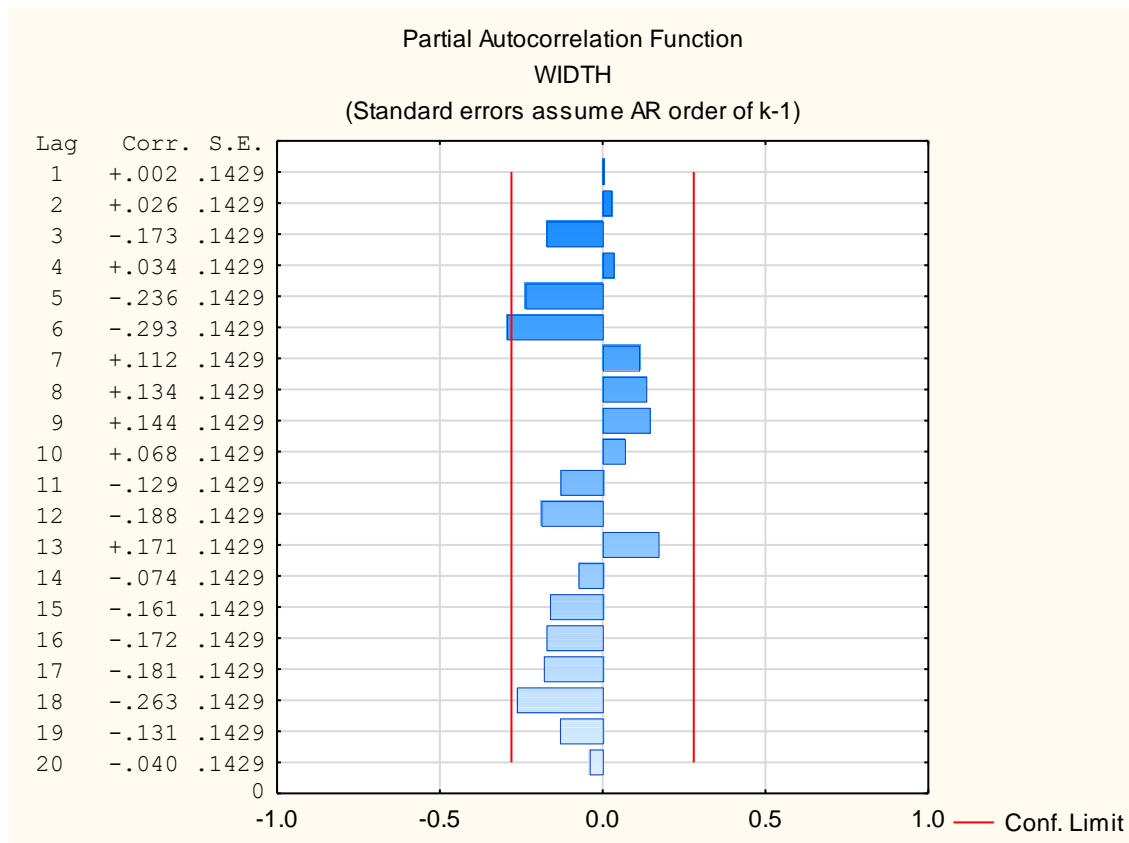


Figure 53: Plot of partial autocorrelation function – Wolseley

The sixth period again becomes a period of interest in the cross-correlations, but so too does the 8th period in the past (period -8), as seen in Figure 54. Due to both the -8th and 6th periods exceeding the confidence limit set out for the cross-correlation function, the possibility of a 2, 6 or 8-year cycle was investigated through spectral analyses. Whilst it was already known to be unlikely that there was a 6 or 8-year cycle given that neither the positive 8th period nor the 12th period (a factor of 6) exceeded the confidence limit, the possibility was not outrightly excluded. The possibility of a two year cycle was included as two is a factor of both six and eight, and as both periods had exceedances the cycle could be a factor common to both – although, again, it was unlikely to be the case as neither the 2nd nor the 4th period had an exceedance.

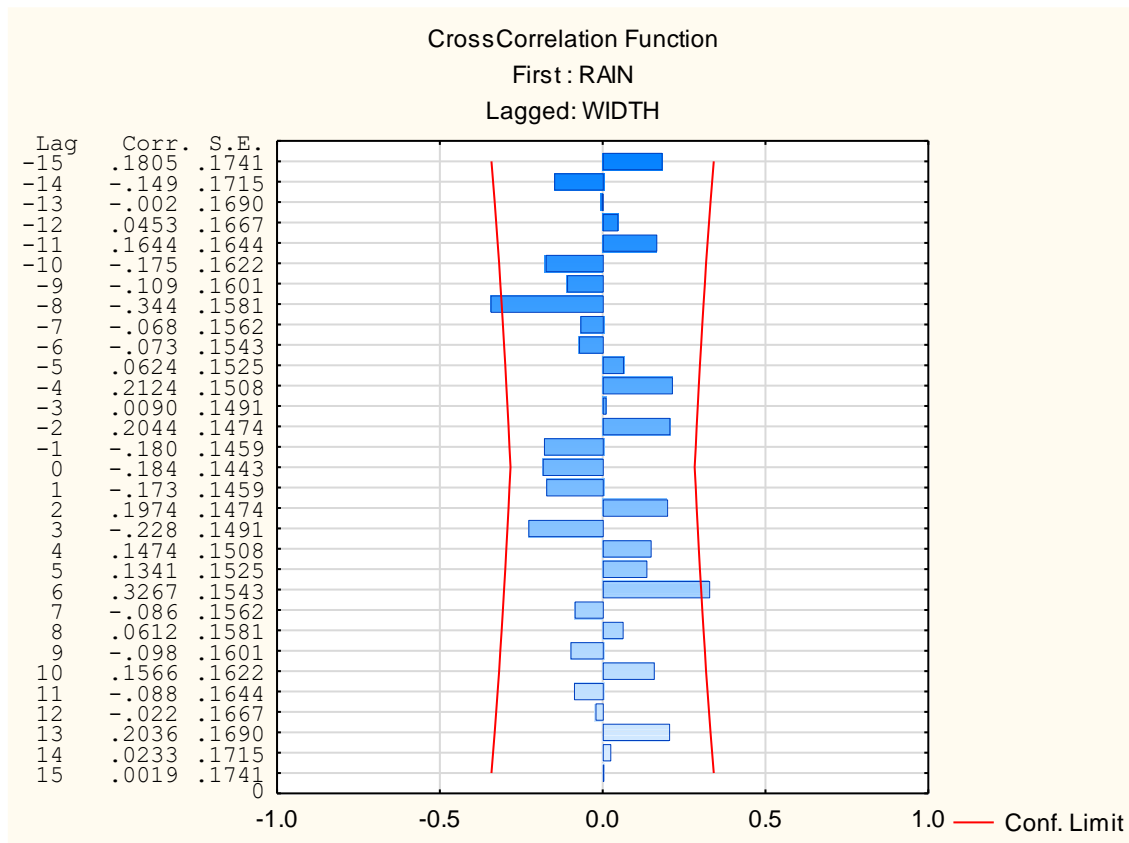


Figure 54: Plot of cross-correlation function – Wolseley

Upon evaluation of the smoothed periodogram (Figure 55), it is apparent that there is not a regular cycle or distinct lag pattern followed within the growth chronology. Whilst the noted exceedance does result in variation within the periodogram, these exceedances remain inconsistent and thus cannot be clearly categorised as a suitable lag period by which the chronology may be shifted.

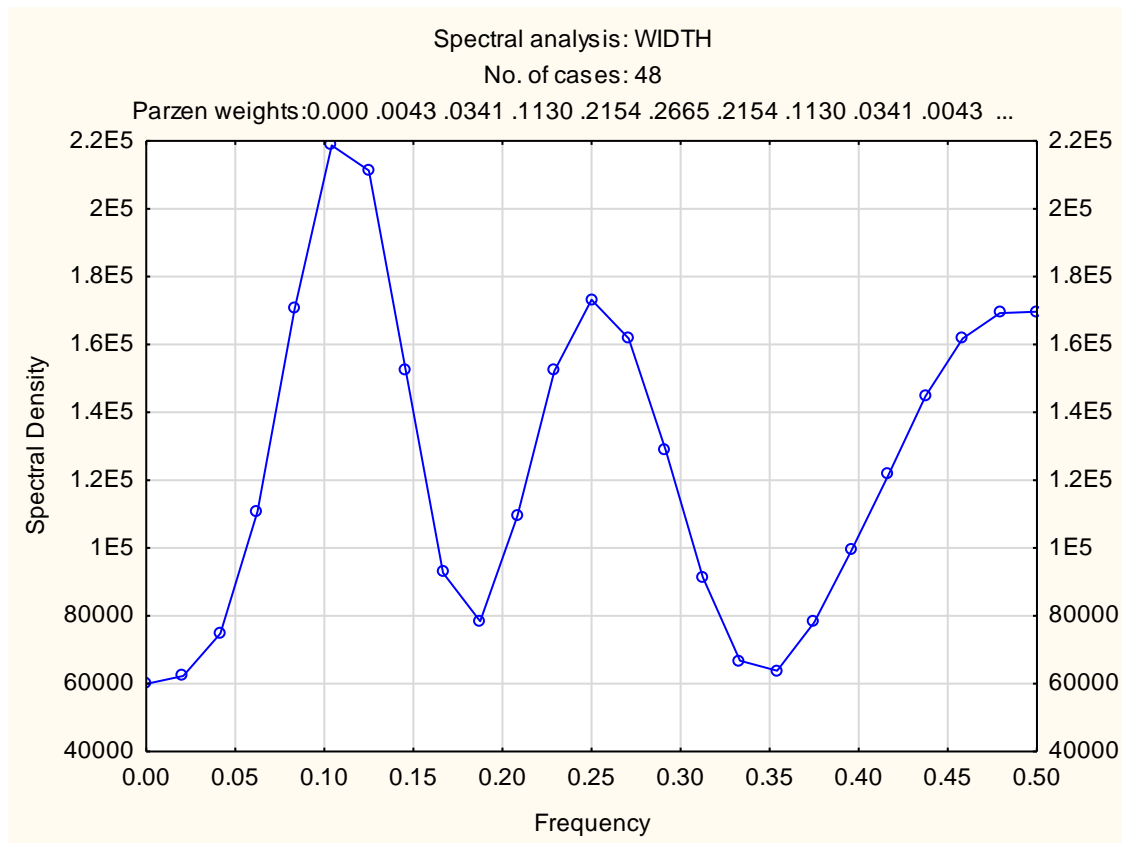


Figure 55: Periodogram, smoothed with Parzen filter, on width chronology – Wolseley

4.2.4 Regression and ARMA model results

This section will detail the results of the initial least squares regression completed on the data sets and, where appropriate, define the ARMA model generated to best approximate and analyse the data.

4.2.4.1 Bishopscourt

For Bishopscourt it was determined that an ARMA model was required, as the Durbin-Watson statistic calculated from the least squares regression was only 1.38 – well below the ideal value of 2. The entire results of this regression, as calculated in *EViews*, can be found in Appendix B.2 Table B5.

As an ARMA model was required, the order of the model was determined by the results of the Bishopscourt ACF and PACF, where the periods exceeding the confidence limits are considered viable orders for the model. As both the ACF and PACF highlighted the first and 10th periods, a composite of order 10 was generated within *EViews*. Table 7, below, summarises the results of the ARMA(10) model, which was deemed sufficient as the Durbin-Watson statistic of 1.96 is near to the requisite 2.

Table 7: Summary of Bishopscourt ARMA model results

Variable	Coefficient	Standard Error
C	547.245	141.231
Rain	-0.174	0.219
AR(10)	0.286	0.109
Descriptive Statistics		
R^2		0.161
Adjusted R^2		0.12
Durbin-Watson		1.96

As defined in the descriptive statistics of the above table, the correlation coefficient (R^2) for the Bishopscourt chronology is weak at 16.1% for a 10-year cycle. There is, thus, no possibility of reliably extending or modelling with the Bishopscourt rainfall record.

4.2.4.2 Tokai

As the Tokai data set was not originally stationary, the log-retained values were utilised in the analyses where the width series remained the dependent variable series. The original, unlogged data set was, however, also analysed through the same techniques as the logged, stationary data – primarily to illustrate the effect of stationarity on the correlation results.

4.2.4.2.1 Original, non-stationary data set

The completed least squares regression yielded a Durbin-Watson statistic of 0.696, which is significantly below the required value of 2 thereby necessitating the generation of an ARMA model to analyse the non-stationary Tokai chronology with respect to the rainfall. The complete least squares regression, completed in *EViews*, can be found in Appendix B.2 Table B6.

Utilising the results of the ACF and PACF, the order of the Tokai ARMA model could be resolved for the original data set – although the correlation plots highlighted multiple possible lag periods, thus leaving many options for the ARMA model's order. As ARMA models must be parsimonious, a first attempt at constructing the ARMA model was completed using the orders of one, two and three (i.e. AR(1), AR(2) and AR(3) were all compared). The complete results of this calculation can be found in Appendix B.3 Table B11.

The results of this first attempt make it clear that a model comprised of all three is not necessary, with AR(2) yielding a significantly higher probability (48.14%) than AR(1) (0%) or AR(3) (0.3%). It thus follows that AR(2) is an unnecessary inclusion within the model, and a second calculation was completed only with AR(1) and AR(3) as the possible orders.

The results of the second ARMA estimations validate the unnecessary inclusion of AR(2) as an order, with the AR(3) model successfully producing a satisfactory Durbin-Watson statistic of 2.137. The results of the model are summarised by Table 8:

Table 8: Summary of Tokai ARMA model results - original

Variable	Coefficient	Standard Error
C	578.193	195.95
Rain	-0.181	0.197
AR(3)	0.356	0.088
Descriptive Statistics		
R^2	0.53	
Adjusted R^2	0.513	
Durbin-Watson	2.137	

As expected given that it is the best correlation amongst precursory analysis methods, the correlation of coefficient for the Tokai series, at 53%, outstrips all the other samples to be the best match within in the research – nevertheless, this is still not statistically significant enough to accurately extend a rainfall record or model the microclimate within Tokai although it does serve to prove the potential when using more alien samples for further study. Additionally, this model serves mostly as an estimator of the forecast as it is not recommended to use AR techniques on non-stationary data although it is worth noting that this is the only correlation to be somewhat within the realm of reasonable correlation.

4.2.4.2.2 Logged, stationary data set

As with the non-stationary data set, the Durbin-Watson statistic was resolved for a least squares approximation of the logged width, dependent on the logged rainfall and was determined to be more than the requisite 2 at a value of 2.662. As such, it is possible that there is slight negative autocorrelation and investigation into modelling by means of an ARMA process is required. The complete least squares results, as processed in *EViews*, can be found in Appendix B.2 Table B7.

As with the original data set, the ACF and PACF can be used to identify possible orders of the ARMA process which best suits the stationary data set. From the ACF and PACF, periods 1, 2 and 5 were noted as potential orders, however, to remain parsimonious orders which resulted in a significant probability (i.e. substantially greater than zero) were excluded from the final model. The complete results and development of the ARMA model can be found in Appendix B.3 Table B12.

When undertaking the evaluation for which order the process is, AR processes of both the third and second order resulted in unsatisfactorily high probabilities – when processing AR(1) through AR(3), AR(3) resulted in a 38.11% probability whilst AR(2) resulted in a 4.07% probability. The Durbin-Watson statistic was also an unsatisfactory 1.96, thereby necessitating the removal of the third and second orders resulting in just a first order model.

The AR(1) process, which yielded a satisfactory Durbin-Watson statistic of 2.122 was, however, not the final consideration. Recalling the Monseraud suggested that ARMA(1,1) is the perfect “universal” model, an ARMA(1,1) process was fitted to the stationary Tokai data and another satisfactory Durbin-Watson statistic of 1.96 was determined. The resulting correlation coefficient is also improved by using the ARMA(1,1) process, with the correlation improving from 13.45% to 20.4%. The final results for the stationary Tokai data set, using ARMA(1,1) is summarised by Table 9:

Table 9: Summary of Tokai ARMA results - logged

Variable	Coefficient	Standard Error
C	-0.016	0.0186
Rain (logged)	-0.059	0.251
AR(1)	0.219	0.171
MA(1)	-0.726	0.134
Descriptive Statistics		
R^2	0.204	
Adjusted R^2	0.175	
Durbin-Watson	1.958	

As illustrated in Table 9, the R^2 is a weak 20.4%, which is an unsatisfactory result that does not support the extension of the stationary rainfall record for Tokai or the use of the Tokai chronology for climatic modelling.

4.2.4.3 Wolseley

The least squares regression completed on the Wolseley width chronology yielded a Durbin-Watson statistic of 2.1, which is very near to the ideal value of 2, thereby dismissing the need for an AR, MA or ARMA model as the least square regression adequately models the series. The complete, tabulated results from the least squares regression can be found in Appendix B.2 Table B8, whilst the key information, such as the correlation coefficient, is summarised by Table 10.

Table 10: Summary of Wolseley least squares regression results

Variable	Coefficient	Standard Error
C	606.723	153.84
Rain	-0.314	0.25
Descriptive Statistics		
R^2	0.033	
Adjusted R^2	0.012	
Durbin-Watson	2.104	

The results of this chronology's correlation are, however, even poorer than the other two locations' chronologies with a near negligible correlation coefficient of 3.32%. The Wolseley chronology can therefore not be used for climatic modelling or to extend the Wolseley rainfall record.

4.3 Application of statistical methods on existing chronology

Given that none of the samples obtained for this research yielded satisfactory correlations, additional consideration was given to applying the analysis techniques on an existing, validated chronology built from more samples, namely the "Die Bos" study completed in 1979 by LaMarche and Dunwiddie.

The standardised width indices for the "Die Bos" study were provided in the report compiled by LaMarche and Dunwiddie, and the chronology extends from 1564 to 1976. This 416-year old chronology is not only an improvement upon the sample chronologies used in this research because of its length, but also as it is comprised of 32 samples which were all cross-dated and referenced to compile a far more extensive chronology.

As discussed in the literature, the original “Die Bos” study concluded that whilst there was significant correlation to be found between the chosen rainfall record and width chronology, the correlation was only successful for an 18-month period after which there appeared to be discord between the two series, with the rainfall and width increasing and decreasing in different periods.

Whilst the exact, original rainfall record used in the “Die Bos” study is not elucidated upon in the report, or available on the ITRDB, the new CRU gridded rainfall data from the National Centre for Atmospheric Research allows for nearly the exact region’s rainfall record for 1901 to 2017 to be obtained. Given that the “Die Bos” location was provided as 32° 24’ S; 19° 14’ E, the rainfall could be interpolated from the CRU gridded data at 32°25 S; 18° 75’ E and 32°25 S; 19° 25’ E, with the used rainfall record being for the near-site location of 32°25 S; 19° 14’ E.

Once this alternative rainfall record was obtained, the same process of resolving the ACF and PACF to seek out lag periods and characteristic periods can be completed, in addition to trying to fit a suitable model to define the correlation between the common period of 1901 to 1976 of the alternative rainfall record and standardised chronology.

4.3.1 Lag results

The lag of the “Die Bos” study’s standardised width chronology was investigated, as before, by correlograms. The resulting ACF and PACF, see Figure 56, illustrates that the first and second periods are in exceedance of the confidence limits for both the ACF and PACF, thus making these periods the main periods of interest as potential lags. Other periods, such as the third through to the seventh also exceeded the confidence limits in the ACF plot although they did not exceed in the PACF plot. For the PACF, only the first, second and ninth periods exceeded the confidence intervals.

Autocorrelation	Partial Correlation	AC	PAC	Q-Stat	Prob	
		1	0.601	0.601	150.12	0.000
		2	0.430	0.108	227.22	0.000
		3	0.315	0.031	268.63	0.000
		4	0.216	-0.015	288.14	0.000
		5	0.187	0.055	302.78	0.000
		6	0.156	0.019	313.03	0.000
		7	0.095	-0.046	316.82	0.000
		8	0.059	-0.014	318.31	0.000
		9	-0.025	-0.100	318.58	0.000
		10	-0.068	-0.038	320.54	0.000
		11	-0.045	0.046	321.39	0.000
		12	-0.059	-0.025	322.86	0.000
		13	-0.087	-0.057	326.10	0.000
		14	-0.102	-0.030	330.61	0.000
		15	-0.076	0.049	333.10	0.000
		16	-0.080	-0.024	335.85	0.000
		17	-0.073	-0.011	338.18	0.000
		18	-0.036	0.042	338.74	0.000
		19	0.009	0.052	338.77	0.000
		20	-0.004	-0.037	338.78	0.000
		21	-0.025	-0.040	339.05	0.000
		22	-0.062	-0.062	340.73	0.000
		23	-0.019	0.059	340.89	0.000
		24	0.013	0.036	340.96	0.000
		25	0.056	0.056	342.35	0.000
		26	0.093	0.036	346.17	0.000
		27	0.073	-0.029	348.52	0.000
		28	0.039	-0.022	349.19	0.000
		29	0.042	0.026	349.99	0.000
		30	0.025	-0.031	350.26	0.000
		31	0.021	-0.024	350.45	0.000
		32	0.015	-0.002	350.56	0.000
		33	0.012	0.023	350.62	0.000
		34	0.008	-0.004	350.65	0.000
		35	0.001	-0.001	350.65	0.000
		36	-0.019	-0.022	350.81	0.000

Figure 56: Plots of the autocorrelation and partial autocorrelation functions – Die Bos

It is, however, worth noting that the factors of these periods (one and two), namely the fourth, sixth, eighth, etc. periods are not in exceedance of the confidence limits, thus rendering the possibility of there being a consistent cycle or lag unlikely. Nevertheless, the cross-correlogram (Figure 57) was generated and it confirmed that there is no consistent lag period within the mutual 77 observed years of rainfall and ring widths.

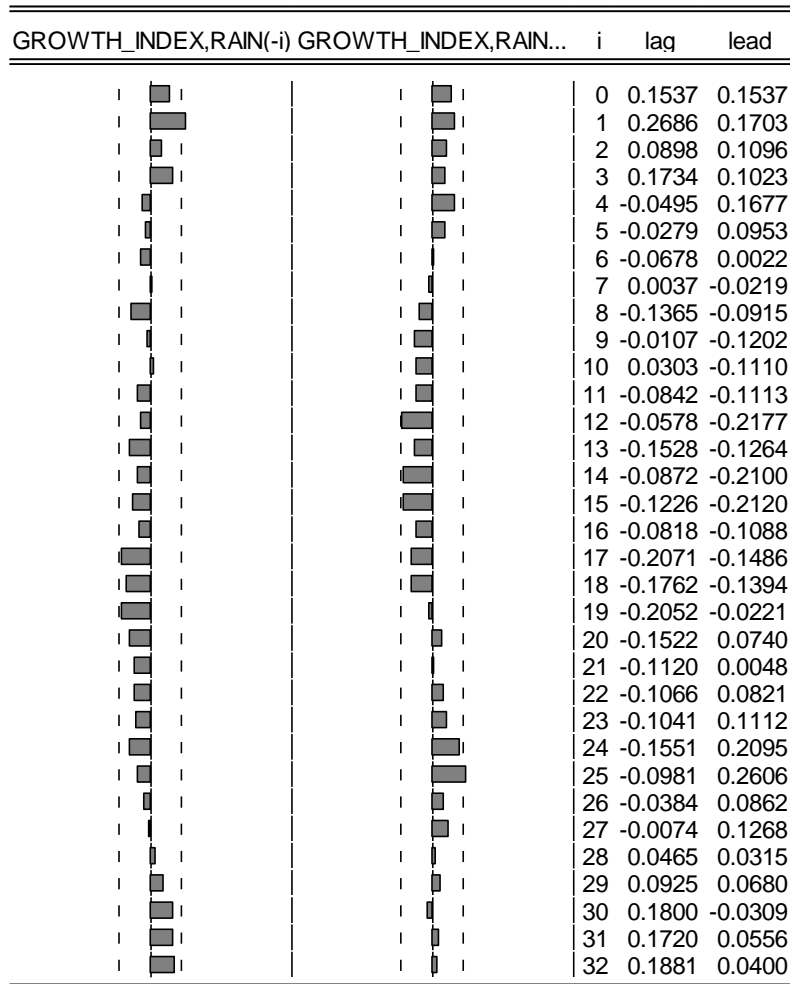


Figure 57: Plot of cross-correlogram - Die Bos

4.3.2 Regression and ARMA results

Initially, as with the previous assessments of Bishopscourt, Tokai and Wolseley, the least squares regression is resolved for the data sets by means of *EViews*. The resulting least square regression, which can be found in Appendix B.2 Table B9, yielded a poor Durbin-Watson statistic of 0.833, therefore necessitating an ARMA model.

Given that the ACF and PACF both highlighted the first and second periods as exceeding, these periods were initially all considered suitable orders for the ARMA model. Combinations of ARMA(2,2) and ARMA(1,1) were all investigated with ARMA(1,1) being the best of the ARMA models, as suggested by Monseraud when he posited that it was the “universal” growth model, although all three models failed to satisfy the requirements for the Durbin-Watson statistic with ARMA(1,1) having a Durbin-Watson statistic of 1.93. As such AR-only models were then investigated, with orders ranging from 1 to 9, as these are the periods that exhibited exceedances in either the ACF or PACF.

When executing the analyses in *EViews*, it became clear that including the second to ninth orders (i.e. AR(2) to AR(9)) was superfluous, as these terms do not enhance the model. The superfluity of these terms are illustrated by the Durbin-Watson statistic, where the value of the Durbin-Watson does not become

much closer to 2 by including these terms, as well as by the high probabilities (p-values) associated with these terms. As such, a final model was tested, namely AR(1). This final model was not only parsimonious, but also met the requirements set out by the Durbin-Watson test with a value of 2.11. The complete results from *EViews* can be found in Appendix B.3 Table B13. though the results of this model are summarised in the table below:

Table 11: Summary of Die Bos ARMA results

Variable	Coefficient	Standard Error
C	113.188	11.84
Rain	-0.026	0.027
AR(1)	0.686	0.085
Descriptive Statistics		
R^2		0.401
Adjusted R^2		0.377
Durbin-Watson		2.107

Notably, the correlation is still, however, not significant across the 77 mutual years between the rainfall and standardised growth series. Nevertheless, for completeness to illustrate the methodology and given the quality of the chronology, the historic rainfall pre-dating 1900 was theoretically resolved.

4.3.3 Historic extension of rainfall

To resolve the rainfall, the equation resolved by the final AR process can be used, where X_t is the amount of rainfall in a given year and the standardised width index is the dependent variable Y_t :

$$Y_t = C + a(\text{Rainfall amount at time } t) + b(\text{AR}(1))$$

Which can also be generally represented as:

$$Y_t = C + \rho Y_{t-1} + \beta X_t + \varepsilon_t \quad \text{Equation 10}$$

where:

ρ is the resolved AR(1) coefficient

β is the resolved coefficient for rain

ε_t is the resolved standard error for Y_t and X_t

The historic rainfall, given that the historic ring width indices are known, can thus be resolved by:

$$X_t = \frac{1}{\beta}(Y_t - \rho Y_{t-1} - \varepsilon_t - C) \quad \text{Equation 11}$$

The values for the standard error and coefficients for Equation 10, and thus Equation 11, are resolved by *EViews* for the final model. The substituted values for Equation 10 and 11 are thus:

Table 12: Substitution values for historic extension

Variable	Value
C	113.188
ρ	0.686
β	-0.026
ε_t	0.112

The rainfall-resolving equation, Equation 11, when substituted with the relevant values from Table 12 thus equates to:

$$X_t = -38.462Y_t + 26.385Y_{t-1} + 4357.692$$

Therefore, by using Equation 11 the historic rainfall can be estimated although it is critical to note that given that the correlation between the rainfall and annual growth is weak, the equation is a rough approximation resulting in a margin of error within the resolved rainfall. When validating the equation with known values (e.g. for 1950 where all the parameters are known), this error was noted as the resulting answer varies by approximately 9% from the actual, recorded answer. When cross-referencing with a few other randomly selected years, the error in estimation ranges from a lesser 8.67% (1950) to a more noticeable error of 155% (1930). A set of the calculated difference errors, which is calculated as the percentage dividend of the difference between the calculated and given growth and the given growth (i.e. $(Y_t' - Y_t)/Y_t$), for six randomly selected sequential years is illustrated in Table 13:

Table 13: Calculation of growth estimation error

Year	Rainfall (X_t)	Given Growth (Y_t)	Calculated Growth (Y_t')	Difference (%)
1949	334.92	139	192.40	38.42
1950	334.08	184	199.97	8.67
1951	389.87	167	229.39	37.36
1952	416.34	131	217.04	65.68
1953	477.66	127	190.75	50.19
1954	461.42	120	188.42	57.02

This error also relates to the incongruity between the rainfall and growth – which was already highlighted by LaMarche and Dunwiddie, whom pointed out that the rainfall and growth data appears to increase in inverse periods, with the negative coefficient for rain implying that as the rain increases, the growth of the tree decreases.

The resolved historic rainfall is thus inherently incorrect given that the relationship defined by Equation 11 is poorly correlated and implies that the growth decreases in scenarios where the rain increases. The resulting estimates of the historic rainfall were thus resolved through Equation 11 however the resulting rainfall values were inherently incorrect due to the poor correlation and incongruity between the rainfall and growth data sets. The error is also compounded, as the regressive growth term carries through and exacerbates the previous errors when calculating the succeeding term. As such, only a theoretical extension of the historic rainfall data was possible - the definition of which is expanded upon within this subsection.

To theoretically obtain the estimated historic rainfall values, there should be a significant and logical correlation between rainfall and growth, an equation such as Equation 10 must be obtained following the resolution of a final regressive model. The equation, based on the regressive model, must account for the fact that the rain and growth are related thus implying, as it is with Equation 10, that the growth is the dependent variable (Y_t) and the rainfall the independent variable (X_t). The independent and dependent variables are then related in terms of the selected analysis method, which for this research was predominately an AR model which is a form of a linear equation with constants and scaled coefficients. The coefficients of the independent and dependent variables within the equation, like the constants in the linear expression, are obtained through the evaluation in *EViews* for this research and the general expression of an AR process, with order p , is:

$$Y_t = C + \alpha_1 Y_{t-1} + \alpha_2 Y_{t-2} \dots + \alpha_p Y_{t-p} + \beta X_t + \varepsilon_t \quad \text{Equation 12}$$

Once the constant and coefficients for Equation 12 are resolved, the equation can be rearranged, as it was for Die Bos where the independent rainfall (X_t) becomes the subject of the formula so that historic rainfall, where historic growth values are known, can be resolved. The resolution of the historic rainfall is thus reasonably simple given that it is a linear substitution, however as previously expressed the correlation is poor thereby resulting in Equation 11 inherently being flawed and unable, in this scenario, to be used for accurate extension. The same can be said for the other three samples, all which failed to have statistically significant correlations and therefore could not be used to generate any sort of extension, historic or future-focused let alone used to assess the potential climatic patterns.

4.4 Results summary

For all the data sets analysed, including the “Die Bos” data obtained from the original study, there appeared to be an overall negative correlation between the rainfall and growth of the tree which would be considered incongruous as the logic demonstrated in literature, as well as practically, would imply that with increased rainfall there would be increased growth. Whilst this result is what has been found within other Western Cape studies, such as the “Die Bos” one included in this analysis it may also suggest a greater lag effect is in play although no clear, consistent lag periods were detected in the evaluation of the correlograms. It thus follows that there may be better methods of evaluation, perhaps through machine learning principles or multiple variable regressions which would consider other climatic factors such as temperature or humidity.

The results of all the data, given all the techniques utilised in this research, are summarised in Table 14.

Table 14: Summary of results

Location	Method	Correlation	Action
Bishopscourt	TSAP-Win generated moving average	-1.4% ∴ 0%	Insufficient correlation - no extension accepted
	EViews AR(10) model	16.1%	
Tokai	TSAP-Win generated moving average	-13.8% ∴ 0%	Insufficient correlation - no extension accepted
	EViews AR(3) model*	53%	
	EViews ARMA(1,1) model**	20.4%	
Wolseley	TSAP-Win generated moving average	-18.6% ∴ 0%	Insufficient correlation - no extension accepted
	EViews least squares regression	3.32%	
Die Bos	EViews AR(1) model	40.1%	Insufficient correlation – no extension accepted

* on original, unlogged width data set

** on log-retuned, stationary width data set

Recommendations

Following the results, this chapter summarises recommendations made upon this research, which includes recommendations how the results of the analyses may be utilised productively.

5.1 Recommendations

Whilst there was a limited possibility of extending the rainfall records or modelling climate from the outset given the small number of samples, both more conventional TSAP-based dendroclimatological and time series analyses could successfully be carried out, allowing this research to take the form of a novel analysis which seeks to define any correlations in addition to evaluating the appropriateness of using time series analysis techniques. Despite a multitude of analysis techniques used in this research the chronologies generally do not correlate with the rainfall records with the Wolseley chronology only correlating a meagre 3.32% at best, when the rainfall and annual growth rings are related through a least squares regression.

The traditional TSAP analyses all produce poor results, with all three of the chronologies failing to present any significant correlation leaving the onus of returning successful correlations with the time series analyses. Through analyses typically utilised in econometrics, such as log-returns, the lack of correlation between the rainfall and annual growth rings was again quantified. Furthermore, any cyclicity and consistent lag in growth following rainfall events was quantified through spectral density and Fourier analyses although there was not a discernible cycle or lag period found within any of the samples and, as such, regression and ARMA processes were executed on the unshifted (original) time series with the exception of the Tokai chronology having the processes executed on the stationary, log-returned chronology.

Through an AR(3) process, the stationary Tokai composite chronology yielded the best correlation at 53%, however as the chronology is only comprised of two trees within the Tokai plantation stand and cross-dated against a singular sample from a nearby-but-not-immediate area this moderate correlation could be anomalous within the greater stand and thus not representative of the true relationship between annual growth and rainfall within the region and, therefore, cannot be relied upon for accurate climatic modelling and further analyses as the correlation is, simply, not significant enough to overlook the limited sample size.

As such, consideration was given to investigating validating the analysis techniques through completing an analysis and historic extension with an established width chronology, leaving only the options of the four ITRDB listed chronologies as options. LaMarche and Dunwiddie's 1979 "Die Bos" study was selected for the purposes of methodological validation as it was an established chronology that not only bore minor correlations, but also had previously been recommended for further analysis. Given that there are now newer rainfall records available through the CRU gridded rainfall data, attempting to apply this research's methodology to the standardised ring width indices of the "Die Bos" study is easily justifiable in furthering work done with the "Die Bos" study. Whilst analysis on the "Die Bos" data set did not yield a statistically significant correlation; an accurate historic extension could, thus, not be completed although the relationship could be quantified by means of an equation and a procedure elucidated.

It is thus the recommendation of this study to not abandon evaluating alien species for dendroclimatological analyses in the Western Cape and greater Southern Africa but rather to pursue a greater collaboration with parties or researchers able to assist in obtaining a significant number (i.e. greater than 20) of well selected, thoroughly reviewed tree samples. Consideration could then also be given to alternative methods of obtaining width data, such as through the use of the less invasive resistograph. Additionally, more robust analysis techniques can also be employed, such as multiple variate regression analysis which would support the evaluation of the effect of factors such as temperature or humidity, in addition to rainfall, on growth and, therefore, potentially provide better correlations that may be used for climatic modelling and record extensions. As the ARMA processes did not yield the best results, critically appraising and employing approaches rooted in disciplines beyond pure statistical analyses may also be advantageous. Such techniques include those related to machine learning, for example random forest analyses which supports both regression analysis and classification tasks whilst utilising multiple decision trees, rather than the traditional one, to more accurately model a scenario.

Summary and Conclusion

This chapter summarises the entire research, with key results being highlighted and explained in addition to conclusions being drawn with further discussion on the limitations of the work. The lessons learnt from undertaking this research are also included in this chapter and in conjunction with the previous recommendations form the basis of the discussion on the potential for future work related to the study.

6.1 Summary of research

This research ultimately was aimed at defining any correlation between the annual growth of the selected samples and the respective rainfall, which could then be used, should a successful correlation be found, to extend rainfall records and develop predictive climatic models. Before completing the calculations for quantifying the correlations between the growth and rainfall, however, a comprehensive review of previous dendroclimatological studies within South Africa and the greater African continent was completed in addition to reviewing climatic patterns in Southern Africa, and the Western Cape. Furthermore, the origins and process of dendroclimatology, sampling, recording and analysis techniques – which includes statistical and computer-aided methods – were also researched and defined. From these reviews, it became evident that there has yet to be a completely successful dendroclimatological study in the Western Cape of South Africa, with most of the research highlighting the difficulties of obtaining enough samples and suggesting alternative species being used. Most of the studies, however, have only considered using indigenous species, therefore this study's use of alien species – although novel – is unique in encouraging the use of alien species for dendroclimatological studies.

Four cross-sectional, alien samples, resulting in three chronologies, were recorded and defined through TSAP-Win (provided by the University of Stellenbosch's Department of Forestry and Wood Science) and subsequently used for the research's analyses. A preliminary correlation value was calculated once the chronologies were constructed, however the results of interest are those from the time series analyses. The time series techniques utilised in this research are log-returns, least squares regression, spectral density/Fourier analysis and ARMA models. The log-return approach was largely included to ascertain the stationarity of the data sets. The correlations between the log-returns of the samples' width and respective rainfall records was calculated but none of the samples yielded successful correlations.

6.2 Findings, conclusions and lessons learned

Of the completed analyses, none of the methods yielded a strong enough correlation that could be used to extend the respective rainfall record nor are the correlations strong enough to be used to develop an accurate, reliable climatic model. The Wolseley chronology yielded the poorest results, with the calculated correlation following a least squares regression being a near-insubstantial 3.32%. The Bishopscourt chronology's correlation to rainfall was marginally better at 16.1%, although still insufficient to be useful in any extending any records or performing any climatic analyses. The Tokai composite chronology, however, returned a moderate correlation following an AR(3) process being applied to the stationary (log-returned) width chronology. The moderate correlation of 53% is still considered insufficient for any reconstruction, as the correlation is not the most accurate representation given that the chronology is comprised of only two samples. Rather, due to the limited number of samples that were used in generating the chronology, additional consideration was given to not overzealously model the climate

from moderate results, as the moderate correlation may be anomalous and thus not representative of the entire stand's response or the true climatic influence within the region. It thus follows that the main lesson learnt in undertaking this research is the value of adequate samples and sample size, which leads into the importance of collaboration.

Nevertheless, the methodology of extending the rainfall record was implemented through applying the analysis techniques to the standardised width indices of LaMarche and Dunwiddie's 1979 "Die Bos" study. When completing the analyses with the standardised indices and the CRU gridded rainfall data, a correlation of 40.1% was determined. As this is not statistically significant, an attempt at estimating the historic rainfall for the 1564-1899 period could not be reliably made, although the process on how to approach the extension of a rainfall record was included for completeness.

6.3 Limitations and future work

This research was largely limited by the availability of samples, thus rendering the study more novel than anticipated as statistical surety could not be provided with the results found from the four provided samples. It is therefore recommended that future studies do the utmost in trying to obtain a greater number of samples, as a larger sample size will inherently bear more statistical significance and support the generation of more accurate chronologies.

The nature of the research was also collaborative with skill areas ranging from forestry to stochastic statistical analyses of data sets. Given the context and purpose of this research, it was encouraged to collaborate with other disciplines to acquire additional, valuable skills required for analysis.

There is, thus, much scope for future collaborative work to be completed on alien samples in the Western Cape that could be more comprehensively researched. Consideration could be given to alternate statistical methods such as multiple variate regression, which would involve the analysis of not only the effect of rainfall but also temperature or humidity, amongst other climatic variables, on growth and thus the associated possibility of using these climatic variables as proxies for climate records. Machine learning techniques, such as a random forest which accounts for a greater number of possibilities in solutions and variables, may also yield better analysis results.

Nevertheless, the possibility of future work in Southern Africa, particularly the Western Cape, with larger sets of alien species yielding successes is present – particularly when considering non-traditional approaches, as seen with the two samples from Tokai (non-stationary set) yielding a 53% correlation and previous indigenous studies, such as "Die Bos" study, reaching a similar conclusion.

References

- Genders, 2018. *Meet a Tree*. [Online] Available at: <http://6enders.weebly.com/meet-a-tree.html> [Accessed 20 August 2018].
- Applied Centre for Climate and Earth Systems Studies, 2017. *ACCESS Position on the Winter Rainfall in the Western Cape Region*. [Online] Available at: <https://www.access.ac.za/access-position-on-the-winter-rainfall-in-the-western-cape/> [Accessed 16 November 2018].
- Benhin, J. K. A., 2006. *Climate Change and South African Agriculture: Impacts and Adaptation Options*. Pretoria, Centre for Environmental Economics and Policy in Africa.
- Bhugeloo, A., 2014. *Assessing the dendrochronological and dendroclimatological potential of Acacia nilotica in northern KwaZulu-Natal*, Durban: University of KwaZulu-Natal.
- Biology Dictionary Editors, 2017. *Angiosperms vs Gymnosperms: A definition*. [Online] Available at: <https://biologydictionary.net/angiosperm-vs-gymnosperm/> [Accessed 14 July 2018].
- Biology Dictionary Editors, 2017. *Angiosperms: A definition*. [Online] Available at: <https://biologydictionary.net/angiosperm/> [Accessed 14 July 2018].
- Black, B. A. et al., 2016. The value of crossdating to retain high-frequency variability, climate signals, and extreme events in environmental proxies. *Global Change Biology*, Volume 22, pp. 2582-2595.
- Bremaud, P., 2014. Fourier Analysis of Time Series. In: *Fourier Analysis and Stochastic Processes*. s.l.:Springer International Publishing, pp. 181-258.
- Bretting, D., 2014. *Working with TSAP-Win*, Munich: Technical University of Munich.
- Brown, C. L., 1971. Primary Growth. In: *Trees: Structure and Function*. New York: Springer-Verlag, pp. 1-60.
- Cane, M. A., Eshel, G. & Buckland, R., 1994. Forecasting Zimbabwean maize yield using eastern equatorial Pacific sea surface temperature. *Nature*, Volume 370, pp. 204-205.
- Carleton College, 2018. *Fourier Spectral Analysis*. Northfield(Minnesota): Carleton College.
- City of Cape Town, 2017. *Day Zero: When is it, What is it, and how can we avoid it?*. [Online] Available at: <http://www.capetown.gov.za/Media-and-news/Day%20Zero%20when%20is%20it,%20what%20is%20it,%20and%20how%20can%20we%20avoid%20it> [Accessed 15 October 2018].
- City of Cape Town, 2018. *Water Outlook 2018 Report*, Cape Town: City of Cape Town.
- Climate Data Organisation, 2018. *Climate Cape Town*. [Online] Available at: <https://en.climate-data.org/africa/south-africa/western-cape/cape-town-788/> [Accessed 16 October 2018].
- Climate Data Organisation, 2019. *Climate Data: Climate Wolseley*. [Online] Available at: <https://en.climate-data.org/africa/south-africa/western-cape/wolseley-189801/> [Accessed 26 February 2019].
- Cook, E. R., 1985. *A Time Series Analysis Approach to Tree Ring Standardization*, Tucson: University of Arizona.
- Cook, E. R. & Kairiukstis, L., 1989. *Methods of Dendrochronology*. 1st ed. s.l.:Academic Publishers.
- De Waal, J. H., Chapman, A. & Kemp, J., 2017. Extreme 1-day rainfall distributions: Analysing change in the Western Cape. *South African Journal of Science*, 113(7/8), pp. 1-8.
- Dennis, I. & Dennis, R., 2012. Climate change vulnerability index for South African aquifers. *Water SA*, 38(3), pp. 417-426.
- Department of Agriculture, Forestry and Fisheries, 2014. *About SA: Forestry*. [Online] Available at: <https://www.gov.za/about-sa/forestry> [Accessed 15 October 2018].

- Department of Water and Sanitation, 2017. *Water Quality Data Exploration Tool: Layers*, s.l.: South African Department of Water and Sanitation.
- Department of Water and Sanitation, 2018. *The Direct Runoff Hydrograph Method*, s.l.: South African Department of Water and Sanitation.
- Diaz, S. C., Touchan, R. & Swetnam, T. W., 2001. A Tree-Ring Reconstruction of Past Precipitation for Baja California Sur, Mexico. *International Journal of Climatology*, Volume 21, pp. 1007-1019.
- Donaldson, R., 2009. *Rainfall, Flooding and Infrastructure Damage in the Breede River Winelands Municipality: A Focus on Cut-off Low Events 2003-2008*, Stellenbosch: Stellenbosch University.
- Donat, M. et al., 2013. Updated analyses of temperature and precipitation extreme indices since the beginning of the twentieth century: The HadEX2 dataset. *Journal of Geophysical Research: Atmospheres*, Volume 118, pp. 2098-2118.
- Du Plessis, J. A. & Schloms, B., 2017. An investigation into the evidence of seasonal rainfall pattern shifts in the Western Cape, South Africa. *Journal of the South African Institution of Civil Engineering*, 59(4), pp. 47-55.
- Dunwiddie, P. W. & LaMarche, V. C., 1980. A climatically responsive tree-ring record from Widdringtonia cedarbergensis, Cape Province, South Africa. *Nature*, Volume 286, pp. 796-797.
- Easterling, D. R. et al., 2000. Observed Variability and Trends in Extreme Climate Events: A Brief Review. *Bulletin of the American Meteorological Society*, Volume 81, pp. 417-425.
- Fischer, P. M., 2011. *Delta-13 Carbon as Indicator of Soil Water Availability and Drought Stress in Pinus Radiata stands in South Africa*, Stellenbosch: University of Stellenbosch.
- Fitchler, E. et al., 2004. Climatic signals in tree rings of *Burkea africana* and *Pterocarpus angolensis* from semiarid forests in Namibia. *Trees*, Volume 18, pp. 442-451.
- Fritts, H. C., 1976. Basic Physiological Processes. In: *Tree Rings and Climate*. London: Academic Press Inc (Ltd), p. 148.
- Fritts, H. C., 1976. *Tree Rings and Climate*. London: Academic Press Inc (Ltd).
- Fritz, E. & Averill, J. L., 1924. Discontinuous Growth Rings in California Redwood. *Journal of Forestry*, 22(6), pp. 31-38.
- Gebrekirstos, A., Brauning, A., Sass-Klassen, U. & Mbow, C., 2014. Opportunities and applications of dendrochronology in Africa. *Current Opinion in Environmental Sustainability*, Volume 6, pp. 48-53.
- Gebrekirstos, A., Mitlohner, R., Teketay, D. & Worbes, M., 2008. Climate-growth relationships of the dominant tree species from semi-arid savanna woodland in Ethiopia. *Trees*, Volume 22, pp. 631-641.
- Government of South Africa, 2019. *About SA: Geography and Climate*. [Online] Available at: <https://www.gov.za/about-sa/geography-and-climate> [Accessed 21 March 2019].
- Groisman, P. Y. et al., 2005. Trends in Intense Precipitation in the Climate Record. *Journal of Climate*, Volume 18, pp. 1326-1350.
- Haglof, 2018. *Haglof Increment Borers*. [Online] Available at: <http://www.haglofcg.com/index.php/en/products/instruments/survey/389-increment-borers> [Accessed 14 November 2018].
- Harlow, W. M., Harrar, E. S. & White, F. M., 1978. *Textbook of Dendrology*. 6th ed. New York: McGraw-Hill.
- Hunter, S., 2016. *There's a Very Good Reason They're Cutting Down The Whole of Tokai Forest*. [Online] Available at: <https://www.2oceansvibe.com/2016/09/01/theres-a-very-good-reason-theyre-cutting-down-the-whole-of-tokai-forest/> [Accessed 26 February 2019].
- Hyndman, R. J. & Athanasopoulos, G., 2018. Chapter 8.3: Autoregressive models. In: *Forecasting: Principles and Practice*. 2nd ed. Melbourne: OTexts.
- Hyndman, R. J. & Athanasopoulos, G., 2018. Chapter 8.4: Moving Average Models. In: *Forecasting: Principles and Practice*. 2nd ed. Melbourne: OTexts.

- Ineson, S. et al., 2011. Solar forcing of winter climate variability in the Northern Hemisphere. *Nature: Geoscience*, November, Volume 4, pp. 753-757.
- International Research Institute for Climate and Society - Columbia University, 2018. *What is ENSO?*. Palisades(New York): s.n.
- Jansen van Vuuren, A., Jordaan, H. & Van der Walt, E., 2003. *Limpopo Water Management Area: Water Resources Situation Assessment*, s.l.: South African Department of Water and Sanitation.
- Jury, M. R., 1995. A Review of Research on Ocean-Atmosphere Interactions and South African Climate Variability. *South African Journal of Science*, Volume 91, pp. 289-293.
- Jury, M. R., 2018. Climate trends across South Africa since 1980. *Water SA*, 44(2), pp. 297-307.
- Kang, E., 2017. *Time Series: Check Stationarity*. San Francisco(California): Medium.
- Kozlowski, T. T., 1971. *Growth and Development of Trees*. 1st ed. New York: Academic Press.
- Kruger, A. C. & Nxumalo, M. P., 2017. Historical rainfall trends in South Africa: 1921-2015. *Water SA*, April, 43(2), pp. 285-297.
- Lawal, K. A., 2015. *Understanding the Variability and Predictability of Seasonal Climates over West and Southern Africa using Climate Models*, Cape Town: University of Cape Town.
- Lilly, M., 1977. *An Assessment of the Dendrochronological Potential of Indigenous Tree Species in South Africa*, Johannesburg: University of Witwatersrand.
- Lindesay, J., Harrison, M. & Haffner, M., 1986. The Souther Oscillation and South African Rainfall. *South African Journal of Science*, Volume 82, pp. 196-198.
- Mackellar, N., New, M. & Jack, C., 2014. Observed and Modelled Trends in Rainfall and Temperature for South Africa: 1960-2010. *South African Journal of Science*, 110(7/8), pp. 1-13.
- Mason, S. J., 2001. El Nino, climate change, and Southern African climate. *Environmetrics*, Volume 12, pp. 327-345.
- Mathias, C. W., 2012. Sensitivity. In: N. J. Salkind, ed. *Encyclopedia of Research Design*. Thousand Oaks: SAGE Publications, Inc., pp. 1338-1339.
- Maxwell, R. S., Wixom, J. A. & Hessler, A. E., 2011. A Comparison of Two Techniques for Measuring and Crossdating Tree Rings. *Dendrochronologia*, Volume 29, pp. 237-243.
- Midgley, J. C., 2002. *A Dendrochronological Investigation of Pinus Radiata from Silvermine Nature Reserve*, Cape Town: University of Cape Town.
- Molekwa, S., 2013. *Cut-off lows over South African and their contribution to the total rainfall of the Eastern Cape Province*, Pretoria: University of Pretoria.
- Monserud, R. A., 1986. Time-Series Analyses of Tree-Ring Chronologies. *Forest Science* , 32(2), pp. 349-372.
- Monserud, R. A. & Marshall, J. D., 2001. Time-series analysis of d13C from tree rings. I. Time trends and autocorrelation. *Tree Physiology*, Issue 21, pp. 1087-1101.
- Montgomery, D. C., Jennings, C. L. & Kulahci, M., 2008. *Introduction to Time Series Analysis and Forecasting*. 1st ed. Hoboken(New Jersey): John Wiley and Sons, Inc..
- National Center for Atmospheric Research, 2017. *The Climate Data Guide: CRU TS Gridded precipitation and other meteorological variables since 1901*. [Online] Available at: <https://climatedataguide.ucar.edu/climate-data/cru-ts-gridded-precipitation-and-other-meteorological-variables-1901> [Accessed 29 March 2019].
- National Institute of Standards and Technology (USA), 2016. *Box-Ljung Test*. Boulder(Colorado): National Institute of Standards and Technology (NIST USA).
- National Sun Yat-sen University Department of Applied Mathematics, 2018. *Durbin Watson Test*. Gushan(Kaohsiung): National Sun Yat-sen University.
- Nau, R., 2019. *Introduction to ARIMA: nonseasonal models*. Durham(North Carolina): Duke University Fuqua School of Business.

- Neukom, R. et al., 2013. Multi-proxy Summer and Winter Precipitation Reconstruction for Southern Africa over the last 200 years. *Climate Dynamics*, 4 August, Volume 42, pp. 2713-2726.
- North Carolina Forestry Association, 2018. *Parts of a Tree*. [Online] Available at: <https://www.ncforestry.org/teachers/parts-of-a-tree/> [Accessed 20 August 2018].
- Norton, D., 1989. Dendrochronology in Southern Hemisphere. In: E. R. Cook & L. A. Kairiukstis, eds. *Methods of Dendrochronology*. Dordrecht: Kluwer Academic Publishers, p. 18.
- OECD, 2013. *Glossary of Statistical Terms: Time Series*. [Online] Available at: <https://stats.oecd.org/glossary/detail.asp?ID=2708> [Accessed 27 February 2019].
- Ortegren, J. T., 2008. *Tree-Ring Based Reconstruction of Multi-Year Summer Droughts in Piedmont and Coastal Plain Climate Divisions of Southeastern US, 1690-2006*, Greensboro: University of North Carolina.
- Parzen, E., 1967. The Role of Spectral Analysis in Time Series Analysis. *Review of the International Statistical Institute*, 35(2), pp. 125-141.
- Philippon, N., Rouault, M., Richard, Y. & Favre, A., 2012. The influence of ENSO on winter rainfall in South Africa. *International Journal of Climatology*, Volume 32, pp. 2333-2347.
- Phipps, R. L., 1985. *Collecting, Preparing, Crossdating and Measuring Tree Increment Cores*, Reston: US Geological Survey.
- Pickup, M., 2015. Autogressive Moving Average Models. In: *Introduction to Time Series Analysis*. Thousand Oaks: SAGE Publications, Inc., pp. 113-164.
- Pickup, M., 2015. Fundamental Concepts in Time Series Analysis. In: *Introduction to Time Series Analysis*. Thousand Oaks: SAGE Publications, Inc., pp. 19-50.
- Precop, 2007. *South Africa Climate and Weather (by regions)*. s.l., s.n.
- Rinntech, 2018. *LINTAB*. [Online] Available at: <http://www.rinntech.de/content/view/16/47/lang,english/index.html> [Accessed 12 December 2018].
- Rinntech, 2018. *Resistograph*. [Online] Available at: <http://www.rinntech.de/content/view/8/34/lang,english/index.html> [Accessed 29 November 2018].
- Rinntech, 2018. *TSAP-Win*. [Online] Available at: <http://www.rinntech.de/index-52147.html> [Accessed 12 December 2018].
- Robinson, W. J., 1989. Historical Background on Dendrochronology. In: E. R. Cook & L. A. Kairiukstis, eds. *Methods of Dendrochronology*. Dordrecht: Kluwer Academic Publishers, pp. 1-3.
- Ruppert, D., 2014. *Statistics and Finance: An Introduction*. 1st ed. s.l.:Springer.
- SA Explorer, 2017. *Cape Town Climate*. [Online] Available at: http://www.saexplorer.co.za/south-africa/climate/cape_town_climate.asp [Accessed 12 December 2018].
- SA Explorer, 2017. *Wolseley Climate*. [Online] Available at: http://www.saexplorer.co.za/south-africa/climate/wolseley_climate.asp [Accessed 26 February 2019].
- SA Venues, 2019. *Tokai Arboretum*. [Online] Available at: <https://www.sa-venues.com/things-to-do/westerncape/tokai-arboretum/> [Accessed 26 February 2019].
- SAS Institute Inc., 2019. *SAS/ETS(R) User's Guide*. [Online] Available at: http://support.sas.com/documentation/cdl/en/etsug/63348/HTML/default/viewer.htm#etsug_timeseries_sect025.htm [Accessed 6 June 2019].
- Schlapp, D. & Butcher, E., 1995. Seasonal and sunspot-cycle changes in the day-to-day variability of Sq.. *Geophysics Journal International*, Volume 120, pp. 173-185.
- Schweingruber, F. H., 1988. *Tree Rings: Basics and Applications of Dendrochronology*. Dordrecht: D. Reidel Publishing Co..
- Schweingruber, F. H., 1993. *Trees and Wood in Dendrochronology*. 1st ed. Berlin: Springer-Verlag.
- Shao, Z., Liu, H., Huang, L. & Liang, E., 2005. Reconstruction of precipitatin variation from tree rings in recent 1000 years in Delingha, Qinghai. *Science in China (Series D: Earth Sciences)*, 48(7), pp. 939-949.
- Sheppard, P. R., 2010. Dendroclimatology: Extracting Climate from Trees. *WIREs Climate Change*, Volume 1, pp. 343-352.

- South African Department of Agriculture, Forestry and Fisheries, 2006. *Woodlands and Indigenous Forest Management*. [Online] Available at: <https://www.daff.gov.za/daffweb3/Branches/Forestry-Natural-Resources-Management/Woodlands-and-Indigenous-Forest-Management/Forestry-Tranfare/Forestry-Transfers> [Accessed 26 February 2019].
- South African Department of Agriculture, Forestry and Fisheries, 2011. *Notice of the List of Protected Tree Species under the National Forests Act, 1998 (No.84)*. Pretoria: South African Department of Agriculture, Forestry and Fisheries.
- South African Department of Agriculture, Forestry and Fisheries, 2016. *Champion Trees*. [Online] Available at: <https://www.daff.gov.za/daffweb3/Branches/Forestry-Natural-Resources-Management/Forestry-Regulation-Oversight/Sustainable-Forestry/Champion-Trees> [Accessed 24 March 2019].
- South African Department of Water and Sanitation, 2019. *Provincial Rainfall*. [Online] Available at: http://www.dwaf.gov.za/hydrology/Provincial%20Rain/Provincial%20Rainfall_files/image009.png [Accessed 25 January 2019].
- South African National Parks, 2019. *Environmental Issues: Tokai and Cecilia Plantation Fact Sheet*. [Online] Available at: <https://www.sanparks.org/parks/tablemountain/environment/tokai.php> [Accessed 26 February 2019].
- Speer, J. H., 2010. *Fundamentals of Tree-Ring Research*. 1st ed. s.l.:University of Arizona Press.
- Stahle, D. W., 1999. Useful Strategies for the Development of Tropical Tree-Ring Chronologies. *IAWA Journal*, 20(3), pp. 249-253.
- Stokes, M. A. & Smiley, T. L., 1968. *An Introduction to Tree-Ring Dating*. 1st ed. Chicago: The University of Chicago Press.
- Stokes, M. A. & Smiley, T. L., 1996. *Introduction to Tree-Ring Dating*. 2nd ed. Tucson: University of Arizona Press.
- Suresh, H., 2012. Do Trees Tell About the Past. *Resonance*, January, pp. 33-43.
- Szewczyk, G., Wasik, R., Leszczynski, K. & Podlaski, R., 2018. Age estimation of different tree species using a special kind of electrically recording resistance drill. *Urban Forestry and Urban Greening*, Volume 34, pp. 249-253.
- Therrell, M. D., Stahle, D. W., Ries, L. P. & Shugart, H. H., 2006. Tree-ring reconstructed rainfall variability in Zimbabwe. *Climate Dynamics*, Volume 26, pp. 677-685.
- TIBCO Software Inc., 2017. *Statistica Help - Parzen Window*. [Online] Available at: <http://documentation.statsoft.com/STATISTICAHelp.aspx?path=Glossary/GlossaryTwo/P/ParzenWindow> [Accessed 6 June 2019].
- TIBCO Software, 2017. *Statistica Help: Transformations of Variables - Fourier Tab*. [Online] Available at: <http://documentation.statsoft.com/STATISTICAHelp.aspx?path=TimeSeries/TimeSeries/Dialogs/TransformationofVariables/TransformationofVariablesFourierTab> [Accessed 6 June 2019].
- University of Arizona Laboratory of Tree Ring Research, 2018. *Research: Collection*. [Online] Available at: lrr.arizona.edu/collection [Accessed 24 05 2018].
- University of Arizona, n.d. *History of Dendrochronology*, Tuscon: University of Arizona.
- University of Massachusetts Dartmouth, 2005. *Spectral Analysis -- Smoother Periodogram Method*. Boston(Massachusetts): University of Massachusettes Dartmouth.
- University of Pennsylvania, 2018. *Introduction to Time Series Regression and Forecasting*. Philedelphia(Pennsylvania): University of Pennsylvania.
- US National Centre for Environmental Information, 2018. *Paleoclimatology Datasets: Tree Ring*. [Online] Available at: <https://www.ncdc.noaa.gov/data-access/paleoclimatology-data/datasets/tree-ring> [Accessed 24 May 2018].
- US National Centres for Environmental Information, 2018. *Paleo Data Search*. [Online] Available at: <https://www.ncdc.noaa.gov/paleo-search/?dataTypeld=18> [Accessed 24 February 2018].

- van Dam, D., 2017. *Cape Town Contends with the Worst Drought in Over a Century*. [Online] Available at: <https://edition.cnn.com/2017/05/31/africa/cape-town-drought/index.html> [Accessed 26 March 2018].
- Wigley, T., Jones, P. & Briffa, K., 1987. Cross-dating Methods in Dendrochronology. *Journal of Archaeological Science*, Volume 14, pp. 51-64.
- Witsuba, M. et al., 2013. Application of eccentric growth of trees as a tool for landslide analyses: The example of *Picea abies* Karst. in the Carpathian and Sudeten Mountains (Central Europe). *Catena*, Volume 111, pp. 41-55.
- Woodborne, S. et al., 2015. A 1000-year Carbon Isotope Rainfall Proxy Record from South African Baobab Trees. *PLoS ONE*, 10(5).
- Woollons, R. & Norton, D., 1990. Time-Series Analyses Applied to Sequences of *Nothofagus* Growth-Ring Measurements. *New Zealand Journal of Ecology*, Volume 13, pp. 9-15.
- Worbes, M., 2002. One hundred years of tree-ring research in the tropics - a brief history and an outlook to future challenges. *Dendrochronologia*, 20(1-2), pp. 217-231.
- Yang, B. et al., 2014. A 3500-year tree-ring record of annual precipitation on the northeastern Tibetan Plateau. *PNAS*, 25 February, 111(8), pp. 2903-2908.
- Zucchini, W. & Hiemstra, L., 1983. A note on the relationship between annual rainfall and tree-ring indices for one site in South Africa. *Water SA*, 9(4), p. 153.

Appendix A

This appendix contains the Microsoft *Excel* spreadsheets with the original width measurements in addition to the spreadsheets that are used for the TSAP-Win and log-return correlation analyses.

A.1 Ring measurements

Table A1: Raw ring measurements - Bishopscourt

RAW DATA			
TREE		RAINFALL	
Year	Width	Year	Rainfall (mm)
1930	1024	1930	465,6
1931	1073	1931	616,6
1932	769	1932	603,1
1933	691	1933	563,1
1934	597	1934	542,4
1935	512	1935	516,9
1936	379	1936	545,1
1937	271	1937	668
1938	191	1938	605,3
1939	245	1939	536
1940	287	1940	621,1
1941	343	1941	837,2
1942	421	1942	702
1943	344	1943	636,3
1944	616	1944	850,2
1945	766	1945	677,6
1946	698	1946	582,7
1947	558	1947	492,7
1948	561	1948	638,1
1949	688	1949	584,2
1950	375	1950	638,8
1951	759	1951	672,9
1952	741	1952	734,7
1953	59	1953	666,1
1954	54	1954	855,1
1955	736	1955	721,7
1956	525	1956	697,8
1957	535	1957	877,7
1958	1056	1958	539,2
1959	415	1959	702,7
1960	676	1960	505,5
1961	782	1961	550,3
1962	777	1962	881,1
1963	293	1963	498
1964	72	1964	594
1965	857	1965	573,5
1966	374	1966	579,1

RAW DATA			
TREE		RAINFALL	
Year	Width	Year	Rainfall (mm)
1967	407	1967	559,9
1968	424	1968	684,4
1969	513	1969	468,7
1970	361	1970	686,3
1971	309	1971	437
1972	215	1972	476,2
1973	325	1973	417,8
1974	62	1974	754,4
1975	669	1975	632,2
1976	42	1976	709,2
1977	335	1977	917,8
1978	404	1978	487,5
1979	644	1979	550,3
1980	49	1980	681
1981	541	1981	647,7
1982	364	1982	549,4
1983	206	1983	605
1984	338	1984	646,6
1985	556	1985	624,4
1986	427	1986	670,3
1987	256	1987	752,8
1988	227	1988	513,6
1989	267	1989	815,1
1990	195	1990	659,9
1991	291	1991	636,2
1992	207	1992	661,2
1993	545	1993	744,6
1994	496	1994	563,9
1995	335	1995	660,5
1996	388	1996	821,6
1997	267	1997	569,1
1998	677	1998	634,1
1999	615	1999	559,7
2000	34	2000	443,5
2001	351	2001	667
2002	222	2002	617
2003	424	2003	468
2004	531	2004	586,1
2005	148	2005	514,8
2006	106	2006	567,4

RAW DATA			
TREE		RAINFALL	
Year	Width	Year	Rainfall (mm)
2007	541	2007	695,4
2008	497	2008	610,6
2009	541	2009	488
2010	461	2010	484,6
2011	474	2011	524,8
2012	29	2012	601,3
2013	169	2013	621,9
2014	378	2014	545
2015	359	2015	442,6
2016	283	2016	420,6
2017	483	2017	347,3

Table A2: Raw ring measurements – Tokai

RAW DATA			
TREE		RAINFALL	
Year	Width	Year	Rainfall (mm)
1903	194	1903	943,862
1904	145	1904	959,66
1905	256	1905	755,874
1906	270	1906	675,384
1907	876	1907	623,146
1908	1011	1908	699,156
1909	996	1909	795,332
1910	821	1910	828,864
1911	701	1911	769,224
1912	478	1912	764,62
1913	648	1913	816,116
1914	499	1914	801,902
1915	567	1915	824,758
1916	759	1916	795,4
1917	713	1917	851,88
1918	688	1918	822,368
1919	560	1919	611,396
1920	750	1920	854,748
1921	813	1921	899,912
1922	754	1922	654,708
1923	468	1923	852,318
1924	196	1924	624,204
1925	928	1925	761,914
1926	468	1926	588,17
1927	400	1927	600,846
1928	1166	1928	563,684
1929	884	1929	635,04
1930	846	1930	558,624
1931	634	1931	707,176
1932	622	1932	727,54
1933	612	1933	676,116
1934	801	1934	603,906
1935	463	1935	618,696
1936	869	1936	641,796
1937	820	1937	809,984
1938	753	1938	714,95
1939	656	1939	596,18
1940	588	1940	724,63

RAW DATA			
TREE		RAINFALL	
Year	Width	Year	Rainfall (mm)
1941	504	1941	976,226
1942	795	1942	824,91
1943	1128	1943	736,464
1944	572	1944	1001,67
1945	822	1945	790,922
1946	777	1946	677,152
1947	679	1947	572,872
1948	507	1948	754,482
1949	1884	1949	671,002
1950	760	1950	770,686
1951	605	1951	785,508
1952	1087	1952	842,208
1953	872	1953	777,994
1954	838	1954	975,766
1955	921	1955	833,696
1956	797	1956	809,592
1957	727	1957	1009,688
1958	628	1958	612,946
1959	568	1959	797,152
1960	664	1960	591,588
1961	553	1961	655,462
1962	441	1962	1003,704
1963	393	1963	599,184
1964	297	1964	699,876
1965	244	1965	681,926
1966	657	1966	680,59
1967	586	1967	660,778
1968	546	1968	818,734
1969	510	1969	551,218
1970	549	1970	797,582
1971	563	1971	491,264
1972	698	1972	559,636
1973	733	1973	502,052
1974	677	1974	913,112
1975	295	1975	753,274
1976	209	1976	857,61
1977	293	1977	1040,302
1978	838	1978	556,86
1979	369	1979	611,398

RAW DATA			
TREE		RAINFALL	
Year	Width	Year	Rainfall (mm)
1980	327	1980	785,04
1981	613	1981	756,84
1982	868	1982	624,88
1983	540	1983	707,612
1984	419	1984	730,852
1985	363	1985	713,14
1986	235	1986	784,642
1987	370	1987	883,87
1988	386	1988	598,974
1989	264	1989	943,722
1990	238	1990	770,672
1991	105	1991	729,02
1992	84	1992	742,392
1993	124	1993	870,57
1994	74	1994	673,652
1995	242	1995	770,762
1996	148	1996	1155
1997	163	1997	666,51
1998	86	1998	729,164
1999	93	1999	666,086
2000	39	2000	499,702
2001	129	2001	802,864
2002	113	2002	730,526
2003	68	2003	512,268
2004	80	2004	681,878
2005	57	2005	623,022
2006	86	2006	630,64
2007	52	2007	851,46
2008	55	2008	750,442
2009	62	2009	593,978
2010	199	2010	531,418
2011	65	2011	553,768
2012	88	2012	679,33
2013	108	2013	748,584
2014	69	2014	664,85
2015	55	2015	494,518
2016	86	2016	500,976
2017	26	2017	403,196

Table A3: Raw ring measurements – Wolseley

RAW DATA			
TREE		RAINFALL	
Year	Width	Year	Rainfall (mm)
1874	275		
1875	368		
1876	315		
1877	279		
1878	292		
1879	273		
1880	820		
1881	507		
1882	582		
1883	427		
1884	438		
1885	665		
1886	695		
1887	243		
1888	284		
1889	584		
1890	632		
1891	382		
1892	651		
1893	549		
1894	522		
1895	712		
1896	332		
1897	279		
1898	380		
1899	451		
1900	770		
1901	839		
1902	547		
1903	391		
1904	239		
1905	256		
1906	637		
1907	677		
1908	490		
1909	474		
1910	506		
1911	540		
1912	873		

RAW DATA			
TREE		RAINFALL	
Year	Width	Year	Rainfall (mm)
1913	283		
1914	469		
1915	417		
1916	453		
1917	690		
1918	163		
1919	211		
1920	448		
1921	694		
1922	806		
1923	518		
1924	327		
1925	238		
1926	196		
1927	311		
1928	138		
1929	320		
1930	393		
1931	812		
1932	754		
1933	565		
1934	639		
1935	414		
1936	152		
1937	668		
1938	260		
1939	280		
1940	126		
1941	195		
1942	141		
1943	499		
1944	533		
1945	721		
1946	437		
1947	398		
1948	276		
1949	364		
1950	439		
1951	482		
1952	585		

RAW DATA			
TREE		RAINFALL	
Year	Width	Year	Rainfall (mm)
1953	504		
1954	303		
1955	191		
1956	306		
1957	353		
1958	233		
1959	219		
1960	176		
1961	322		
1962	405		
1963	492		
1964	181	1964	599
1965	280	1965	549,9
1966	196	1966	516,4
1967	554	1967	678,4
1968	419	1968	496,3
1969	334	1969	624,1
1970	746	1970	419,3
1971	589	1971	399,1
1972	183	1972	456,5
1973	211	1973	735,8
1974	541	1974	629,3
1975	218	1975	586
1976	207	1976	1060,8
1977	330	1977	393,4
1978	1519	1978	417,8
1979	414	1979	495,5
1980	881	1980	774,2
1981	292	1981	437,4
1982	542	1982	697,2
1983	172	1983	665,3
1984	121	1984	830,6
1985	461	1985	575
1986	379	1986	664,4
1987	835	1987	472,8
1988	542	1988	717,8
1989	132	1989	665,7
1990	266	1990	660
1991	595	1991	651
1992	153	1992	761,1

RAW DATA			
TREE		RAINFALL	
Year	Width	Year	Rainfall (mm)
1993	150	1993	521,6
1994	284	1994	426,5
1995	469	1995	955,4
1996	350	1996	506,5
1997	198	1997	561,6
1998	219	1998	721,2
1999	573	1999	386,9
2000	557	2000	618,3
2001	661	2001	726,3
2002	316	2002	387,8
2003	376	2003	465
2004	252	2004	552,4
2005	489	2005	433,1
2006	239	2006	656,1
2007	552	2007	775,3
2008	583	2008	648,6
2009	332	2009	622,7
2010	716	2010	556,1
2011	495	2011	599
2012	530		
2013	647		
2014	716		
2015	212		
2016	255		
2017	533		

A.2 Excel sheets – TSAP-Win

Table A4: TSAP-Win results – Bishopscourt

RAW DATA		RESIDUALS		
TREE		LINEAR REGRESSION (TSAP)	EXPONENTIAL REGRESSION (TSAP)	MOVING AVERAGE (TSAP)
<i>Year</i>	<i>Width</i>	<i>TREE</i>	<i>TREE</i>	<i>TREE</i>
1930	1024	403	41	169
1931	1073	455	465	259
1932	769	155	168	12
1933	691	8	96	6
1934	597	-10	9	-9
1935	512	-92	-70	-13
1936	379	-222	-197	-69
1937	271	-326	-299	-119
1938	191	-403	-372	-162
1939	245	-346	-312	-95
1940	287	-300	-265	-66
1941	343	-241	-203	-43
1942	421	-159	-119	-7
1943	344	-233	-190	-128
1944	616	42	87	97
1945	766	196	243	218
1946	698	131	18	121
1947	558	-6	46	-44
1948	561	1	54	-57
1949	688	131	186	64
1950	375	-178	-121	-248
1951	759	209	268	142
1952	741	194	255	128
1953	59	47	109	-41
1954	54		64	-97
1955	736	199	265	95
1956	525	-8	58	-128
1957	535	5	73	-124
1958	1056	53	599	403
1959	415	-108	-38	-240
1960	676	156	228	13
1961	782	266	338	127
1962	777	264	338	135
1963	293	-217	-142	-324
1964	72	214	29	135
1965	857	354	431	293

RAW DATA		RESIDUALS		
TREE		LINEAR REGRESSION (TSAP)	EXPONENTIAL REGRESSION (TSAP)	MOVING AVERAGE (TSAP)
Year	Width	TREE	TREE	TREE
1966	374	-125	-48	-153
1967	407	-89	-11	-77
1968	424	-69	1	-23
1969	513	24	103	82
1970	361	-125	-45	-54
1971	309	-173	-93	-98
1972	215	-264	-183	-199
1973	325	-151	-69	-92
1974	62	148	23	19
1975	669	2	282	226
1976	42	-46	37	-44
1977	335	-127	-44	-143
1978	404	-55	28	-72
1979	644	189	272	183
1980	49	38	121	46
1981	541	92	176	108
1982	364	-81	2	-60
1983	206	-236	-152	-202
1984	338	-101	-17	-47
1985	556	121	204	202
1986	427	-5	78	95
1987	256	-172	-89	-55
1988	227	-198	-115	-82
1989	267	-155	-72	-48
1990	195	-223	-141	-121
1991	291	-124	-42	-27
1992	207	-205	-123	-119
1993	545	137	218	193
1994	496	91	172	112
1995	335	-66	14	-74
1996	388	-10	69	-38
1997	267	-128	-49	-161
1998	677	286	364	25
1999	615	227	305	194
2000	34	-45	32	-70
2001	351	-30	46	-40
2002	222	-156	-80	-156
2003	424	5	124	55
2004	531	16	234	17

<i>RAW DATA</i>		<i>RESIDUALS</i>		
TREE		LINEAR REGRESSION (TSAP)	EXPONENTIAL REGRESSION (TSAP)	MOVING AVERAGE (TSAP)
<i>Year</i>	<i>Width</i>	<i>TREE</i>	<i>TREE</i>	<i>TREE</i>
2005	148	-220	-147	-218
2006	106	-258	-186	-277
2007	541	18	251	146
2008	497	139	21	1
2009	541	187	256	148
2010	461	11	178	7
2011	474	127	194	82
2012	29	-54	12	-98
2013	169	-172	-107	-204
2014	378	41	104	15
2015	359	25	88	1
2016	283	-48	14	-78
2017	483	156	216	114

Table A5: TSAP-Win results – Tokai

RAW DATA		RESIDUALS		
TREE		LINEAR REGRESSION (TSAP)	EXPONENTIAL REGRESSION (TSAP)	MOVING AVERAGE (TSAP)
<i>Year</i>	<i>Width</i>	<i>TREE</i>	<i>TREE</i>	<i>TREE</i>
1903	194	-649	-1125	-137
1904	145	-692	-1142	-247
1905	256	-575	-999	-206
1906	270	-555	-954	-262
1907	876	57	-318	285
1908	1011	198	-153	366
1909	996	189	-139	311
1910	821	20	-286	114
1911	701	-94	-379	-13
1912	478	-311	-576	-227
1913	648	-135	-380	-29
1914	499	-277	-503	-150
1915	567	-203	-411	-69
1916	759	-5	-195	116
1917	713	-45	-217	53
1918	688	-64	-220	16
1919	560	-186	-325	-99
1920	750	10	-114	90
1921	813	79	-30	166
1922	754	26	-68	132
1923	468	-254	-334	-155
1924	196	-520	-586	-440
1925	928	218	165	271
1926	468	-236	-277	-201
1927	400	-298	-327	-281
1928	1166	474	457	469
1929	884	198	192	162
1930	846	166	171	116
1931	634	-40	-25	-90
1932	622	-46	-21	-109
1933	612	-50	-15	-117
1934	801	145	189	93
1935	463	-187	-134	-235
1936	869	225	286	181
1937	820	182	251	129
1938	753	121	198	45
1939	656	30	114	-60
1940	588	-32	59	-135

RAW DATA		RESIDUALS		
TREE		LINEAR REGRESSION (TSAP)	EXPONENTIAL REGRESSION (TSAP)	MOVING AVERAGE (TSAP)
Year	Width	TREE	TREE	TREE
1941	504	-110	-12	-232
1942	795	187	291	61
1943	1128	526	636	400
1944	572	-24	92	-200
1945	822	232	353	10
1946	777	193	320	-61
1947	679	101	233	-186
1948	507	-65	71	-370
1949	1884	1318	1458	999
1950	760	200	345	-145
1951	605	51	199	-305
1952	1087	539	691	181
1953	872	330	485	-17
1954	838	302	460	-15
1955	921	391	552	127
1956	797	273	437	28
1957	727	209	375	-6
1958	628	116	284	-50
1959	568	63	232	-57
1960	664	165	336	97
1961	553	60	233	29
1962	441	-46	128	-55
1963	393	-88	88	-87
1964	297	-178	-1	-175
1965	244	-225	-48	-227
1966	657	194	372	181
1967	586	129	308	90
1968	546	95	274	19
1969	510	65	244	-50
1970	549	110	289	-29
1971	563	130	309	-10
1972	698	271	450	152
1973	733	312	491	196
1974	677	262	440	153
1975	295	-114	63	-209
1976	209	-194	-18	-280
1977	293	-104	72	-195
1978	838	447	621	349
1979	369	-16	157	-124

RAW DATA		RESIDUALS		
TREE		LINEAR REGRESSION (TSAP)	EXPONENTIAL REGRESSION (TSAP)	MOVING AVERAGE (TSAP)
Year	Width	TREE	TREE	TREE
1980	327	-52	120	-173
1981	613	240	411	106
1982	868	501	670	365
1983	540	179	346	54
1984	419	64	230	-35
1985	363	14	178	-66
1986	235	-108	54	-155
1987	370	33	193	34
1988	386	55	212	102
1989	264	-61	94	18
1990	238	-81	72	19
1991	105	-208	-58	-92
1992	84	-223	-75	-95
1993	124	-177	-32	-34
1994	74	-221	-79	-68
1995	242	-47	93	112
1996	148	-135	2	24
1997	163	-114	20	40
1998	86	-185	-54	-33
1999	93	-172	-44	-19
2000	39	-220	-96	-65
2001	129	-124	-3	36
2002	113	-134	-16	27
2003	68	-172	-59	-12
2004	80	-154	-44	3
2005	57	-171	-65	-22
2006	86	-136	-33	5
2007	52	-164	-65	-28
2008	55	-155	-60	-28
2009	62	-142	-50	-24
2010	199	1	89	112
2011	65	-127	-43	-23
2012	88	-98	-18	2
2013	108	-72	4	24
2014	69	-105	-33	-12
2015	55	-113	-45	-22
2016	86	-76	-12	14
2017	26	-130	-70	-45

Table A6: TSAP-Win results – Wolseley

RAW DATA		RESIDUALS		
TREE		LINEAR REGRESSION (TSAP)	EXPONENTIAL REGRESSION (TSAP)	MOVING AVERAGE (TSAP)
<i>Year</i>	<i>Width</i>	<i>TREE</i>	<i>TREE</i>	<i>TREE</i>
1874	275	-190	-136	-31
1875	368	-97	-42	43
1876	315	-149	-93	-32
1877	279	-185	-128	-97
1878	292	-171	-114	-110
1879	273	-190	-132	-153
1880	820	358	416	365
1881	507	45	104	20
1882	582	120	180	76
1883	427	-34	26	-84
1884	438	-23	38	-75
1885	665	205	266	154
1886	695	235	297	201
1887	243	-216	-154	-252
1888	284	-175	-112	-214
1889	584	125	189	80
1890	632	174	238	117
1891	382	-76	-11	-132
1892	651	194	259	141
1893	549	92	158	37
1894	522	66	132	19
1895	712	256	323	216
1896	332	-124	-56	-173
1897	279	-176	-108	-238
1898	380	-75	-6	-138
1899	451	-3	66	-61
1900	770	316	386	271
1901	839	386	456	345
1902	547	94	165	40
1903	391	-61	10	-122
1904	239	-213	-141	-270
1905	256	-196	-123	-242
1906	637	186	259	153
1907	677	226	300	182
1908	490	40	114	-19
1909	474	24	99	-51
1910	506	57	132	-28
1911	540	91	167	10

RAW DATA		RESIDUALS		
TREE		LINEAR REGRESSION (TSAP)	EXPONENTIAL REGRESSION (TSAP)	MOVING AVERAGE (TSAP)
Year	Width	TREE	TREE	TREE
1912	873	424	501	351
1913	283	-165	-88	-221
1914	469	21	99	-13
1915	417	-30	48	-44
1916	453	6	85	3
1917	690	244	322	238
1918	163	-283	-204	-293
1919	211	-235	-155	-260
1920	448	3	83	-21
1921	694	249	330	236
1922	806	362	443	364
1923	518	74	156	101
1924	327	-116	-34	-75
1925	238	-205	-122	-141
1926	196	-246	-163	-169
1927	311	-131	-47	-52
1928	138	-304	-220	-239
1929	320	-121	-37	-94
1930	393	-48	37	-61
1931	812	372	457	333
1932	754	314	400	248
1933	565	126	212	50
1934	639	200	287	129
1935	414	-25	63	-65
1936	152	-286	-199	-280
1937	668	230	318	296
1938	260	-177	-89	-73
1939	280	-157	-68	-36
1940	126	-310	-221	-195
1941	195	-241	-151	-144
1942	141	-294	-204	-220
1943	499	64	154	130
1944	533	98	189	143
1945	721	287	378	311
1946	437	3	95	6
1947	398	-35	57	-49
1948	276	-157	-65	-180
1949	364	-68	24	-82
1950	439	7	100	12

RAW DATA		RESIDUALS		
TREE		LINEAR REGRESSION (TSAP)	EXPONENTIAL REGRESSION (TSAP)	MOVING AVERAGE (TSAP)
Year	Width	TREE	TREE	TREE
1951	482	50	144	74
1952	585	154	248	186
1953	504	73	168	117
1954	303	-127	-33	-68
1955	191	-239	-144	-153
1956	306	-123	-28	-11
1957	353	-76	20	56
1958	233	-196	-99	-57
1959	219	-209	-113	-68
1960	176	-252	-155	-116
1961	322	-105	-8	28
1962	405	-22	76	102
1963	492	66	163	177
1964	181	-245	-147	-149
1965	280	-145	-47	-78
1966	196	-229	-130	-191
1967	554	129	229	155
1968	419	-5	94	18
1969	334	-90	10	-76
1970	746	323	423	329
1971	589	166	267	180
1972	183	-239	-139	-212
1973	211	-211	-110	-205
1974	541	119	221	103
1975	218	-203	-101	-255
1976	207	-214	-112	-284
1977	330	-90	12	-191
1978	1519	1099	1202	976
1979	414	-5	98	-125
1980	881	462	565	357
1981	292	-127	-23	-217
1982	542	124	228	45
1983	172	-246	-142	-301
1984	121	-296	-192	-302
1985	461	44	149	53
1986	379	-37	68	-21
1987	835	419	524	434
1988	542	127	232	152
1989	132	-283	-177	-252

RAW DATA		RESIDUALS		
TREE		LINEAR REGRESSION (TSAP)	EXPONENTIAL REGRESSION (TSAP)	MOVING AVERAGE (TSAP)
Year	Width	TREE	TREE	TREE
1990	266	-149	-43	-109
1991	595	181	287	240
1992	153	-261	-154	-178
1993	150	-263	-156	-152
1994	284	-129	-22	-20
1995	469	57	164	145
1996	350	-62	46	2
1997	198	-214	-106	-167
1998	219	-192	-84	-173
1999	573	162	271	167
2000	557	147	255	143
2001	661	251	360	250
2002	316	-93	16	-102
2003	376	-33	76	-54
2004	252	-156	-47	-177
2005	489	81	191	60
2006	239	-169	-59	-195
2007	552	145	255	105
2008	583	176	287	108
2009	332	-74	36	-175
2010	716	310	421	193
2011	495	90	201	-24
2012	530	125	236	12
2013	647	242	354	142
2014	716	312	424	223
2015	212	-192	-80	-270
2016	255	-148	-36	-209
2017	533	130	243	78

A.3 Excel sheets – log-return

Table A7: Log-returned data - Bishopscourt

RAW DATA		RESIDUALS	
TREE		LOG RETURNS	
<i>Year</i>	<i>Width</i>	<i>Tree</i>	<i>Rainfall</i>
1930	1024		
1931	1073	0,046742	0,280894
1932	769	-0,33312	-0,02214
1933	691	-0,10695	-0,06863
1934	597	-0,14622	-0,03745
1935	512	-0,15359	-0,04815
1936	379	-0,30079	0,05312
1937	271	-0,33542	0,203319
1938	191	-0,34985	-0,09856
1939	245	0,248985	-0,12159
1940	287	0,158224	0,147358
1941	343	0,178248	0,298571
1942	421	0,204902	-0,17613
1943	344	-0,20199	-0,09826
1944	616	0,582605	0,289801
1945	766	0,217935	-0,22691
1946	698	-0,09296	-0,15088
1947	558	-0,22386	-0,16777
1948	561	0,005362	0,258595
1949	688	0,204068	-0,08825
1950	375	-0,60686	0,089348
1951	759	0,705076	0,052005
1952	741	-0,024	0,087866
1953	59	-2,53046	-0,09802
1954	54	-0,08855	0,249779
1955	736	2,612246	-0,16961
1956	525	-0,33783	-0,03368
1957	535	0,018868	0,229372
1958	1056	0,679977	-0,48722
1959	415	-0,93396	0,264843
1960	676	0,487915	-0,32938
1961	782	0,145662	0,084916
1962	777	-0,00641	0,470708
1963	293	-0,97527	-0,57057
1964	72	-1,40351	0,176279
1965	857	2,476772	-0,03512
1966	374	-0,82918	0,009717

RAW DATA		RESIDUALS	
TREE		LOG RETURNS	
Year	Width	Tree	Rainfall
1967	407	0,084557	-0,03372
1968	424	0,04092	0,200784
1969	513	0,190542	-0,37858
1970	361	-0,3514	0,381352
1971	309	-0,15554	-0,45138
1972	215	-0,3627	0,085905
1973	325	0,413187	-0,13084
1974	62	-1,65669	0,59092
1975	669	2,37865	-0,17672
1976	42	-2,76811	0,114932
1977	335	2,076461	0,257842
1978	404	0,187284	-0,63269
1979	644	0,466284	0,121173
1980	49	-2,57588	0,213099
1981	541	2,401599	-0,05013
1982	364	-0,39627	-0,1646
1983	206	-0,56928	0,096402
1984	338	0,49517	0,066499
1985	556	0,497722	-0,03494
1986	427	-0,26398	0,070934
1987	256	-0,51161	0,116074
1988	227	-0,12023	-0,38235
1989	267	0,162299	0,461866
1990	195	-0,31425	-0,21122
1991	291	0,400324	-0,03658
1992	207	-0,3406	0,038543
1993	545	0,968067	0,118791
1994	496	-0,09421	-0,27797
1995	335	-0,39245	0,15812
1996	388	0,146875	0,218257
1997	267	-0,37376	-0,3672
1998	677	0,930423	0,108151
1999	615	-0,09605	-0,12481
2000	34	-2,89526	-0,2327
2001	351	2,334426	0,408092
2002	222	-0,45811	-0,07792
2003	424	0,647056	-0,2764
2004	531	0,225029	0,225022
2005	148	-1,27755	-0,12971
2006	106	-0,33377	0,097286

<i>RAW DATA</i>		<i>RESIDUALS</i>	
TREE		LOG RETURNS	
<i>Year</i>	<i>Width</i>	<i>Tree</i>	<i>Rainfall</i>
2007	541	1,62998	0,203423
2008	497	-0,08483	-0,13005
2009	541	0,084829	-0,22413
2010	461	-0,16002	-0,00699
2011	474	0,027809	0,079693
2012	29	-2,79391	0,136077
2013	169	1,762603	0,033685
2014	378	0,804995	-0,13199
2015	359	-0,05157	-0,20812
2016	283	-0,23788	-0,05098
2017	483	0,53457	-0,19149

Table A8: Log-returned data – Tokai

RAW DATA		RESIDUALS	
TREE		LOG RETURNS	
<i>Year</i>	<i>Width</i>	<i>Tree</i>	<i>Rainfall</i>
1903	194		
1904	145	-0,291124417	0,016599086
1905	256	0,568443702	-0,238704359
1906	270	0,053244515	-0,112593278
1907	876	1,176944132	-0,080500577
1908	1011	0,143329128	0,115093052
1909	996	-0,014947961	0,128885744
1910	821	-0,193224148	0,041296451
1911	701	-0,158015222	-0,074673874
1912	478	-0,382897155	-0,006003236
1913	648	0,304279964	0,065177523
1914	499	-0,261284601	-0,017570096
1915	567	0,127753208	0,028103604
1916	759	0,291642474	-0,036244877
1917	713	-0,062520357	0,068600539
1918	688	-0,035692582	-0,035257688
1919	560	-0,205852054	-0,296443116
1920	750	0,292136423	0,335061822
1921	813	0,080657903	0,051490292
1922	754	-0,075338742	-0,318107646
1923	468	-0,476924072	0,263770362
1924	196	-0,870353637	-0,311482459
1925	928	1,554917074	0,19935645
1926	468	-0,684563437	-0,258817667
1927	400	-0,157003749	0,02132264
1928	1166	1,06986982	-0,063844851
1929	884	-0,276877304	0,119194178
1930	846	-0,043937703	-0,128211372
1931	634	-0,288470405	0,235802957
1932	622	-0,019108862	0,028389406
1933	612	-0,01620781	-0,073304321
1934	801	0,269128665	-0,112946102
1935	463	-0,548133893	0,024195481
1936	869	0,629616071	0,036656459
1937	820	-0,058038785	0,232743998
1938	753	-0,085239112	-0,124801884
1939	656	-0,137904439	-0,181669975
1940	588	-0,109433841	0,195118545
1941	504	-0,15415068	0,298032937

RAW DATA		RESIDUALS	
TREE		LOG RETURNS	
Year	Width	Tree	Rainfall
1942	795	0,455765847	-0,168419828
1943	1128	0,349859317	-0,113413935
1944	572	-0,679062441	0,307563531
1945	822	0,362601404	-0,236224533
1946	777	-0,056300045	-0,155303586
1947	679	-0,134819223	-0,167233462
1948	507	-0,292110124	0,275369115
1949	1884	1,312641452	-0,117259303
1950	760	-0,907834022	0,13850891
1951	605	-0,228089975	0,019049615
1952	1087	0,585948429	0,069696372
1953	872	-0,220387463	-0,079308203
1954	838	-0,039771323	0,226503992
1955	921	0,094441936	-0,157353976
1956	797	-0,144605357	-0,02933841
1957	727	-0,091928201	0,220866234
1958	628	-0,146386311	-0,499119811
1959	568	-0,100418748	0,262768535
1960	664	0,156160731	-0,298234929
1961	553	-0,182924148	0,102529884
1962	441	-0,226313126	0,426112106
1963	393	-0,115235264	-0,515883706
1964	297	-0,280077473	0,155334447
1965	244	-0,196563914	-0,025982029
1966	657	0,990515793	-0,001961079
1967	586	-0,114364229	-0,02954214
1968	546	-0,070700814	0,214341316
1969	510	-0,06820825	-0,39562887
1970	549	0,073687716	0,369454276
1971	563	0,025181187	-0,484602989
1972	698	0,214939475	0,130304911
1973	733	0,048926599	-0,108582872
1974	677	-0,079474429	0,598154846
1975	295	-0,830695917	-0,192429506
1976	209	-0,344641104	0,129720411
1977	293	0,337838357	0,193116884
1978	838	1,050845491	-0,624952473
1979	369	-0,820221456	0,093434276
1980	327	-0,120836473	0,249986534
1981	613	0,628404765	-0,036582801

RAW DATA		RESIDUALS	
TREE		LOG RETURNS	
Year	Width	Tree	Rainfall
1982	868	0,347826779	-0,191592239
1983	540	-0,474622575	0,12433629
1984	419	-0,25369822	0,032315056
1985	363	-0,143468086	-0,024533222
1986	235	-0,43481732	0,095549808
1987	370	0,453917491	0,11908243
1988	386	0,042334364	-0,389091802
1989	264	-0,379888266	0,45461344
1990	238	-0,103678429	-0,20256877
1991	105	-0,818310324	-0,055561695
1992	84	-0,223143551	0,018176239
1993	124	0,389464767	0,159270764
1994	74	-0,516216472	-0,256434512
1995	242	1,184872633	0,134665979
1996	148	-0,491725452	0,404475987
1997	163	0,096537927	-0,54980048
1998	86	-0,639402905	0,089843529
1999	93	0,078252197	-0,090479881
2000	39	-0,869037847	-0,287406871
2001	129	1,196250758	0,474173414
2002	113	-0,132424586	-0,094420512
2003	68	-0,507880114	-0,354916897
2004	80	0,162518929	0,286002831
2005	57	-0,338975367	-0,090268925
2006	86	0,411296028	0,012153346
2007	52	-0,503103578	0,300217346
2008	55	0,056089467	-0,126290157
2009	62	0,1198012	-0,233820085
2010	199	1,16617044	-0,111293376
2011	65	-1,118917555	0,041196921
2012	88	0,302949545	0,204361192
2013	108	0,204794413	0,097076404
2014	69	-0,448024723	-0,118621971
2015	55	-0,226773319	-0,2959779
2016	86	0,447014111	0,012974645
2017	26	-1,196250758	-0,2171354

Table A9: Log-returned data – Wolseley

RAW DATA		RESIDUALS	
TREE		LOG RETURNS	
Year	Width	Tree	Rainfall
1874	275		
1875	368	0,291311841	
1876	315	-0,155510299	
1877	279	-0,121360857	
1878	292	0,04554202	
1879	273	-0,067282007	
1880	820	1,099832545	
1881	507	-0,480793337	
1882	582	0,137959444	
1883	427	-0,309686435	
1884	438	0,025434897	
1885	665	0,41756813	
1886	695	0,044124805	
1887	243	-1,050850402	
1888	284	0,155912795	
1889	584	0,720926745	
1890	632	0,078988411	
1891	382	-0,503468786	
1892	651	0,533089034	
1893	549	-0,170411201	
1894	522	-0,050430854	
1895	712	0,310410324	
1896	332	-0,762942942	
1897	279	-0,173923187	
1898	380	0,308959471	
1899	451	0,171296087	
1900	770	0,534923175	
1901	839	0,085820192	
1902	547	-0,427761904	
1903	391	-0,335741242	
1904	239	-0,492244008	
1905	256	0,068713893	
1906	637	0,911592211	
1907	677	0,060901617	
1908	490	-0,323265882	
1909	474	-0,033198069	
1910	506	0,065329348	
1911	540	0,06503247	
1912	873	0,480366416	

RAW DATA		RESIDUALS	
TREE		LOG RETURNS	
Year	Width	Tree	Rainfall
1913	283	-1,126488658	
1914	469	0,505155871	
1915	417	-0,117516547	
1916	453	0,082805904	
1917	690	0,420799472	
1918	163	-1,442941397	
1919	211	0,258107933	
1920	448	0,752935099	
1921	694	0,437678728	
1922	806	0,149611782	
1923	518	-0,4421085	
1924	327	-0,460015071	
1925	238	-0,317689497	
1926	196	-0,194156014	
1927	311	0,461678253	
1928	138	-0,812539227	
1929	320	0,841067311	
1930	393	0,205488616	
1931	812	0,725690728	
1932	754	-0,074107972	
1933	565	-0,288566637	
1934	639	0,123078723	
1935	414	-0,434038481	
1936	152	-1,001985453	
1937	668	1,480407653	
1938	260	-0,943606543	
1939	280	0,074107972	
1940	126	-0,798507696	
1941	195	0,436717652	
1942	141	-0,324239668	
1943	499	1,263846205	
1944	533	0,065915328	
1945	721	0,302117713	
1946	437	-0,500705942	
1947	398	-0,09348119	
1948	276	-0,36605114	
1949	364	0,276753002	
1950	439	0,187345545	
1951	482	0,093444701	
1952	585	0,193667733	

RAW DATA		RESIDUALS	
TREE		LOG RETURNS	
Year	Width	Tree	Rainfall
1952	585	0,193667733	
1953	504	-0,149035579	
1954	303	-0,508843463	
1955	191	-0,461459377	
1956	306	0,471311674	
1957	353	0,142882955	
1958	233	-0,415429603	
1959	219	-0,061966724	
1960	176	-0,218587735	
1961	322	0,604067551	
1962	405	0,229335522	
1963	492	0,194591649	
1964	181	-0,999981685	
1965	280	0,436292572	-0,085525155
1966	196	-0,356674944	-0,062854785
1967	554	1,039050028	0,272855426
1968	419	-0,279293767	-0,312556502
1969	334	-0,226729927	0,229130029
1970	746	0,803584607	-0,397723958
1971	589	-0,236299417	-0,049374642
1972	183	-1,168940031	0,134376688
1973	211	0,142371981	0,477369643
1974	541	0,941561145	-0,156350252
1975	218	-0,908924216	-0,071288301
1976	207	-0,05177627	0,59345883
1977	330	0,466373861	-0,991951713
1978	1519	1,526714848	0,060175943
1979	414	-1,299941529	0,170564505
1980	881	0,755191652	0,446262884
1981	292	-1,104303824	-0,57098213
1982	542	0,618512199	0,466224205
1983	172	-1,147771525	-0,046834247
1984	121	-0,351703931	0,221910264
1985	461	1,337607497	-0,36777829
1986	379	-0,195861838	0,144514337
1987	835	0,78989552	-0,340211912
1988	542	-0,432165723	0,417518513
1989	132	-1,412464079	-0,07535186
1990	266	0,700694386	-0,008599284

RAW DATA		RESIDUALS	
TREE		LOG RETURNS	
Year	Width	Tree	Rainfall
1991	595	0,805065097	-0,013730193
1992	153	-1,358123484	0,156255113
1993	150	-0,019802627	-0,377863745
1994	284	0,638338944	-0,201288644
1995	469	0,50162853	0,806517734
1996	350	-0,292669614	-0,634605777
1997	198	-0,569666124	0,103265529
1998	219	0,100804699	0,250126639
1999	573	0,961813987	-0,62275023
2000	557	-0,028320477	0,468807515
2001	661	0,1711886	0,160989376
2002	316	-0,738011626	-0,62747341
2003	376	0,17384693	0,181547663
2004	252	-0,400160056	0,172235016
2005	489	0,662933402	-0,243303773
2006	239	-0,715898938	0,415344568
2007	552	0,837084494	0,166936835
2008	583	0,05463914	-0,178433857
2009	332	-0,563052217	-0,040751332
2010	716	0,768545198	-0,113116728
2011	495	-0,369122404	0,074313464
2012	530	0,068319244	
2013	647	0,199469288	
2014	716	0,101333872	
2015	212	-1,217093892	
2016	255	0,18467727	
2017	533	0,737257879	

Appendix B

This appendix contains all the resulting tables from processing the various statistical components in *Statistica* and *EViews*. The first sub-chapter includes the resulting tables for all the samples' partial and autocorrelations. Finally, the second sub-chapter includes the results from the regression analyses completed on the width data of each sample.

B.1 Correlation function results

Table B1: Autocorrelation function results from *Statistica* - *Bishopscourt*

AUTOCORRELATION FUNCTION: ON WIDTH				
Lag	Autocorrelation	Standard Error	Box-Ljung Q	p
1	0.27253	0.104809	6.74764	0.009391
2	0.121424	0.104205	8.10545	0.017384
3	0.201835	0.103597	11.90122	0.007737
4	0.138969	0.102986	13.42211	0.008246
5	-0.061426	0.102371	14.08215	0.015111
6	0.029988	0.101752	14.16901	0.027828
7	-0.034215	0.101130	14.28347	0.046397
8	-0.147345	0.100504	16.43282	0.036621
9	-0.066596	0.099874	16.87744	0.050713
10	0.217028	0.099240	21.66000	0.016960
11	0.018958	0.098601	21.69697	0.026865
12	0.042084	0.097959	21.88153	0.038916
13	0.175120	0.097312	25.11998	0.022297
14	0.189936	0.096661	28.98106	0.010537
15	0.047003	0.096006	29.22072	0.015097
16	0.158556	0.095346	31.98611	0.010069
17	0.152787	0.094682	34.59009	0.007061
18	-0.002960	0.094013	34.59108	0.010667
19	-0.024441	0.093339	34.65965	0.015385
20	0.064715	0.092660	35.14743	0.019381

Table B2: Partial autocorrelation function results from Statistica - Bishopscourt

PARTIAL AUTOCCORELATION FUNCTION - WIDTH		
Lag	Partial autocorrelation	Standard Error
1	0.272253	0.106600
2	0.051089	0.106600
3	0.169533	0.106600
4	0.046306	0.106600
5	-0.143269	0.106600
6	0.043610	0.106600
7	-0.080713	0.106600
8	-0.111702	0.106600
9	0.017458	0.106600
10	0.281427	0.106600
11	-0.041455	0.106600
12	0.051652	0.106600
13	0.077898	0.106600
14	0.082850	0.106600
15	-0.022285	0.106600
16	0.060793	0.106600
17	0.070584	0.106600
18	-0.025639	0.106600
19	-0.029416	0.106600
20	-0.016903	0.106600

Table B3: Autocorrelation function results from Statistica - Wolsey

AUTOCORRELATION FUNCTION: ON WIDTH				
Lag	Autocorrelation	Standard Error	Box-Ljung Q	p
1	0.002378	0.138592	0.00029	0.986309
2	0.025670	0.137141	0.03533	0.982490
3	-0.172307	0.135674	1.64826	0.648501
4	0.031777	0.134191	1.70433	0.789929
5	-0.237270	0.132692	4.90175	0.428007
6	-0.244219	0.131175	8.36797	0.212406
7	0.087381	0.129641	8.82228	0.265708
8	0.190089	0.128088	11.02469	0.200353
9	0.197811	0.126516	13.46929	0.142551
10	0.047165	0.124925	13.61183	0.191504
11	-0.02484	0.123313	13.64998	0.253028
12	-0.148297	0.121680	15.13534	0.234183
13	0.024835	0.120024	15.17815	0.296424
14	-0.202970	0.118345	18.11961	0.201465
15	-0.145843	0.116642	19.68297	0.184518
16	-0.115430	0.114914	20.69197	0.190744
17	0.095289	0.113160	21.40107	0.208953
18	-0.097759	0.111378	22.17147	0.224554
19	-0.073713	0.109566	22.62409	0.254397
20	0.060290	0.107725	22.93732	0.291970

Table B4: Partial autocorrelation function results from Statistica - Wolseley

PARTIAL AUTOCCORELATION FUNCTION - WIDTH		
Lag	Partial autocorrelation	Standard Error
1	0.002378	0.142857
2	0.025664	0.142857
3	-0.172542	0.142857
4	0.033706	0.142857
5	-0.236426	0.142857
6	-0.293075	0.142857
7	0.111630	0.142857
8	0.133596	0.142857
9	0.144458	0.142857
10	0.068147	0.142857
11	-0.129411	0.142857
12	-0.188193	0.142857
13	0.171388	0.142857
14	-0.073836	0.142857
15	-0.161451	0.142857
16	-0.172273	0.142857
17	-0.180651	0.142857
18	-0.263114	0.142857
19	-0.131317	0.142857
20	-0.039916	0.142857

B.2 Regression results

Table B5: EViews regression results - Bishopscourt

Dependent Variable: WIDTH
 Method: Least Squares
 Date: 05/14/19 Time: 09:49
 Sample: 1930 2017
 Included observations: 88

Variable	Coefficient	Std. Error	t-Statistic	Prob.
C	487.6790	138.3000	3.526240	0.0007
RAIN	-0.089005	0.221490	-0.401845	0.6888
R-squared	0.001874	Mean dependent var		433.0455
Adjusted R-squared	-0.009732	S.D. dependent var		236.6679
S.E. of regression	237.8167	Akaike info criterion		13.80334
Sum squared resid	4863885.	Schwarz criterion		13.85965
Log likelihood	-605.3471	Hannan-Quinn criter.		13.82603
F-statistic	0.161480	Durbin-Watson stat		1.380914
Prob(F-statistic)	0.688795			

Table B6: EViews regression results - Tokai

Dependent Variable: WIDTH
 Method: Least Squares
 Date: 05/09/19 Time: 11:57
 Sample: 1903 2017
 Included observations: 115

Variable	Coefficient	Std. Error	t-Statistic	Prob.
C	379.7166	167.5361	2.266477	0.0253
RAIN	0.164803	0.226717	0.726910	0.4688
R-squared	0.004654	Mean dependent var		499.4609
Adjusted R-squared	-0.004154	S.D. dependent var		326.7412
S.E. of regression	327.4191	Akaike info criterion		14.43760
Sum squared resid	12113973	Schwarz criterion		14.48534
Log likelihood	-828.1619	Hannan-Quinn criter.		14.45697
F-statistic	0.528398	Durbin-Watson stat		0.695819
Prob(F-statistic)	0.468784			

Table B7: EViews regression results – Tokai (logged)

Dependent Variable: RWIDTH
 Method: Least Squares
 Date: 08/13/19 Time: 15:02
 Sample (adjusted): 1904 2017
 Included observations: 114 after adjustments

Variable	Coefficient	Std. Error	t-Statistic	Prob.
C	-0.017713	0.047521	-0.372734	0.7101
RRAIN	-0.011152	0.208558	-0.053473	0.9575
R-squared	0.000026	Mean dependent var		-0.017629
Adjusted R-squared	-0.008903	S.D. dependent var		0.504871
S.E. of regression	0.507113	Akaike info criterion		1.497223
Sum squared resid	28.80235	Schwarz criterion		1.545227
Log likelihood	-83.34173	Hannan-Quinn criter.		1.516705
F-statistic	0.002859	Durbin-Watson stat		2.661934
Prob(F-statistic)	0.957450			

Table B8: EViews regression results - Wolseley

Dependent Variable: WIDTH
 Method: Least Squares
 Date: 05/14/19 Time: 09:27
 Sample (adjusted): 1964 2011
 Included observations: 48 after adjustments

Variable	Coefficient	Std. Error	t-Statistic	Prob.
C	606.7239	153.8399	3.943865	0.0003
RAIN	-0.313690	0.249589	-1.256829	0.2152
R-squared	0.033199	Mean dependent var		418.8333
Adjusted R-squared	0.012182	S.D. dependent var		253.0444
S.E. of regression	251.4984	Akaike info criterion		13.93352
Sum squared resid	2909566.	Schwarz criterion		14.01149
Log likelihood	-332.4046	Hannan-Quinn criter.		13.96299
F-statistic	1.579618	Durbin-Watson stat		2.104426
Prob(F-statistic)	0.215160			

Table B9: EViews regression results - Die Bos

Dependent Variable: GROWTH_INDEX
 Method: Least Squares
 Date: 08/22/19 Time: 09:22
 Sample (adjusted): 337 413
 Included observations: 77 after adjustments

Variable	Coefficient	Std. Error	t-Statistic	Prob.
C	85.21708	12.22803	6.968996	0.0000
RAIN	0.046350	0.034399	1.347426	0.1819
R-squared	0.023635	Mean dependent var		101.2727
Adjusted R-squared	0.010617	S.D. dependent var		24.22191
S.E. of regression	24.09298	Akaike info criterion		9.227349
Sum squared resid	43535.39	Schwarz criterion		9.288227
Log likelihood	-353.2529	Hannan-Quinn criter.		9.251700
F-statistic	1.815557	Durbin-Watson stat		0.812770
Prob(F-statistic)	0.181900			

B.3 ARMA results

Table B10: EViews ARMA results - Bishopscourt

Dependent Variable: WIDTH
 Method: ARMA Maximum Likelihood (BFGS)
 Date: 05/14/19 Time: 09:52
 Sample: 1930 2017
 Included observations: 88
 Convergence achieved after 6 iterations
 Coefficient covariance computed using outer product of gradients

Variable	Coefficient	Std. Error	t-Statistic	Prob.
C	547.2449	141.2308	3.874827	0.0002
RAIN	-0.174077	0.219390	-0.793458	0.4298
AR(1)	0.300965	0.089061	3.379324	0.0011
AR(10)	0.285558	0.108961	2.620738	0.0104
SIGMASQ	46465.21	8705.377	5.337530	0.0000
R-squared	0.160902	Mean dependent var		433.0455
Adjusted R-squared	0.120464	S.D. dependent var		236.6679
S.E. of regression	221.9557	Akaike info criterion		13.70995
Sum squared resid	4088938.	Schwarz criterion		13.85071
Log likelihood	-598.2379	Hannan-Quinn criter.		13.76666
F-statistic	3.978941	Durbin-Watson stat		1.961339
Prob(F-statistic)	0.005290			
Inverted AR Roots	.92	.75-.51i	.75+.51i	.30+.83i
	.30-.83i	-.24-.84i	-.24+.84i	-.69-.52i
	-.69+.52i	-.86		

Table B11: EViews ARMA results - Tokai

Dependent Variable: WIDTH
 Method: ARMA Maximum Likelihood (BFGS)
 Date: 05/09/19 Time: 12:03
 Sample: 1903 2017
 Included observations: 115
 Convergence achieved after 8 iterations
 Coefficient covariance computed using outer product of gradients

Variable	Coefficient	Std. Error	t-Statistic	Prob.
C	576.1956	210.9338	2.731642	0.0074
RAIN	-0.185621	0.211136	-0.879153	0.3813
AR(1)	0.433837	0.077798	5.576454	0.0000
AR(2)	0.093604	0.132480	0.706548	0.4814
AR(3)	0.317424	0.107766	2.945482	0.0039
SIGMASQ	49354.70	3961.344	12.45908	0.0000
R-squared	0.533648	Mean dependent var		499.4609
Adjusted R-squared	0.512256	S.D. dependent var		326.7412

S.E. of regression	228.1917	Akaike info criterion	13.75869
Sum squared resid	5675790.	Schwarz criterion	13.90190
Log likelihood	-785.1246	Hannan-Quinn criter.	13.81682
F-statistic	24.94582	Durbin-Watson stat	2.045231
Prob(F-statistic)	0.000000		

Inverted AR Roots	.92	-.24+.54i	-.24-.54i
-------------------	-----	-----------	-----------

Dependent Variable: WIDTH
 Method: ARMA Maximum Likelihood (BFGS)
 Date: 05/09/19 Time: 12:04
 Sample: 1903 2017
 Included observations: 115
 Convergence achieved after 7 iterations
 Coefficient covariance computed using outer product of gradients

Variable	Coefficient	Std. Error	t-Statistic	Prob.
C	578.1834	195.9502	2.950665	0.0039
RAIN	-0.181320	0.196837	-0.921171	0.3590
AR(1)	0.474581	0.070916	6.692192	0.0000
AR(3)	0.356349	0.088247	4.038090	0.0001
SIGMASQ	49767.77	4056.340	12.26913	0.0000

R-squared	0.529745	Mean dependent var	499.4609
Adjusted R-squared	0.512645	S.D. dependent var	326.7412
S.E. of regression	228.1007	Akaike info criterion	13.74944
Sum squared resid	5723293.	Schwarz criterion	13.86878
Log likelihood	-785.5925	Hannan-Quinn criter.	13.79788
F-statistic	30.97892	Durbin-Watson stat	2.137252
Prob(F-statistic)	0.000000		

Inverted AR Roots	.91	-.22+.59i	-.22-.59i
-------------------	-----	-----------	-----------

Table B12: EViews ARMA results – Tokai (logged)

Dependent Variable: RWIDTH
Method: ARMA Maximum Likelihood (OPG - BHHH)
Date: 08/13/19 Time: 14:50
Sample: 1904 2017
Included observations: 114
Convergence achieved after 26 iterations
Coefficient covariance computed using outer product of gradients

Variable	Coefficient	Std. Error	t-Statistic	Prob.
C	-0.013970	0.028478	-0.490571	0.6247
RRAIN	-0.069169	0.255385	-0.270842	0.7870
AR(1)	-0.473474	0.094797	-4.994626	0.0000
AR(2)	-0.262224	0.126622	-2.070921	0.0407
AR(3)	-0.081932	0.093153	-0.879546	0.3811
SIGMASQ	0.206428	0.024375	8.468967	0.0000
R-squared	0.182976	Mean dependent var		-0.017629
Adjusted R-squared	0.145150	S.D. dependent var		0.504871
S.E. of regression	0.466794	Akaike info criterion		1.367729
Sum squared resid	23.53282	Schwarz criterion		1.511739
Log likelihood	-71.96054	Hannan-Quinn criter.		1.426174
F-statistic	4.837402	Durbin-Watson stat		1.964149
Prob(F-statistic)	0.000496			
Inverted AR Roots	-.05+ .47i	-.05- .47i	-.37	

Dependent Variable: RWIDTH
Method: ARMA Maximum Likelihood (OPG - BHHH)
Date: 08/13/19 Time: 15:14
Sample: 1904 2017
Included observations: 114
Convergence achieved after 3 iterations
Coefficient covariance computed using outer product of gradients

Variable	Coefficient	Std. Error	t-Statistic	Prob.
C	-0.014613	0.037356	-0.391182	0.6964
RRAIN	-0.066656	0.239746	-0.278028	0.7815
AR(1)	-0.374059	0.096634	-3.870894	0.0002
SIGMASQ	0.218674	0.027648	7.909290	0.0000
R-squared	0.134508	Mean dependent var		-0.017629
Adjusted R-squared	0.110904	S.D. dependent var		0.504871
S.E. of regression	0.476052	Akaike info criterion		1.389201
Sum squared resid	24.92883	Schwarz criterion		1.485208
Log likelihood	-75.18448	Hannan-Quinn criter.		1.428165
F-statistic	5.698458	Durbin-Watson stat		2.122388
Prob(F-statistic)	0.001155			
Inverted AR Roots	-.37			

Dependent Variable: RWIDTH
 Method: ARMA Maximum Likelihood (OPG - BHHH)
 Date: 08/13/19 Time: 16:05
 Sample: 1904 2017
 Included observations: 114
 Convergence achieved after 16 iterations
 Coefficient covariance computed using outer product of gradients

Variable	Coefficient	Std. Error	t-Statistic	Prob.
C	-0.015604	0.018576	-0.839975	0.4028
RRAIN	-0.058511	0.251287	-0.232845	0.8163
AR(1)	0.218938	0.170785	1.281950	0.2026
MA(1)	-0.725519	0.133520	-5.433799	0.0000
SIGMASQ	0.201107	0.023159	8.683907	0.0000
R-squared	0.204037	Mean dependent var	-0.017629	
Adjusted R-squared	0.174827	S.D. dependent var	0.504871	
S.E. of regression	0.458620	Akaike info criterion	1.325630	
Sum squared resid	22.92619	Schwarz criterion	1.445638	
Log likelihood	-70.56089	Hannan-Quinn criter.	1.374334	
F-statistic	6.985264	Durbin-Watson stat	1.957970	
Prob(F-statistic)	0.000048			
Inverted AR Roots	.22			
Inverted MA Roots	.73			

Table B13: EViews ARMA results – Die Bos

Dependent Variable: GROWTH_INDEX
 Method: ARMA Maximum Likelihood (OPG - BHHH)
 Date: 08/20/19 Time: 10:50
 Sample: 337 413
 Included observations: 77
 Convergence achieved after 24 iterations
 Coefficient covariance computed using outer product of gradients

Variable	Coefficient	Std. Error	t-Statistic	Prob.
C	110.8042	12.89406	8.593426	0.0000
RAIN	-0.017371	0.028706	-0.605133	0.5470
AR(1)	0.794065	0.115364	6.883140	0.0000
MA(1)	-0.221392	0.190505	-1.162131	0.2490
SIGMASQ	338.4393	51.00051	6.635999	0.0000
R-squared	0.415558	Mean dependent var	101.2727	
Adjusted R-squared	0.383089	S.D. dependent var	24.22191	
S.E. of regression	19.02477	Akaike info criterion	8.800654	
Sum squared resid	26059.83	Schwarz criterion	8.952849	
Log likelihood	-333.8252	Hannan-Quinn criter.	8.861531	
F-statistic	12.79863	Durbin-Watson stat	1.928612	
Prob(F-statistic)	0.000000			
Inverted AR Roots	.79			

Dependent Variable: GROWTH_INDEX
 Method: ARMA Maximum Likelihood (OPG - BHHH)
 Date: 08/20/19 Time: 10:52
 Sample: 337 413
 Included observations: 77
 Convergence achieved after 17 iterations
 Coefficient covariance computed using outer product of gradients

Variable	Coefficient	Std. Error	t-Statistic	Prob.
C	113.1877	11.52833	9.818225	0.0000
RAIN	-0.025950	0.026449	-0.981130	0.3298
AR(1)	0.685717	0.082655	8.296127	0.0000
SIGMASQ	346.5808	51.70844	6.702596	0.0000
R-squared	0.401499	Mean dependent var		101.2727
Adjusted R-squared	0.376903	S.D. dependent var		24.22191
S.E. of regression	19.11993	Akaike info criterion		8.798139
Sum squared resid	26686.72	Schwarz criterion		8.919896
Log likelihood	-334.7284	Hannan-Quinn criter.		8.846841
F-statistic	16.32380	Durbin-Watson stat		2.107418
Prob(F-statistic)	0.000000			
Inverted AR Roots	.69			